
Spectral Representations for Accurate Causal Uncertainty Quantification with Gaussian Processes

Hugh Dance[†]

Peter Orbanz[†]

Arthur Gretton[†]

Abstract

Accurate uncertainty quantification for causal effects is essential for robust decision making in complex systems, but remains challenging in non-parametric settings. One promising framework represents conditional distributions in a reproducing kernel Hilbert space and places Gaussian process priors on them to infer posteriors on causal effects, but requires restrictive nuclear dominant kernels and approximations that lead to unreliable uncertainty estimates. In this work, we introduce a method, IMPspec, that addresses these limitations via a spectral representation of the Hilbert space. We show that posteriors in this model can be obtained explicitly, by extending a result in Hilbert space regression theory. We also learn the spectral representation to optimise posterior calibration. Our method achieves state-of-the-art performance in uncertainty quantification and causal Bayesian optimisation across simulations and a healthcare application.

1 Introduction

In many fields, practitioners aim to make optimal interventions to improve outcomes - such as determining the best cancer treatment for a patient, or the most effective poverty reduction policy for resource allocation. The stakes involved in these decisions can be extremely high, with incorrect actions affecting livelihoods. Causal machine learning (Pearl, 2009a; Rubin, 2005) provides a powerful set of tools to address these questions using observational data. However, for decision-makers to trust and act on the outputs of a machine, it is essential to know when it

might be wrong, so as to inform more robust intervention strategies. This makes it crucial to have methods that reliably estimate both causal effects and measures of uncertainty around those effects.

Accurate uncertainty quantification for flexible, non-parametric causal methods remains difficult. For average causal effects of discrete interventions, doubly robust estimators - which estimate conditional distributions to perform bias corrections - can be used to construct asymptotic confidence intervals (Hines et al., 2022; Kennedy, 2022; Chernozhukov et al., 2018). However, extending these methods to conditional average effects and continuous treatments whilst retaining their beneficial properties is an unresolved challenge (Kennedy, 2023; Singh et al., 2024). A promising recent approach avoids conditional distribution estimation by instead learning distribution embeddings a reproducing kernel Hilbert space (RKHS) (Singh et al., 2024). The resulting causal effect estimators avoid propensity weights and their associated issues, and can overcome the curse of dimensionality under certain conditions, whilst using non-parametric models with minimax optimal rates. They do not address uncertainty quantification however and asymptotics of their method are unknown.

Gaussian processes (GPs) are a powerful non-parametric modelling framework for uncertainty quantification in machine learning (Williams and Rasmussen, 2006), which remain popular due to their good generalisation properties. Since there are close connections between GPs and RKHS-based methods (Kanagawa et al., 2018), a natural Bayesian approach to extend the method in Singh et al. (2024) for causal uncertainty quantification, is to place GP priors on the required RKHS elements and infer posteriors on the causal effect. A first work in this direction is Chau et al. (2021b). However, this approach necessitates the use of so-called nuclear dominant kernels to ensure GP sample paths lie in the RKHS, which we show can lead to pathologies in uncertainty estimates. In this work, we develop a novel approach that places GP priors on non-parametric models with conditional distribution embeddings, which addresses these problems. As a result, our method pro-

[†] Gatsby Unit, University College London. Correspondence to: HD <hugh.dance.15@ucl.ac.uk>.

duces accurate and reliable epistemic uncertainty estimates around causal effects. Below we overview the main ideas and our contributions.

Non-technical summary. Singh et al. (2024) represent a causal function γ as an RKHS inner product

$$\text{causal function } \gamma(z) = \langle f, \mathbb{E}[\psi|z] \rangle \quad (1)$$

for suitable functions f and ψ . See Section 2 for details. One can therefore define a prior on γ by placing Gaussian process priors on f and $\mathbb{E}[\psi|z]$. A nuclear dominant kernel ensures both functions are elements of the RKHS, so that (1) remains valid. Nuclear dominant kernels are rarely available in closed form, are not stationary, and introduce intractabilities that resulted in Chau et al. (2021b) using finite dimensional GP approximations. This leads to pathologies, notably collapse of the variance outside the sample support (Fig. 3) and oversmoothing of the posterior mean (Fig. 2). We develop a novel method, referred to as the Spectral Interventional Mean Process (IMPspec), that uses the spectral representation of RKHSs to avoid these limitations. Our strategy is to express γ exactly as

$$\gamma(z) = \sum_i f_i \mathbb{E}[\psi_i|z] \quad (2)$$

for suitable random components f_i and ψ_i , made precise in Section 3. A key tool is the following idea: If a subset of entries of a finite-dimensional Gaussian distribution are conditioned on the remaining entries, the conditional is again Gaussian, with a covariance of the form $\Sigma_A - \Sigma_{AB}\Sigma_B^{-1}\Sigma_A^T$, where $\Sigma_A, \Sigma_B, \Sigma_{AB}$ are suitable blocks of the input covariance matrix (see e.g. Williams and Rasmussen (2006)). In Section 4 we show an analogous formula holds for Gaussian processes that involve certain unbounded operators, see Theorem 1. Using this fact, we can construct Gaussian process priors on the components of (2) without using nuclear dominant kernels, and obtain posteriors for each. This is Theorem 2. This in turn allows us to obtain posterior moments for γ , see Theorem 3, and to construct a posterior for γ which avoids the pathologies above.

As we explain in Section 5, the possible choices of the representation in (2) can be indexed by a hyperparameter μ . We choose this hyperparameter to optimise posterior calibration, by extending a bootstrap approach recently introduced for Bayesian calibration (Syring and Martin, 2019). Theorem 4 shows our procedure is consistent under well-known conditions for bootstrap consistency. In Section 6 our method achieves state-of-the-art performance in several uncertainty quantification and Bayesian optimisation experiments, including a Healthcare example.

2 Background and Related Work

2.1 Reproducing Kernel Hilbert Spaces and Gaussian Processes

An RKHS \mathcal{H}_k is a Hilbert space of functions $f : \mathcal{X} \rightarrow \mathbb{R}$ constructed by a positive definite kernel function $k : \mathcal{X} \times \mathcal{X} \rightarrow \mathbb{R}$, where $k(x, \cdot) \in \mathcal{H}_k$ for all $x \in \mathcal{X}$. Many popular kernels are ‘universal’ (Micchelli et al., 2006), which means \mathcal{H}_k can approximate any continuous function on a compact subset of \mathcal{X} . The defining property of an RKHS is that point evaluation is continuous and bounded (aka the reproducing property): $f(x) = \langle f, k(x, \cdot) \rangle_{\mathcal{H}_k} \forall f \in \mathcal{H}_k$. It is known that if \mathcal{X} is σ -compact¹ and $k \in L_2(\mu^{\otimes 2})$, where μ is a finite, full support measure, the operator $T_k : f \mapsto \int f(x)k(x, \cdot)d\mu(x)$ has spectral decomposition $(\lambda_i, \phi_i(\cdot))_{i \in \mathbb{N}}$ with positive, summable eigenvalues. Additionally, $(\lambda_i^{\frac{1}{2}}\phi_i(x))_{i \in \mathbb{N}} \in \ell_2(\mathbb{N})$ for every $x \in \mathcal{X}$ and $(\lambda_i^{\frac{1}{2}}\phi_i)_{i \in \mathbb{N}}$ is an orthonormal basis (ONB) of \mathcal{H}_k (Sun, 2005; Steinwart and Scovel, 2012), which means \mathcal{H}_k has the spectral representation.

$$\mathcal{H}_k = \{f = \sum_{i \in \mathbb{N}} a_i \lambda_i^{\frac{1}{2}} \phi_i : (a_i)_{i \in \mathbb{N}} \in \ell_2(I)\} \quad (3)$$

A collection of random variables $(Y(x) : x \in \mathcal{X})$ is a Gaussian process (GP) with mean function $m : \mathcal{X} \rightarrow \mathbb{R}$ and covariance $k : \mathcal{X}^2 \rightarrow \mathbb{R}$ if any finite subcollection are jointly Gaussian; $\mathbb{E}Y(x) = m(x)$; and $\text{Cov}(Y(x), Y(x')) = k(x, x)$ (Kallenberg, 1997). If we replace each a_i in Eq. (3) with $Z_i \sim \mathcal{N}(0, 1)$, then the Karhunen-Loève (KL) Theorem tells us we recover a centered GP with covariance k , in the sense that $f := \sum_{i \in \mathbb{N}} Z_i \lambda_i^{\frac{1}{2}} \phi_i \sim \mathcal{GP}(0, k)$. This process lies outside \mathcal{H}_k almost surely, since $\mathbb{P}((Z_i)_{i \in \mathbb{N}} \notin \ell_2(I)) = 1$. For a GP f to lie in \mathcal{H}_k almost surely, its covariance must be constructed using a kernel r which is nuclear dominant with respect to k (Lukić and Beder, 2001). In practice a popular construction is $r(x, x') = \int k(x, u)k(x', u)d\nu(u)$ for finite ν (Flaxman et al., 2016; Chau et al., 2021b).

2.2 Causal Inference and Do-Calculus

In this work, we aim to quantify causal effects of a treatment/intervention $A \in \mathcal{A}$ on an outcome $Y \in \mathcal{Y} \subseteq \mathbb{R}$, and the epistemic uncertainty around these effects. Using the notation of causal graphical models (Pearl, 2009a), we focus on the *average treatment effect (ATE)*, $\gamma(a) := \mathbb{E}[Y | \text{do}(A = a)]$, the *conditional average treatment effect (CATE)*, $\gamma(a, z) := \mathbb{E}[Y | \text{do}(A = a), Z = z]$, where $Z \in \mathcal{Z}$ are observed covariates, and the *average treatment effect on the treated (ATT)*, $\gamma(a, a') = \mathbb{E}[Y | \text{do}(A = a), A = a']$.

¹ \mathcal{X} is σ -compact if it is a countable union of compact subspaces. This covers any discrete or open subset of \mathbb{R}^d .

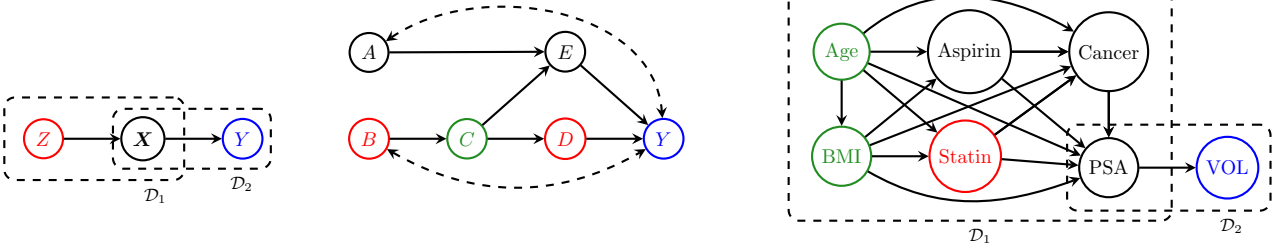


Figure 1: Causal graphs used in experiments. Left: Ablation study. Middle: Synthetic benchmark from Aglietti et al. (2020) with unobserved confounding between $A \leftrightarrow Y$ and $B \leftrightarrow Y$. Right: Healthcare Example from Chau et al. (2021b). \mathcal{D}_1 and \mathcal{D}_2 indicate two different datasets of observations. Blue nodes are outcome variables, red nodes are interventions (not simultaneous), and green nodes are adjustment variables.

Note that in general $\mathbb{E}[Y|do(A = a)] \neq \mathbb{E}[Y|A = a]$. Given a causal directed acyclic graph (DAG) (Pearl, 2009a) over $\mathbf{X} = \{Y, A, O, U\}$, where $O \in \mathcal{O}$ are observed variables and $U \in \mathcal{U}$ unobserved variables, these effects can be identified using the *do-calculus*. Under the popular *back-door* and *front-door* criterion (defined in Appendix A) they are all expressed as

$$\gamma(w, z) = \int_{\mathcal{V}} \mathbb{E}[Y|W = w, V = v] \mathbb{P}_{V|Z}(dv|z) \quad (4)$$

for some $W, V, Z \subseteq \{A, O, \emptyset\}$, or as a marginal expectation of this quantity. Below we demonstrate two examples, with the rest in Appendix A.

Example 1: CATE under back-door. If V satisfies the back-door criterion with respect to (A, Y) ,

$$\mathbb{E}[Y|do(a), z] = \int_{\mathcal{V}} \mathbb{E}[Y|a, v, z] \mathbb{P}_{V|Z}(dv|z) \quad (5)$$

Example 2: ATT under front-door. If V satisfies the front-door criterion with respect to (A, Y) ,

$$\mathbb{E}[Y|do(a), a'] = \int_{\mathcal{V}} \mathbb{E}[Y|a', v] \mathbb{P}_{V|A}(dv|a) \quad (6)$$

Our object of central analysis is therefore Eq. (4). We focus our experiments on the more challenging case where $Z \neq \emptyset$, which covers CATE and ATT, as well as ATE in the setting where one has access to multiple datasets with only partial observations (see Fig. 1). However, our method also works for $Z = \emptyset$.

2.3 Kernel Methods for Causal Functions

Recently, Singh et al. (2024) reduced the problem of estimating Eq. (4) to non-parametric RKHS regression. In particular, they estimate $\mathbb{E}[Y|W, V]$ using functions in a tensor product RKHS $\mathcal{H} := \mathcal{H}_W \otimes \mathcal{H}_V$

$$\mathbb{E}[Y|W, V] = \langle f, \psi(W) \otimes \psi(V) \rangle_{\mathcal{H}} : f \in \mathcal{H} \quad (7)$$

This allows the causal function to be represented as

$$\gamma(w, z) = \langle f, \psi(w) \otimes \mathbb{E}[\psi(V)|Z = z] \rangle_{\mathcal{H}} \quad (8)$$

Many popular kernels k_V are *characteristic*, i.e. the mapping $\mathbb{P} \mapsto \int \psi(v) d\mathbb{P}(v)$ is injective, which means $\mathbb{E}[\psi(V)|Z]$ is an embedding of $\mathbb{P}_{V|Z}$ in \mathcal{H}_V (Simon-Gabriel and Schölkopf, 2018). They proceed to estimate $\mathbb{E}[Y|W, V]$ and $\mathbb{E}[\psi(V)|Z]$ using non-parametric RKHS (i.e. kernel ridge) regression (Steinwart and Christmann, 2008), which gives rise to closed form estimators. The key benefit of this approach is it avoids the need for explicit estimation of $\mathbb{P}_{V|Z}$ or propensity weighting, whilst still enabling one to work with flexible, non-parametric function classes. As a result, it is applicable to both continuous and discrete interventions, and avoids high-variance under insufficient overlap. Singh et al. (2024) prove minimax optimal rates for the conditional expectation estimators, that can avoid the curse of dimensionality by adapting to the smoothness of the regression problems. This implies fast non-parametric rates for γ .

2.4 Bayesian Causal Inference

Bayesian inference has been used to quantify epistemic uncertainty over causal effects since the roadmap of Rubin (1978). We follow recent practice (Oganisian and Roy, 2021) which avoids the need to model counterfactual variables directly. This approach specifies a model $\{\mathbb{P}_{\mathcal{X}^n|\theta} : \theta \in \Theta\}$ over the distribution of $\mathcal{X}^n = (Y_i, W_i, V_i, Z_i)_{i=1}^n$ a prior \mathbb{P}_{θ} on Θ and aims to infer the posterior

$$\mathbb{P}_{\theta|\mathcal{X}^n}(A|x) = \frac{\int_A p_{\mathcal{X}^n|\theta}(x|\theta) \mathbb{P}_{\theta}(d\theta)}{\int_{\Theta} p_{\mathcal{X}^n|\theta}(x|\theta) \mathbb{P}_{\theta}(d\theta)} \quad (9)$$

where $p_{\mathcal{X}^n|\theta}$ is the conditional density with respect to some measure λ . The posterior $\mathbb{P}_{\gamma|\mathcal{X}^n}$ on γ is then derived using Eq. (4) and the posterior $\mathbb{P}_{\theta|\mathcal{X}^n}$.

Whilst Bayes rule provides a probabilistically principled framework for belief updating, for non-parametric priors over infinite-dimensional function spaces, it can be challenging to meaningfully assess the ‘reliability’ or ‘accuracy’ of posterior uncertainties. This has led to an increasing focus on as-

sessing posterior *calibration*² (Müller, 2013; Bissiri et al., 2016; Lyddon et al., 2019; Syring and Martin, 2019; Matsubara et al., 2022). Posteriors are only guaranteed to be calibrated asymptotically in the well-specified regime. We therefore use calibration to assess the *accuracy* of our method’s uncertainty quantification. We analyse *reliability* by whether our model uncertainties are sufficiently under-confident out of distribution, which is a desirable heuristic.

2.5 Related Work

Our work is most related to Chau et al. (2021b), who previously estimated epistemic uncertainty around causal effects using GP priors on RKHS elements in the causal data fusion setting. They establish state-of-the-art performance in causal Bayesian optimisation tasks, however rely on using nuclear dominant kernels. As we demonstrate in our experiments, this leads to key limitations with their method.

Our method avoids these drawbacks and further optimises a spectral hyperparameter to improve posterior calibration. Aglietti et al. (2020) show how to use observational data to construct GP priors for Bayesian Optimisation (BO) of causal functions. Our method can improve their approach by constructing a more informed prior, and demonstrates better performance in experiments. Witty et al. (2020) use GPs for counterfactual inference under structured forms of unobserved confounding. However, their method is instead designed for individual treatment effects, which require structural causal model assumptions and explicit modeling of unobservables. Several methods for calibrating GP predictive distributions have been proposed (Kuleshov et al., 2018; Tran et al., 2019; Capone et al., 2024). However, they are not applicable for calibrating posteriors on latent causal effects. Our calibration approach instead builds on the Bayesian calibration framework in Syring and Martin (2019). We modify their approach to avoid post-hoc variance scaling, instead tuning the spectral representation of the RKHS. By sample splitting, we also ensure consistency of our procedure under general conditions.

3 IMPspec for Causal Uncertainty Quantification

In this section we derive our model (IMPspec), which will be used to infer posteriors on causal functions of the form $\gamma(w, z) = \int_{\mathcal{V}} \mathbb{E}[Y|W = w, V = v] \mathbb{P}_{V|Z}(dv|z)$. From now on, we assume $Y \in \mathbb{R}, V \in \mathcal{V}, W \in \mathcal{W}, Z \in \mathcal{Z}$ where all spaces are σ -compact.

²A posterior α -credible interval $C_\alpha(\mathcal{X}^n)$ for parameter θ is *calibrated* if it has the asserted coverage in repeated experiments, i.e. $\mathbb{P}_{\mathcal{X}_n}(\theta \in C_\alpha(\mathcal{X}^n)) = \alpha$ (Rubin, 1984).

We start from the model in Singh et al. (2024)

$$\mathbb{E}[Y|W, V] = \langle f, \psi(W) \otimes \psi(V) \rangle_{\mathcal{H}_W \otimes \mathcal{H}_V} \quad (10)$$

$$\mathbb{E}[\psi(V)|Z] = L\psi(Z), \quad L \in HS(\mathcal{H}_Z, \mathcal{H}_W) \quad (11)$$

where $HS(\mathcal{H}_Z, \mathcal{H}_W)$ is the class of Hilbert-Schmidt operators $\mathcal{H}_Z \rightarrow \mathcal{H}_W$. We assume the associated kernels k_W, k_V, k_Z are continuous and bounded. This is satisfied by most popular kernels, and allows us to apply Mercer’s theorem in σ -compact domains (Sun, 2005). Whilst one can place GP priors on f, L directly, this requires the use of nuclear dominant kernels so that f and $\psi(W) \otimes \mathbb{E}[\psi(V)|Z = z]$ lie in $\mathcal{H}_W \otimes \mathcal{H}_V$ with probability one, leading to the aforementioned issues. To get around this, our first step is to represent the model using a spectral representation of the RKHS’s $\mathcal{H}_W, \mathcal{H}_V, \mathcal{H}_Z$. In particular, we prove in Proposition 1 in Appendix B that Eq. (10)-Eq. (11) can be equivalently represented as³

$$\mathbb{E}[Y|W, V] = \sum_{(i,j) \in \mathbb{N}} f_{i,j} \lambda_i^{\frac{1}{2}} \lambda_j^{\frac{1}{2}} \phi_i(W) \phi_j(V) \quad (12)$$

$$\mathbb{E}[\phi_i(V)|Z] = \sum_{j \in \mathbb{N}} L_{i,j} \lambda_j^{\frac{1}{2}} \phi_j(Z), \quad \forall i \in \mathbb{N} \quad (13)$$

where $(\lambda_i, \phi_i)_{i \in \mathbb{N}}$ is the eigenspectrum of the operator \mathcal{T}_k defined in Section 2 associated with each kernel (we suppress the dependence on W, V, Z for convenience), and $(f_{i,j})_{(i,j) \in \mathbb{N}^2} \in \ell_2(\mathbb{N})$, $(L_{i,j})_{(i,j) \in \mathbb{N}^2} \in \mathbb{R}^\infty \times \ell_2(\mathbb{N})$. This reduces our problem to constructing an appropriate prior for $(f_{i,j}), (L_{i,j})$. To that end, we expand the function class by allowing $(f_{i,j})_{(i,j) \in \mathbb{N}^2}, (L_{i,j})_{(i,j) \in \mathbb{N}^2} \in \mathbb{R}^\infty \times \mathbb{R}^\infty$ and place independent Gaussian priors on the coefficients:

$$f_{i,j}, L_{i,j} \sim \mathcal{N}(0, 1), \quad \forall (i, j) \in \mathbb{N}^2 \quad (14)$$

As we show in Proposition 2 in Appendix B, the induced spectral processes Eq. (12)-Eq. (13) are distributionally equivalent to nuclear dominant kernel-free GPs for the conditional expectations.

$$\mathbb{E}[Y|W, V] \sim \mathcal{GP}(0, k_W \otimes k_V) \quad (15)$$

$$\mathbb{E}[\phi_i(V)|Z] \sim \mathcal{GP}(0, k_Z), \quad \forall i \in \mathbb{N} \quad (16)$$

The spectral representation allows us to construct nuclear dominant kernel free priors on the one-dimensional co-ordinates $\mathbb{E}[\phi_i(V)|Z]$, but the eigenvalues still ensure that $(\lambda_i^{\frac{1}{2}} \mathbb{E}[\phi_i(V)|Z])_{i \in \mathbb{N}} \in \ell_2(\mathbb{N})$. However, we will not need to estimate the eigenvalues. A consequence of our models being defined without nuclear dominant kernels, is that our posterior uncertainties will not suffer their induced problems (see Section 6). Moreover, our model class ensures

³Without loss of generality we assume $\sum_{(i,j) \in \mathbb{N}^2} (\bullet) = \lim_{n \rightarrow \infty} \sum_{i,j}^n (\bullet)$ is a diagonal limit.

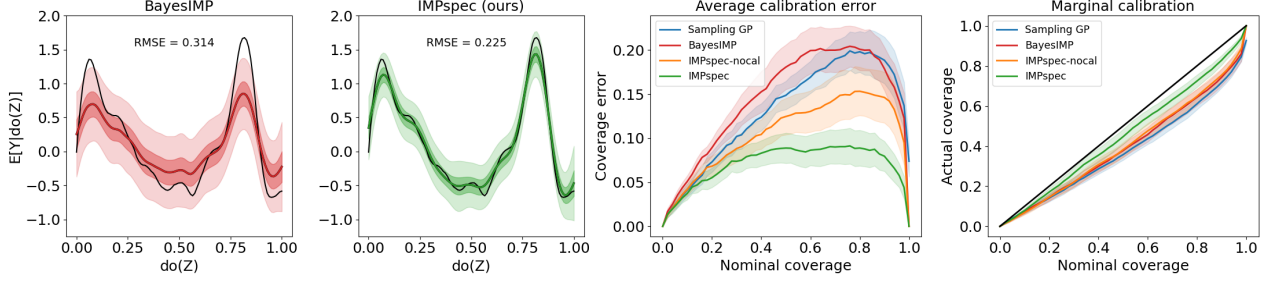


Figure 2: (Ablation Study) LHS plots: Estimated $\mathbb{E}[Y|do(Z)]$ and RMSE, using BayesIMP (Chau et al., 2021b) (red) and our method IMPspec (green). True $\mathbb{E}[Y|do(Z)] =$ black line, posterior mean = colored lines, light shading = 95% credible intervals, dark shading = interquartile range. All quantities are averaged over 50 trials. BayesIMP oversmooths the posterior mean (see Section 6 for discussion). RHS plots: Calibration profiles of different methods estimated from 50 trials, with 95% confidence intervals (shaded regions) estimated using 100 bootstrap replications. Our method is best calibrated and is significantly improved by optimising the spectral representation.

the posterior mean for γ agrees exactly with the estimator $\hat{\gamma}$ in Singh et al. (2024) up to hyperparameter equivalence. The finite sample guarantees in Singh et al. (2024) therefore apply to our method. Since the mean of a GP lies in a smoother RKHS than the sample paths (Kanagawa et al., 2018), using a nuclear dominant kernel would require stronger smoothness assumptions for the same guarantees.

4 Posteriors in Hilbert Spaces

In this section we prove a result that extends existing theory on posteriors for Bayesian regression on Hilbert spaces. In particular, it extends Proposition 3.1 in Knapik et al. (2011) to cover a class of μ -measurable linear transformations (μ -mlt), which are limits of bounded operators μ -almost everywhere (Skorohod, 2012). We use this result to derive exact posteriors with our spectral models Eq. (12)-Eq. (14), and to validate a key assumption we make to derive closed form posteriors for γ (see Section 5.3 and Appendix A for details).

Theorem 1. *Let \mathcal{H}_W be a real, separable Hilbert space with Borel σ -algebra $\mathcal{B}(\mathcal{H}_W)$. Let $W \sim \mathcal{N}(0, \Lambda)$ and $\xi \sim \mathcal{N}(0, \Omega)$ be Gaussian elements in \mathcal{H}_W and \mathbb{R}^n respectively, with trace-class, positive, and injective covariance operators. Let $L : \mathcal{H}_W \rightarrow \mathbb{R}^n$ be a $\mathcal{N}(0, \Lambda)$ -mlt. Then the posterior distribution of $W|Y := LW + \xi$ is $\mathcal{N}(BY, S)$. The posterior is proper and equivalent to $\mathcal{N}(0, \Lambda)$. Additionally, $B : \mathbb{R}^n \rightarrow \mathcal{H}_W$ is continuous and linear, $S : \mathcal{H}_W \rightarrow \mathcal{H}_W$ is positive and trace class and*

$$B = (L\Lambda)^* \left((L\Lambda^{\frac{1}{2}})(L\Lambda^{\frac{1}{2}})^* + \Omega \right)^{-1} \quad (17)$$

$$S = \Lambda - (L\Lambda)^* \left((L\Lambda^{\frac{1}{2}})(L\Lambda^{\frac{1}{2}})^* + \Omega \right)^{-1} (L\Lambda) \quad (18)$$

5 Deriving Posteriors for IMPspec

We now derive the posterior distribution of γ given a dataset \mathcal{X}^n of iid variables $\{\mathbf{X}_i\}_{i=1}^n$, where $\mathbf{X}_i =$

(Y_i, W_i, Z_i, V_i) . We use Theorem 1 to derive explicit posteriors on the scaled coefficients $\tilde{f} = (\lambda_i^{\frac{1}{2}} \lambda_j^{\frac{1}{2}} f_{ij})_{(i,j) \in \mathbb{N}^2}$, $\tilde{L} = (\lambda_i^{\frac{1}{2}} \lambda_j^{\frac{1}{2}} L_{ij})_{(i,j) \in \mathbb{N}^2}$, and then we infer a posterior on γ . In Appendix C we present adaptations of these results for the causal data fusion setting; for the case where $W = \emptyset$; for incremental effects; and for average causal effects (i.e. $Z = \emptyset$). For the sake of brevity, we have suppressed some of the technical assumptions used in the main text. In Appendix C we restate these results more formally with the full set of assumptions used.

For tractable inference, we follow Chau et al. (2021b) and assume the data are noisy observations from the conditional expectations,

$$Y = \mathbb{E}[Y|W, V] + U, \quad U \sim \mathcal{N}(0, \sigma^2) \quad (19)$$

$$\phi(V) = \mathbb{E}[\phi(V)|Z] + \xi, \quad \xi \sim \mathcal{N}(0, I\eta^2) \quad (20)$$

5.1 Posteriors for Spectral Models

Under the above assumption and Theorem 1, we have the following posterior result for f, L

Theorem 2. *Let $\tilde{\Phi}_{W,V} = [\tilde{\phi}(W_1) \otimes \tilde{\phi}(V_1), \dots, \tilde{\phi}(W_n) \otimes \tilde{\phi}(V_n)] \in \ell_2(\mathbb{N}^2)^n$, $\tilde{\Phi}_Z = [\tilde{\phi}(Z_1), \dots, \tilde{\phi}(Z_n)] \in \ell_2(\mathbb{N})^n$ where $\tilde{\phi}_i = \lambda_i^{\frac{1}{2}} \phi_i$ for each $i \in \mathbb{N}$. Let $\Lambda : (h_{ij})_{(i,j) \in \mathbb{N}^2} \mapsto (\lambda_i \lambda_j h_{ij})_{(i,j) \in \mathbb{N}^2}$. Then, given the model in Eq. (12)-Eq. (14) and Eq. (19)-Eq. (20), we have the posteriors*

$$\mathbb{P}_{\tilde{f}|\mathcal{X}^n} = \mathcal{N}(\mu_{\tilde{f}}, \Sigma_{\tilde{f}}) \quad (21)$$

$$\mathbb{P}_{\tilde{L}_i|\mathcal{X}^n} = \mathcal{N}(\mu_{\tilde{L}_i}, \lambda_i \Sigma_{\tilde{L}_i}) : i \in \mathbb{N} \quad (22)$$

$$\mu_{\tilde{f}} = (\tilde{\Phi}_{W,V} \Lambda^{\frac{1}{2}})^* \left(\tilde{\Phi}_{W,V} \tilde{\Phi}_{W,V}^* + I\sigma^2 \right)^{-1} \mathbf{Y} \quad (23)$$

$$\Sigma_{\tilde{f}} = \Lambda - (\tilde{\Phi}_{W,V} \Lambda^{\frac{1}{2}})^* \left(\tilde{\Phi}_{W,V} \tilde{\Phi}_{W,V}^* + I\sigma^2 \right)^{-1} (\tilde{\Phi}_{W,V} \Lambda^{\frac{1}{2}}) \quad (24)$$

$$\mu_{\tilde{L}_i} = (\tilde{\Phi}_Z \Lambda^{\frac{1}{2}})^* \left(\tilde{\Phi}_Z \tilde{\Phi}_Z^* + I\eta^2 \right)^{-1} \tilde{\Phi}_{V,i} \quad (25)$$

$$\Sigma_{\tilde{L}_i} = \Lambda - (\tilde{\Phi}_Z \Lambda^{\frac{1}{2}})^* \left(\tilde{\Phi}_Z \tilde{\Phi}_Z^* + I\eta^2 \right)^{-1} (\tilde{\Phi}_Z \Lambda^{\frac{1}{2}}) \quad (26)$$

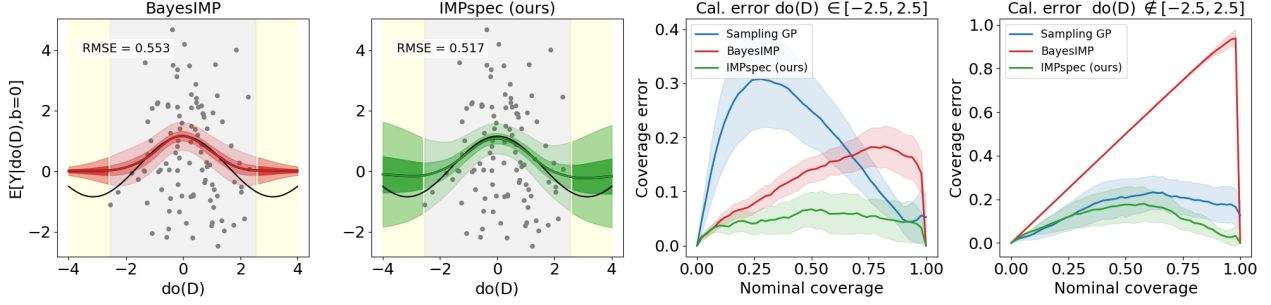


Figure 3: (Synthetic Benchmark) LHS = estimated posterior mean and credible intervals (50% and 95%) for $\mathbb{E}[Y|do(D), b=0]$ using BayesIMP (green) and our IMPSpec (red). Grey dots = example dataset $(D_i, Y_i)_{i=1}^n$ and shading illustrates the training support. RHS = calibration error of different methods (defined as in Fig. 2). BayesIMP’s finite dimensional approximation leads to posterior variance collapse out-of-distribution (see Section 6 and Appendix A for discussion), whilst our method is best calibrated in and out of distribution.

5.2 Posterior Moments for Causal Effects

Using Theorem 2, we can derive the following closed forms for the posterior moments of γ .

Theorem 3. *Given Eq. (12)-Eq. (14) and Eq. (19)-Eq. (20), we have the posterior moments*

$$\mathbb{E}[\gamma(w, z)|\mathcal{X}^n] = \beta(z)^T K_{VV} \alpha(w) \quad (27)$$

$$\text{Var}[\gamma(w, z)|\mathcal{X}^n] = S_1 + S_2 + S_3 \quad (28)$$

$$S_1 = \beta(z)^T K_{VV} (Ik(w, w) - A(w)K_{VV})\beta(z) \quad (29)$$

$$S_2 = \hat{k}(z, z)(\text{Tr}[\tilde{K}_{VV}(\alpha(w)\alpha(w)^T - A(w))]) \quad (30)$$

$$S_3 = \left(\sum_{i \in \mathbb{N}} \lambda_i \right) \hat{k}(z, z)k(w, w) \quad (31)$$

$\alpha(w) = D(w)(K_{WW} \odot K_{VV} + \sigma^2 I)^{-1} \mathbf{Y}$, $A(w) = D(w)(K_{WW} \odot K_{VV} + \sigma^2 I)^{-1} D(w)$, $D(w) = \text{diag}(\mathbf{k}(w))$, $\beta(z) = (K_{ZZ} + \eta^2 I)^{-1} \mathbf{k}(z)$, $\hat{k}(z, z) = k(z, z) - \mathbf{k}(z)^T \beta(z)$, $\tilde{K}_{V,V} = \int \mathbf{k}(v)\mathbf{k}(v)^T d\mu(v)$.

The ATT and CATE under the front-door and back-door criterion are of the form $\gamma(w, z)$ for the appropriately chosen variables W, Z in each scenario, and so Theorem 3 gives the posterior moments for these causal effects. For the ATE one must average γ wrt a subset of (W, V) . By using the empirical distribution to estimate this expectation, one can straightforwardly modify Theorem 2 for the ATE. One can also calculate (i) the posterior moments of incremental effects such as $\mathbb{E}[Y|do(Z=z), W=w] - \mathbb{E}[Y|do(Z=z'), W=w]$, by deriving $\text{Cov}[\gamma(w, z), \gamma(w, z')|\mathcal{X}_n]$, and (ii) the posterior in the causal data fusion setting. We present these formulae in Appendix C.

We note the gram matrix \tilde{K}_{VV} in S_2 resembles a nuclear dominant kernel, where μ defines the ONB $(\lambda_i^{\frac{1}{2}} \phi_i)_{i \in \mathbb{N}}$ of \mathcal{H}_V . However, this term is only computed once at inference time, and can be approximated to arbitrary precision using a very large number of samples (e.g., $m \gg 10^6$) at a cost of $\mathcal{O}(m)$ and error of $\mathcal{O}(m^{-1/2})$, or computed in closed form

if available. Additionally, it only affects the posterior variance. Therefore, we still avoid the aforementioned issues with nuclear dominant kernels, as demonstrated in Section 6. The eigenvalue sum in S_3 is $\sum_{i \in \mathbb{N}} \lambda_i = k(0, 0)$ for any translation invariant kernel. In the following section we outline an approach to optimise posterior calibration with respect to μ .

5.3 Posterior Construction and Calibration

Whilst the first and second moments of γ are available in closed form, the posterior is not. To construct credible intervals, we take the same approach as Chau et al. (2021b) and Kullback-Leibler project the posterior into the space of Gaussians, since

$$(\mathbb{E}[\gamma(w, z)|\mathcal{X}^n], \text{Var}[\gamma(w, z)|\mathcal{X}^n]) = \quad (32)$$

$$\underset{\mu, \sigma}{\text{argmin}} \{KL(\mathbb{P}_{\gamma(w, z)|\mathcal{X}^n} \parallel \mathcal{N}(\mu(w, z), \sigma(w, z)))\} \quad (33)$$

Although the credible regions of this posterior are approximate, they are still closely calibrated in our experiments. Additionally, in Appendix A, we use Theorem 1 to derive a truncated posterior for \tilde{f} and $\mathbb{E}[\tilde{\phi}(V)|Z]$ along one of the sum directions. A large enough truncation can approximate the full posterior arbitrarily well, but is not computationally practical. We implement this in a simulation in Appendix D to assess the validity of our KL projection approach, and find it does not significantly improve calibration.

Since the posterior variance depends on the spectral representation through the measure μ , we learn it to optimise the calibration of the posterior coverage probabilities for $\gamma(w, v)$, by extending the framework in Syring and Martin (2019). In particular, letting $C_{w, z, \alpha, \omega}(\mathcal{X}^n)$ be the highest-posterior density (HPD) α -credible region for γ and $M = \{\mu_\omega : \Omega\}$ a parametric model for μ , we aim to minimise

$$\sum_{(w, z, \alpha) \in \Theta} |\mathbb{P}_{\mathcal{X}^n}(\gamma(w, z) \in C_{w, z, \alpha, \omega}(\mathcal{X}^n)) - \alpha| \quad (34)$$

where Θ is a user-defined grid of values of interest. For instance, if purely interested in 95% credible regions one could just fix $\alpha = 0.95$ and vary w, v discretely and uniformly over a range of interest. Our experiments have continuous variables and so we use the parameterisation $\mu_\omega = \mathcal{N}(\bar{V}, \omega^2 I)$. For discrete variables, one could specify $\omega \in \Delta_k$ for the finite case and $\text{Pois}(\omega)$ for the countably infinite case.

(34) can be optimised wrt ω using grid-search or gradient descent, however it is unobserved and so needs estimating. Syring and Martin (2019) propose to do this using the empirical bootstrap $\hat{\mathbb{P}}_{\mathcal{X}^n} = \mathbb{P}_{\mathcal{Z}^n | \mathcal{X}^n}$ and a plug-in estimator for $\gamma(w, z)$. In our case there is no obvious empirical plug-in estimator, so we use the estimator in Singh et al. (2024) as its convergence rates are well established and it agrees with our posterior mean up to hyperparameter equivalence. Consistency of the empirical bootstrap for black-box statistics has been established under certain stability and smoothness conditions (Austern and Syrgkanis, 2020; Tang and Westling, 2024). However, the consistency of $\hat{\mathbb{P}}_{\mathcal{Z}^n | \mathcal{X}^n}(\hat{\gamma}(w, z) \in C_{w,z,\alpha,\mu}(\mathcal{X}^n))$ jointly in $\hat{\gamma}$ and $\hat{\mathbb{P}}_{\mathcal{Z}^n | \mathcal{X}^n}$ is unclear, particularly given the non-parametric estimator $\hat{\gamma}$. Below we show that under sample splitting, this estimator is consistent whenever the empirical bootstrap $\mathbb{P}_{\mathcal{Z}^n | \mathcal{X}^n}$ is consistent and the distribution function is sufficiently smooth, under the conditions for uniform consistency of $\hat{\gamma}$ in (Singh et al., 2024). For simplicity, we prove the result for cumulative rather than HPD regions, but the result extends under analogous conditions.

Theorem 4. *Under the conditions of Theorem 3, let $\{\mathcal{X}^n, \mathcal{X}^m\}$ be a partition of the dataset for $n, m > 0$. Let $\mu_{w,z} = \mathbb{E}[\gamma(w, z) | \mathcal{X}^n]$, $\sigma_{w,z} = \text{Var}[\gamma(w, z) | \mathcal{X}^n]$, $F_\alpha(t) = \mathbb{P}_{\mathcal{X}^n}(\mu_{w,z} + t_\alpha \sigma_{w,z} \leq t)$ and t_α be the $(1 - \alpha)$ quantile of $\mathcal{N}(0, 1)$. Let $\hat{\gamma}_m$ be the estimator for γ in Singh et al. (2024) using \mathcal{X}^m . Then, under the assumptions of Theorem 6.1 in Singh et al. (2024) and L -Lipschitzness of F_α*

$$\begin{aligned} & \|\mathbb{P}_{\mathcal{X}^n}(\gamma(w, z) \leq \mu_{w,z} + t_\alpha \sigma_{w,z}) \\ & - \hat{\mathbb{P}}_{\mathcal{Z}^n | \mathcal{X}^n}(\hat{\gamma}_m(w, z) \leq \mu_{w,z} + t_\alpha \sigma_{w,z})\|_{L_1(\mathbb{P}_{\mathcal{X}^m})} \\ & \leq \|\mathcal{D}(\mathbb{P}_{\mathcal{X}^n}, \mathbb{P}_{\mathcal{Z}^n | \mathcal{X}^n})\|_{L_1(\mathbb{P}_{\mathcal{X}^n})} + \mathcal{O}\left(m^{-\frac{1}{2} \frac{c-1}{c+b}}\right) \end{aligned} \quad (35)$$

\mathcal{D} is the Kolmogorov metric, $c \in (1, 2]$, $b \in [1, \infty)$.

The constants c and b describe the smoothness and effective dimensionality of the underlying regression problems Singh et al. (2024). Whilst sample splitting calibrates the posterior given only a subset of the dataset, we find sample splitting leads to better calibration performance (see Appendix D).

Method	RMSE	Calibration error
Sampling GP	0.279 \pm 0.061	0.130 \pm 0.010
BayesIMP	0.314 \pm 0.082	0.143 \pm 0.011
IMPspec-nocal (ours)	0.223 \pm 0.046	0.098 \pm 0.010
IMPspec (ours)	0.223 \pm 0.046	0.065 \pm 0.008

Table 1: Ablation study mean \pm standard deviation of RMSE and calibration error from 50 trials.

Method	RMSE	Cal. error	Cal. error (OOD)
Sampling GP	0.540 \pm 0.168	0.190 \pm 0.028	0.156 \pm 0.031
BayesIMP	0.544 \pm 0.098	0.107 \pm 0.011	0.485 \pm 0.003
IMPspec (ours)	0.517 \pm 0.192	0.047 \pm 0.015	0.108 \pm 0.026

Table 2: Synthetic benchmark mean \pm standard deviation RMSE and calibration error from 50 trials.

5.4 Hyperparameter Optimisation

The remaining model hyperparameters are the kernel parameters $(\theta_W, \theta_V, \theta_Z)$ and noise parameters (σ^2, η^2) , which can be trained using our distributional equivalences Eq. (15) and Eq. (16). In particular, $(\theta_W, \theta_V, \sigma^2)$ can be trained by maximising the log marginal likelihood $\log p(\mathbf{y} | \mathbf{w}, \mathbf{v})$,

$$LL(\theta_{W,V}, \sigma^2) = \log \mathcal{N}(\mathbf{y} | \mathbf{0}, K_{VV} \odot K_{WW} + \eta^2 I) \quad (36)$$

Unfortunately, we cannot learn the hyperparameters (θ_V, σ^2) this way, since $\tilde{\phi}(V)$ is unobserved. Instead, we propose optimising the *weighted* likelihood sum

$$\begin{aligned} LL_\lambda(\theta_Z, \eta^2) &= \sum_{i \in \mathbb{N}} \lambda_i \log p(\phi_i | z) \\ &= c - \frac{1}{2}(\tau \log |K_{ZZ}| - \frac{1}{2} \text{Tr}[(K_{ZZ} + \eta^2 I)^{-1} K_{VV}]) \end{aligned} \quad (37)$$

where $\phi_i = (\phi_i(v_1), \dots, \phi_i(v_n))$ and $\tau := \sum_{i \in \mathbb{N}} \lambda_i = k_V(0, 0)$ for any translation invariant k_V . Note that if we had not used the spectral representation, we would instead have had to use the objective in Chau et al. (2021b), which again requires working with nuclear dominant kernels. Eq. (36) and Eq. (38) have $\mathcal{O}(n^3)$ complexity. Therefore, for large datasets (e.g. $n \geq 10^4$) one could use established approximation methods such as inducing points (Titsias, 2009; Hensman et al., 2013) or minibatching (Chen et al., 2020; Dance and Paige, 2022) to reduce this.

6 Experiments

We now implement our method, IMPspec, in several simulations and a Healthcare example. All experiment and implementation details are in Appendix D.

6.1 Ablation Study

We first implement IMPspec along with BayesIMP (Chau et al., 2021b) and the sampling based GP in (Witty et al., 2020) in an ablation study with causal data fusion, where we isolate some key benefits of

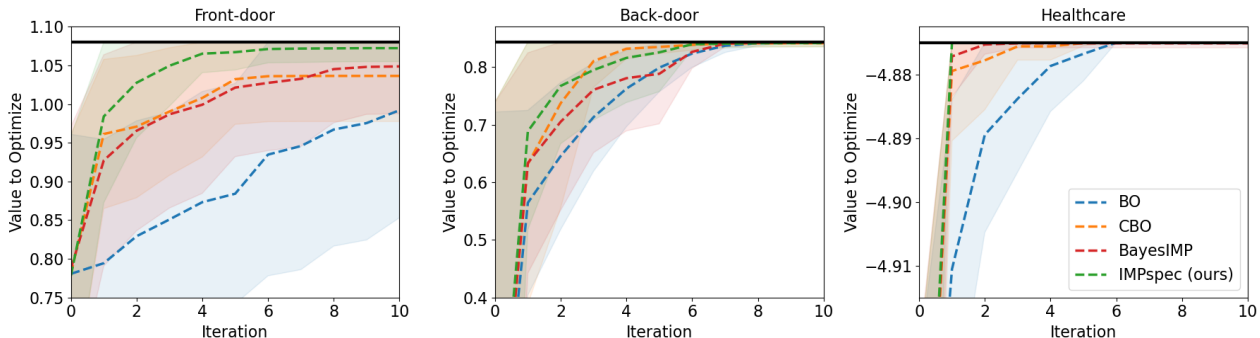


Figure 4: BO best values per iteration (50 trials). LHS: Synthetic benchmark targeting $\max_b \mathbb{E}[Y|do(b), B = 0]$ via front-door criterion, Middle: Synthetic benchmark targeting $\min_d \mathbb{E}[Y|do(d), B = 0]$ via back-door criterion, Right: Healthcare example from Aglietti et al. (2020) targeting $\min_s \mathbb{E}[\text{Vol}|do(\text{Statin} = s)]$ via back-door criterion. Dashed lines = mean, shading = standard deviation, black line = best obtainable value. Our method (IMPspec) converged fastest on average in all three experiments.

our method. We simulate two independent datasets $\mathcal{D}_1 = \{X_i^{(1)}, Y_i^{(1)}\}_{i=1}^{100}$, $\mathcal{D}_2 = \{Z_j^{(2)}, X_j^{(2)}\}_{j=1}^{100}$ from the LHS causal graph in Fig. 1 and use them to estimate $\mathbb{E}[Y|do(Z)]$ for a range of values z_1, \dots, z_K . Average RMSE and calibration estimates from 50 trials are displayed in Fig. 2 and Table 1.

We see (RHS of Fig. 2) that IMPspec performed best in terms of calibration and is generally well-calibrated, with coverage errors significantly smaller than 0.1. Additionally, it is clear that our spectral hyperparameter optimisation procedure significantly improved calibration performance. Note, the coverage error profile computes the absolute error *before* averaging over the tested values of $do(z)$. The marginal calibration profile (RHS) can be perfect even if a method is mis-calibrated at every $do(z)$, but we produce it as standard practice in calibration.

Our method also achieved the best RMSE on average and fit the causal function well. By contrast, BayesIMP systematically oversmoothed the posterior mean, resulting in underfitting. We believe this may be caused by the fact that the nuclear dominant kernel used in BayesIMP is nonstationary. This could make it challenging to fit the extreme points of the function without using an excessively small length-scale. Nonstationarity is difficult to avoid when the input support is \mathbb{R}^d , due to the requirement that the integrating measure in the nuclear dominant construction is finite. In this experiment, the nuclear dominant kernel had a closed form. In other situations it must be Monte Carlo approximated during training and inference. We found this approximation had a significant negative effect on performance (see Appendix D), demonstrating another limitation. The baseline sampling GP posterior mean doesn't have the same finite-sample guarantees our method, and performed worse than our method on average. In Appendix D we report results for several (additional) ablations of IMPspec and BayesIMP.

Method	Front-door	Back-door	Healthcare
BO	1.753 ± 1.326	0.760 ± 0.519	0.064 ± 0.029
CBO	0.656 ± 0.604	0.383 ± 0.427	0.008 ± 0.018
BayesIMP	0.698 ± 0.825	0.570 ± 0.555	0.003 ± 0.010
IMPspec (ours)	0.247 ± 0.284	0.335 ± 0.420	0.000 ± 0.000

Table 3: BO experiments mean \pm standard deviation cumulative regret for $\mathbb{E}[Y|do(B), b = 0]$ (front-door), $\mathbb{E}[Y|do(D), b = 0]$ (back-door) on synthetic benchmark, and $\mathbb{E}[\text{Vol}|do(\text{Statin})]$ from 50 trials.

6.2 Synthetic Benchmark

We next implement the same methods on the middle causal graph of Fig. 1, which is a synthetic benchmark studied in Aglietti et al. (2020); Chau et al. (2021b). We aim to estimate the conditional average treatment effect $\mathbb{E}[Y|do(D = d), B = b]$, which is identified under the back-door criterion using C as an adjustment set. Table 2 and Fig. 3 display equivalent results to the ablation study from 50 trials of $n = 100$ datapoints. We fix $b = 0$ and vary d using a grid of values to assess how each method's uncertainty estimates generalise out of distribution. Table 2 and Fig. 3 show our method performed best in overall RMSE, and in calibration both in and out of distribution. Whilst BayesIMP performed well in distribution, it performed considerably worse out of distribution. This is a direct consequence of the finite dimensional GP approximations used for tractability with the nuclear dominant kernel, which lead to collapse of the posterior variance out of distribution. We expand on this in Appendix A.

6.3 CBO and Example in Healthcare

We now showcase the usefulness of IMPspec's uncertainty estimates on various causal Bayesian optimisation tasks. This includes a Healthcare example with a known causal graph (RHS Fig. 1) for which we construct a simulator based on real data. The objective in these tasks is to efficiently identify the optimal value of the average causal effect

$\mathbb{E}[Y|do(X = x)]$ (or the conditional average effect $\mathbb{E}[Y|do(X = x), Z = z]$) with respect to x , using the fewest possible BO iterations. In causal Bayesian optimisation (CBO) (Aglietti et al., 2020), one uses observational data to construct a more informed GP prior on the interventional effect. Since our method produces a GP posterior for the causal effect from observational data, we can use this posterior to construct a BO prior (as in BayesIMP). We compare this approach against BayesIMP, the original CBO approach in (Aglietti et al., 2020), and a naive BO algorithm which doesn't use observational data to construct the GP prior. Note that in practice, each iteration corresponds to running a large-scale experiment to recover (e.g.) a pair $(x_i, \hat{\mathbb{E}}[Y|do(X = x_i)])$. Running many iterations is therefore typically not feasible in practice, nor ethical in healthcare scenarios. We therefore focus on performance up to 10 iterations, and emphasise that performance improvements by just a few iterations can have a large practical impact. Table 3 displays cumulative regret scores after 10 iterations for two different causal effects on the synthetic benchmark (middle causal graph of Fig. 1) and for the average causal effect of `statin` on `cancer_vol` in the healthcare example. Fig. 4 displays convergence profiles. IMPspec converged fastest and obtained the lowest cumulative regret scores across all three tasks. In one experimental setup, ours was the only method that could find the approximate optimum value within the specified number of iterations. This demonstrates the practical usefulness of our method's uncertainty estimates in aiding optimal decision making.

References

- Aglietti, V., Lu, X., Paleyes, A., and González, J. (2020). Causal bayesian optimization. In *International Conference on Artificial Intelligence and Statistics*, pages 3155–3164. PMLR.
- Austern, M. and Syrgkanis, V. (2020). Asymptotics of the empirical bootstrap method beyond asymptotic normality. *arXiv preprint arXiv:2011.11248*.
- Baker, C. R. (1973). Joint measures and cross-covariance operators. *Transactions of the American Mathematical Society*, 186:273–289.
- Bissiri, P. G., Holmes, C. C., and Walker, S. G. (2016). A general framework for updating belief distributions. *Journal of the Royal Statistical Society: Series B (Statistical Methodology)*, 78(5):1103–1130.
- Capone, A., Hirche, S., and Pleiss, G. (2024). Sharp calibrated gaussian processes. *Advances in Neural Information Processing Systems*, 36.
- Carvalho, G. F., Daudi, S. N., Kan, D., Mondo, D., Roehl, K. A., Loeb, S., and Catalona, W. J. (2010). Correlation between serum prostate-specific antigen and cancer volume in prostate glands of different sizes. *Urology*, 76(5):1072–1076.
- Chau, S. L., Bouabid, S., and Sejdinovic, D. (2021a). Deconditional downscaling with gaussian processes. *Advances in Neural Information Processing Systems*, 34:17813–17825.
- Chau, S. L., Ton, J.-F., González, J., Teh, Y., and Sejdinovic, D. (2021b). Bayesimp: Uncertainty quantification for causal data fusion. *Advances in Neural Information Processing Systems*, 34:3466–3477.
- Chen, H., Zheng, L., Al Kontar, R., and Raskutti, G. (2020). Stochastic gradient descent in correlated settings: A study on gaussian processes. *Advances in neural information processing systems*, 33:2722–2733.
- Chernozhukov, V., Chetverikov, D., Demirer, M., Duflo, E., Hansen, C., Newey, W., and Robins, J. (2018). Double/debiased machine learning for treatment and structural parameters. *The Econometrics Journal*, 21(1):C1–C68.
- Dance, H. and Paige, B. (2022). Fast and scalable spike and slab variable selection in high-dimensional gaussian processes. In *International Conference on Artificial Intelligence and Statistics*, pages 7976–8002. PMLR.
- Flaxman, S., Sejdinovic, D., Cunningham, J. P., and Filippi, S. (2016). Bayesian learning of kernel embeddings. In *Proceedings of the Thirty-Second Conference on Uncertainty in Artificial Intelligence*, pages 182–191.
- Geiger, D., Verma, T., and Pearl, J. (1990). d-separation: From theorems to algorithms. In *Machine Intelligence and Pattern Recognition*, volume 10, pages 139–148. Elsevier.
- Grenander, U. (1963). *Probability on algebraic structures*. Almqvist & Wiksell.
- Hensman, J., Fusi, N., and Lawrence, N. D. (2013). Gaussian processes for big data. In *Uncertainty in Artificial Intelligence*, page 282. Citeseer.
- Hines, O., Dukes, O., Diaz-Ordaz, K., and Vansteelandt, S. (2022). Demystifying statistical learning based on efficient influence functions. *The American Statistician*, 76(3):292–304.
- Kallenberg, O. (1997). *Foundations of modern probability*, volume 2. Springer.
- Kanagawa, M., Hennig, P., Sejdinovic, D., and Sriperumbudur, B. K. (2018). Gaussian processes and kernel methods: A review on connections and equivalences. *arXiv preprint arXiv:1807.02582*.
- Kennedy, E. H. (2022). Semiparametric doubly robust targeted double machine learning: a review. *arXiv preprint arXiv:2203.06469*.

- Kennedy, E. H. (2023). Towards optimal doubly robust estimation of heterogeneous causal effects. *Electronic Journal of Statistics*, 17(2):3008–3049.
- Klesov, O. I. (1996). Almost sure convergence of multiple series of independent random variables. *Theory of Probability & Its Applications*, 40(1):52–65.
- Knapik, B. T., Van Der Vaart, A. W., and van Zanten, J. H. (2011). Bayesian inverse problems with gaussian priors.
- Kuleshov, V., Fenner, N., and Ermon, S. (2018). Accurate uncertainties for deep learning using calibrated regression. In *International conference on machine learning*, pages 2796–2804. PMLR.
- Le Gall, J.-F. (2016). *Brownian motion, martingales, and stochastic calculus*. Springer.
- Lukić, M. and Beder, J. (2001). Stochastic processes with sample paths in reproducing kernel hilbert spaces. *Transactions of the American Mathematical Society*, 353(10):3945–3969.
- Lyddon, S. P., Holmes, C., and Walker, S. (2019). General bayesian updating and the loss-likelihood bootstrap. *Biometrika*, 106(2):465–478.
- Matsubara, T., Knoblauch, J., Briol, F.-X., and Oates, C. J. (2022). Robust generalised bayesian inference for intractable likelihoods. *Journal of the Royal Statistical Society Series B: Statistical Methodology*, 84(3):997–1022.
- Micchelli, C. A., Xu, Y., and Zhang, H. (2006). Universal kernels. *Journal of Machine Learning Research*, 7(12).
- Müller, U. K. (2013). Risk of bayesian inference in misspecified models, and the sandwich covariance matrix. *Econometrica*, 81(5):1805–1849.
- Oganisian, A. and Roy, J. A. (2021). A practical introduction to bayesian estimation of causal effects: Parametric and nonparametric approaches. *Statistics in medicine*, 40(2):518–551.
- Pearl, J. (1995). Causal diagrams for empirical research. *Biometrika*, 82(4):669–688.
- Pearl, J. (2009a). Causal inference in statistics: An overview.
- Pearl, J. (2009b). *Causality*. Cambridge university press.
- Rahimi, A. and Recht, B. (2007). Random features for large-scale kernel machines. *Advances in neural information processing systems*, 20.
- Richardson, T. S. and Robins, J. M. (2013). Single world intervention graphs (swigs): A unification of the counterfactual and graphical approaches to causality. *Center for the Statistics and the Social Sciences, University of Washington Series. Working Paper*, 128(30):2013.
- Rubin, D. B. (1978). Bayesian inference for causal effects: The role of randomization. *The Annals of statistics*, pages 34–58.
- Rubin, D. B. (1984). Bayesianly justifiable and relevant frequency calculations for the applied statistician. *The Annals of Statistics*, pages 1151–1172.
- Rubin, D. B. (2005). Causal inference using potential outcomes: Design, modeling, decisions. *Journal of the American Statistical Association*, 100(469):322–331.
- Ryabov, G. (2008). Finite absolute continuity of gaussian measures on infinite-dimensional spaces. *Ukrainian Mathematical Journal*, 60(10).
- Shahriari, B., Swersky, K., Wang, Z., Adams, R. P., and De Freitas, N. (2015). Taking the human out of the loop: A review of bayesian optimization. *Proceedings of the IEEE*, 104(1):148–175.
- Shawe-Taylor, J., Williams, C. K., Cristianini, N., and Kandola, J. (2005). On the eigenspectrum of the gram matrix and the generalization error of kernel-pca. *IEEE Transactions on Information Theory*, 51(7):2510–2522.
- Shpitser, I. and Pearl, J. (2012). Effects of treatment on the treated: Identification and generalization. *arXiv preprint arXiv:1205.2615*.
- Simon-Gabriel, C.-J. and Schölkopf, B. (2018). Kernel distribution embeddings: Universal kernels, characteristic kernels and kernel metrics on distributions. *Journal of Machine Learning Research*, 19(44):1–29.
- Singh, R., Xu, L., and Gretton, A. (2024). Kernel methods for causal functions: dose, heterogeneous and incremental response curves. *Biometrika*, 111(2):497–516.
- Skorohod, A. V. (2012). *Integration in Hilbert space*, volume 79. Springer Science & Business Media.
- Steinwart, I. (2024). Conditioning of banach space valued gaussian random variables: An approximation approach based on martingales. *arXiv preprint arXiv:2404.03453*.
- Steinwart, I. and Christmann, A. (2008). *Support vector machines*. Springer Science & Business Media.
- Steinwart, I. and Scovel, C. (2012). Mercer’s theorem on general domains: On the interaction between measures, kernels, and rkhs. *Constructive Approximation*, 35(3):363–417.
- Sun, H. (2005). Mercer theorem for rkhs on noncompact sets. *Journal of Complexity*, 21(3):337–349.
- Syring, N. and Martin, R. (2019). Calibrating general posterior credible regions. *Biometrika*, 106(2):479–486.

- Tang, Z. and Westling, T. (2024). Consistency of the bootstrap for asymptotically linear estimators based on machine learning. *arXiv preprint arXiv:2404.03064*.
- Titsias, M. (2009). Variational learning of inducing variables in sparse gaussian processes. In *Artificial intelligence and statistics*, pages 567–574. PMLR.
- Tran, G.-L., Bonilla, E. V., Cunningham, J., Michiardi, P., and Filippone, M. (2019). Calibrating deep convolutional gaussian processes. In *The 22nd International Conference on Artificial Intelligence and Statistics*, pages 1554–1563. PMLR.
- Williams, C. K. and Rasmussen, C. E. (2006). *Gaussian processes for machine learning*, volume 2. MIT press Cambridge, MA.
- Witty, S., Takatsu, K., Jensen, D., and Mansinghka, V. (2020). Causal inference using gaussian processes with structured latent confounders. In *International Conference on Machine Learning*, pages 10313–10323. PMLR.

Supplementary Materials for “Spectral representations for accurate causal uncertainty quantification with Gaussian Processes”

Contents

A Additional Details	12
A.1 Causal Graphical Models	12
A.2 Formula for Treatment Effects of Interest	12
A.3 Causal Data Fusion	13
A.4 Truncated Posterior Approximations	13
A.5 Problems with Nuclear Dominant Kernels in BayesIMP	14
B Assumptions and Auxilliary Results	15
B.1 Assumptions in Technical Results	15
B.2 Auxilliary Results	16
C Proofs of Main Results and Extensions of Results	19
C.1 Proof of Theorem 1	19
C.2 Proof of Theorem 2	21
C.3 Proof of Theorem 3	23
C.4 Proof of Theorem 4	27
C.5 Theorem 3 for Incremental Effects	28
C.6 Theorem 3 for Average Causal Effects	29
D Experiments	29
D.1 Ablation Study	29
D.2 Synthetic Benchmark	31
D.3 CBO on Synthetic Benchmark and Healthcare Example	32
D.4 Additional Results	34

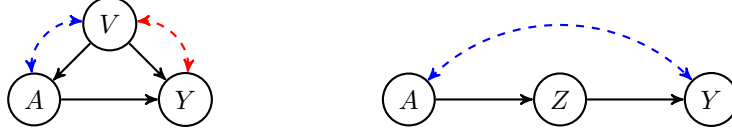


Figure 5: LHS: causal graph where V satisfies the back-door criterion wrt. (A, Y) . RHS: causal graph where Z satisfies the front-door criterion wrt (A, Y) . Dashed edges indicate unobserved confounding (red and blue cannot occur simultaneously in LHS).

A Additional Details

A.1 Causal Graphical Models

Below we describe some key concepts used in the causal graphical modelling literature (Pearl, 2009b).

Graphs: A Graph \mathcal{G} is a set of directed edges E and indices $[m] = \{1, \dots, m\}$. The edges of \mathcal{G} can be encoded by a parent function $\text{pa} : [m] \rightarrow 2^{[m-1]}$ in the sense that $l \in \text{pa}(j) \Leftrightarrow l \rightarrow j$ in \mathcal{G} . If j has no incoming edges then $\text{pa}(j) = \emptyset$. In this case, one can write $\mathcal{G} = (E, \text{pa})$.

Causal DAGs: a graph $\mathcal{G} = (\mathbf{X}, \text{pa})$ is a causal DAG over random variables $\mathbf{X} := (X_i)_{i=1}^m \sim \mathbb{P}$, if the factorisation $\mathbb{P} = \prod_i \mathbb{P}_{i|\text{pa}(i)}$ holds and conditionals $(\mathbb{P}_{j|\text{pa}(j)})_{j=1}^m$ describe real (e.g., physical) data generating mechanisms for observations.

Definition 1 (Back-door criterion (Pearl, 1995)). *Take a causal DAG \mathcal{G} over $(X_i)_{i=1}^m$, and let $(A, V, Y) \subseteq (X_i)_{i=1}^m$. V satisfies the back-door criterion with respect to (A, Y) if*

1. No node in V is a descendent of A .
2. V blocks every path between A and Y that contains an edge pointing into A

Definition 2 (Front-door criterion (Pearl, 1995)). *Take a causal DAG \mathcal{G} over $(X_i)_{i=1}^m$, and let $(A, Z, Y) \subseteq (X_i)_{i=1}^m$. Z satisfies the front-door criterion with respect to (A, Y) if*

1. Z intercepts all directed paths from A to Y .
2. There is no back-door path between A, Z .
3. Every back-door path between Z and Y is blocked by A .

A.2 Formula for Treatment Effects of Interest

In the following we present the known formulae for all causal effects of interest in this work. All these effects take the form of Eq. (4) in the main text, or a marginal expectation of it. Details for ATE and CATE can be found in (Pearl, 2009b) and for ATT in (Shpitser and Pearl, 2012).

Effects under the back-door criterion: In the following A is the treatment, Y is the outcome, and $V = (W, Z)$ satisfy the back-door criterion wrt (A, Y) (see Fig. 5 LHS).

$$\text{ATE}_{BD}(a) = \int_{\mathcal{V}} \mathbb{E}[Y|A = a, V = v] \mathbb{P}_V(dv) \quad (39)$$

$$\text{CATE}_{BD}(a, z) = \int_{\mathcal{W}} \mathbb{E}[Y|A = a, W = w, Z = z] \mathbb{P}_{W|Z}(dw|z) \quad (40)$$

$$\text{ATT}_{BD}(a, a') = \int_{\mathcal{V}} \mathbb{E}[Y|A = a, V = v] \mathbb{P}_{V|A}(dv|a') \quad (41)$$

Effects under the front-door criterion: In the following A is the treatment, Y is the outcome, and Z satisfies the front-door criterion wrt (A, Y) (see Fig. 5 RHS).

$$\text{ATE}_{FD}(a) = \int_{\mathcal{A}} \int_{\mathcal{Z}} \mathbb{E}[Y|A = a', Z = z] \mathbb{P}_{Z|A}(dz|a) \mathbb{P}_A(da') \quad (42)$$

$$\text{ATT}_{FD}(a, a') = \int_{\mathcal{Z}} \mathbb{E}[Y|A = a', Z = z] \mathbb{P}_{Z|A}(dz|a) \quad (43)$$

A.3 Causal Data Fusion

As we discuss in the main text, our method can be used both in situations where \mathcal{X}^n is a single dataset of i.i.d. observations from a causal graph, or in certain situations where \mathcal{X}^n is comprised of two (i.i.d.) datasets $\mathcal{D}_1, \mathcal{D}_2$ of partial observations from the causal graph. Following [Chau et al. \(2021b\)](#), we refer to the latter situation as the *causal data fusion* setting. In general, to estimate a causal effect of the form $\gamma(w, z)$ as defined in Eq. (4) in the main text, one must have access to observation sets $\mathcal{D}_1 = (Y_i^{(1)}, W_i^{(1)}, V_i^{(1)})_{i=1}^{m_1}$ and $\mathcal{D}_2 = (Z_i^{(2)}, V_i^{(2)})_{i=1}^{m_2}$ (in the case where $W = \emptyset$ it suffices to have $\mathcal{D}_1 = (Y_i^{(1)}, V_i^{(1)})_{i=1}^{m_1}$).

The theorems in the main text are derived for the single dataset case. These theorems can be straightforwardly modified to the causal data fusion setting, and we do so in Appendix C. Our experiments include both single dataset and causal data fusion scenarios. In Appendix D we explain how we implement IMPspec in each case, with reference to the relevant results in Appendix C.

A.4 Truncated Posterior Approximations

One cannot sample from the posterior model we derive for $\gamma(w, z)$ because it requires sampling infinite-dimensional elements of an RKHS. As explained in Section 5.3, our solution is to approximate the posterior for $\gamma(w, z)$ using a Gaussian with the true posterior mean and variance. This corresponds to Kullback-Leibler projecting the true posterior into the space of Gaussians. Another approach to approximate the posterior of $\gamma(w, z)$ is to truncate the spectral representation along one of the directions. The approach enables one to control the degree of posterior approximation error through the size of the truncation. In particular, suppose that at inference time, we truncate the model for $\mathbb{E}[Y|W, V]$ as

$$\mathbb{E}[Y|W, V]_m = \sum_{i \in \mathbb{N}} \sum_{j=1}^m f_{i,j} \tilde{\phi}_i(W) \tilde{\phi}_j(V) \quad (44)$$

In this case, we get

$$\gamma_m(w, z) = \sum_{j=1}^m \left(f_j[\tilde{\phi}(w)] \right) \left(L_j[\tilde{\phi}(z)] \right) \quad (45)$$

where $f_j[\tilde{\phi}(w)] := \sum_{i \in \mathbb{N}} f_{i,j} \tilde{\phi}_i(w)$ and $L_j[\tilde{\phi}(z)] = \sum_{i \in \mathbb{N}} L_{i,j} \tilde{\phi}_i(z)$. By using the posteriors on \tilde{f} and \tilde{L} derived in Theorem 2, and applying Proposition 3.2 in [Knapik et al. \(2011\)](#) we get that,

$$f_{1:m}[\tilde{\phi}(w)] | \mathcal{X}^n \sim \mathcal{N}(\mathbf{m}_f, C_f) \quad (46)$$

$$L_{1:m}[\tilde{\phi}(z)] | \mathcal{X}^n \sim \mathcal{N}(\mathbf{m}_L, C_L) \quad (47)$$

where the posterior moments are

$$\mathbf{m}_f = (\tilde{\Phi}_{V,m} D(w))^T (K_{WW} \odot K_{VV} + I\sigma^2)^{-1} \mathbf{Y} \quad (48)$$

$$C_f = I_m k(w, w) - (\tilde{\Phi}_{V,m} D(w))^T (K_{WW} \odot K_{VV} + I\sigma^2)^{-1} ((\tilde{\Phi}_{V,m} D(w))^T) \quad (49)$$

$$\mathbf{m}_L = \mathbf{k}(z) (K_{ZZ} + I\eta^2)^{-1} \tilde{\Phi}_{V,m} \quad (50)$$

$$C_L = \Lambda_m (k(z, z) - \mathbf{k}(z)^T (K_{ZZ} + I\eta^2)^{-1} \mathbf{k}(z)) \quad (51)$$

and $[\tilde{\Phi}_{V,m}]_{l,j} = \tilde{\phi}_l(V_j)$, $[\Lambda_m]_{i,j} = \delta(i=j)\lambda_j$.

One can approximate any posterior quantity of interest by sampling from this model. Under some regularity conditions, the posterior moments of γ_m converge to the true posterior moments of γ at the rate of decay of $\sum_{j>m} \lambda_j$ wrt m . In practice, to recover the features and eigenvalues one can use an eigendecomposition of the gram matrix. Specifically, since $(\lambda_i, \phi_i)_{i \in \mathbb{N}}$ are the solutions to

$$\int_{\mathcal{V}} k(v, v') \phi_i(v') d\mu(v') = \lambda_i \phi_i(v) \quad (52)$$

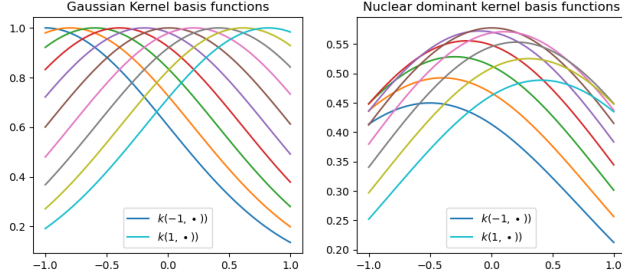


Figure 6: Basis functions for (LHS) Gaussian kernel $k(x, x') = \exp(-(x - x')^2)$ and (RHS) nuclear dominant kernel $r(x, x') = \int k(x, t)k(x', t)\mathcal{N}(dt|0, 1)$. The nuclear dominant kernel is nonstationary, which manifests in the basis function modes being biased towards zero, and the scales decaying away from zero.

one can approximate this using samples from the integrating measure μ :

$$\frac{1}{S} \sum_{s=1}^T k(v, \tilde{V}_s) \phi_i(\tilde{V}_s) \approx \lambda_i \phi_i(v) : (\tilde{V}_s)_{s=1}^S \sim \mu \quad (53)$$

Using this approach, if $\hat{K}_{V,V}$ is the $S \times S$ matrix with (s, t) entry $k(\tilde{V}_s, \tilde{V}_t)$, its eigenvectors $(\mathbf{u}_i)_{i=1}^n$ approximate $(\phi_i(\tilde{\mathbf{V}}))_{i=1}^n$ and its eigenvalues approximate $(\lambda_i)_{i=1}^n$. These can then be used with Eq. (53) to recover the features at the training points $(\phi_j(V_i))_{j=1}^m$ each $i \in \{1, \dots, n\}$. This introduces an additional approximation error of roughly $\mathcal{O}(T^{-\frac{1}{2}})$ (Shawe-Taylor et al., 2005), which for most stationary kernels (e.g. the Gaussian kernel) will dominate the approximation error induced by the truncation. In Appendix D we use this approach (with large $T = 10^4$) to assess whether IMPspec’s approach of KL-projecting the posterior into the space of Gaussians significantly affects calibration performance, and we find that it does not. We also implement another truncation approach where we replace the eigenfeatures ϕ_j with Random Fourier Features (Rahimi and Recht, 2007) ϕ_{ω_j} and the eigenvalues λ_j by the appropriate scaling m^{-1} . The advantage of this approach is it only introduces a single source of truncation error of size $\mathcal{O}(m^{-\frac{1}{2}})$.

A.5 Problems with Nuclear Dominant Kernels in BayesIMP

A.5.1 Nonstationarity and Oversmoothing

In the Ablation study in Section 6 we observe that BayesIMP’s posterior mean systematically underfits the true causal function $\mathbb{E}[Y|do(Z)]$. Here we demonstrate the root of the problem, which is the nonstationarity of the nuclear dominant kernel. Chau et al. (2021b) use the popular nuclear dominant construction

$$r(x, x') = \int_{\mathcal{X}} k(x, t)k(t, x')d\mu(t), \quad (54)$$

where they set $\mu = \mathcal{N}(0, \varsigma)$. The resulting kernel is non-stationary and the particular form of this nonstationarity can lead to pathological underfitting. Fig. 6 displays how the basis function $x \mapsto r(x, x')$ changes wrt x' , and how this compares to a standard Gaussian kernel. Smoothing the kernel with a Gaussian measure centered at zero biases the basis function modes towards zero, and results in the scales of the basis functions shrinking as we move x' away from zero. Since ς controls the degree of nonstationarity, we tried treating it as an additional hyperparameter in the Ablation study and optimising the marginal likelihood. Whilst this improved performance (see Appendix D), it did not fully resolve the underfitting problem.

A.5.2 Finite Dimensional Approximation and Variance Collapse

In the synthetic benchmark in Section 6, we observed that BayesIMP’s posterior variance collapsed out of distribution. Here we show that this occurs as a consequence of the finite dimensional GP approximations they use for tractability. Abstracting away from this particular experiment, the posterior variance of any causal effect $\gamma(w, z)$ of the form Eq. (4) for BayesIMP is given by

$$\text{Var}[\gamma(w, z)|\mathcal{X}^n] := \text{Var}\langle f, \psi(w) \otimes \mu(z) \rangle_{\mathcal{H}_w \otimes \mathcal{H}_V}, \quad f \sim \mathcal{GP}(\hat{m}_f, \hat{r}_f), \quad \mu(z) \sim \mathcal{GP}(\hat{m}_z, \hat{r}_z) \quad (55)$$

where now \hat{m}_f, \hat{r}_f are posterior functions trained on $\mathcal{D}_1 = (Y_i^{(1)}, W_i^{(1)}, V_i^{(1)})_{i=1}^n$ and \hat{m}_z, \hat{r}_z are posterior functions trained on $\mathcal{D}_2 = (W_i^{(2)}, V_i^{(2)}, Z_i^{(2)})_{i=1}^m$. The non-causal data fusion setting is recovered by $n = m$ and $(W_i^{(1)}, V_i^{(1)}, Z_i^{(1)}) = (W_i^{(2)}, V_i^{(2)}, Z_i^{(2)}) \forall i \in \{1, \dots, n\}$. To ensure tractability of the posterior variance when working with nuclear dominant kernels, Chau et al. (2021b) replace f and μ_z with the finite dimensional approximations

$$\hat{f} = \sum_{i=1}^{n+m} a_i k_{W,V}((W_i, V_i), \bullet), \quad \mathbf{a} \sim \mathcal{N}(\mathbf{m}_a, C_a) \quad (56)$$

$$\hat{\mu}(z) = \sum_{i=1}^{n+m} b_i(z) k_V(V_i, \bullet), \quad \mathbf{b}(z) \sim \mathcal{N}(\mathbf{m}_b(z), C_b(z)) \quad (57)$$

where now $(W_i, V_i)_{i=1}^{n+m}$ are all observations concatenated from $\mathcal{D}_1 \cup \mathcal{D}_2$ (in the single dataset case $m = 0$) and $\mathbf{m}_a = (K_{WW} \odot K_{VV})^{-1} \hat{\mathbf{m}}_f$, $C_a = (K_{WW} \odot K_{VV})^{-1} \hat{R}_f (K_{WW} \odot K_{VV})^{-1}$, $\mathbf{m}_b(z) = K_{VV}^{-1} \hat{\mathbf{m}}_z$, $C_b(z) = K_{VV}^{-1} \hat{R}_z K_{VV}^{-1}$. Here $\hat{\mathbf{m}}_f, \hat{\mathbf{m}}_z, \hat{R}_f, \hat{R}_z$ are the posterior means and covariances of the true $f, \mu(z)$ evaluated on $(W_i, V_i)_{i=1}^{n+m}$. With these approximations, Eq. (55) is then estimated as

$$\hat{\mathbb{V}}ar\langle f, \psi(w) \otimes \mu(z) \rangle_{\mathcal{H}_W \otimes \mathcal{H}_V} = \mathbb{V}ar[\mathbf{a}^T D(w) K_{VV} \mathbf{b}(z)] \quad (58)$$

$$= \mathbf{m}_a^T D(w) K_{VV} C_b(z) K_{VV} D(w) \mathbf{m}_a + \mathbf{m}_b(z)^T D(w) K_{VV} C_a K_{VV} D(w) \mathbf{m}_b(z) + Tr[C_a D(w) K_{VV} C_b(z) K_{VV} D(w)] \quad (59)$$

where $D(w) = \text{diag}(k_W(w, W_1), \dots, k_W(w, W_{n+m}))$. For any universal, stationary kernel k_W (e.g. Gaussian, Cauchy, Matérn, Gamma-exponential), $D(w) \rightarrow 0$ as $w \rightarrow \pm\infty$, which implies $\hat{\mathbb{V}}ar\langle f, \psi(w) \otimes \mu(z) \rangle_{\mathcal{H}_W \otimes \mathcal{H}_V} \rightarrow 0$ as well. Therefore, as w moves out of distribution, we will see the posterior variance collapse to zero. This behaviour can be avoided for certain causal estimands in the causal data fusion setting where $W = \emptyset$. However, for many standard situations of interest (both in the single dataset and causal data fusion setting) $W \neq \emptyset$ and so this pathology will occur.

B Assumptions and Auxilliary Results

B.1 Assumptions in Technical Results

Assumption 1 (Topological assumptions). *Let \mathcal{X} be a topological space. We assume*

1. \mathcal{X} is a measurable space with Borel σ -algebra $\mathcal{B}(\mathcal{X})$.
2. \mathcal{X} is σ -compact

Assumption 2 (Kernel assumptions). *Let $k : \mathcal{X}^2 \rightarrow \mathbb{R}$ be a positive definite kernel. We assume*

1. k is Borel measurable
2. k is continuous and bounded

Assumption 3 (Mercer's theorem). *Let $\mathcal{T}_k : L_2(\mu) \rightarrow L_2(\mu)$, $\varphi \mapsto \int k(x, \bullet) \varphi(x) \mu(dx)$ with μ finite and non-degenerate. We assume*

1. \mathcal{T}_k has eigendecomposition $(\lambda_i, \phi_i)_{i \in I}$ with I countable.
2. $\sum_{i \in I} \lambda_i < \infty$.
3. $(\tilde{\phi}_i)_{i \in I} := (\lambda_i^{-\frac{1}{2}} \phi_i)_{i \in I}$ is an orthonormal basis (ONB) of the RKHS \mathcal{H}_k associated with k .
4. $k(x, x') = \sum_{i \in I} \tilde{\phi}_i(x) \tilde{\phi}_i(x')$ where the convergence is absolute and uniform on any compact $A \times B \subset \mathcal{X}^2$.
5. $\tilde{\phi}(x) \in \ell_2(I)$, $\forall x \in \mathcal{X}$.
6. $\lambda_i > 0$, $\forall i \in I$.

Remark 1. Conditions 1-5 hold in Assumption 3 under Assumption 1 and Assumption 2 (see Proposition 1 and Theorem 3 in Sun (2005)). Condition 6 also holds for many popular universal kernels k (e.g. Gaussian, Matérn, Rational quadratic, and Gamma exponential).

Remark 2. Without loss of generality we will take $I = \mathbb{N}$ in this work for concreteness. When working with multiple kernels k_1, k_2, \dots we will assume they share the same eigendecomposition for notational convenience.

B.2 Auxilliary Results

Lemma 1 (Tensor-product spectral RKHS representation). *Let $\mathcal{X}_1, \mathcal{X}_2$ satisfy Assumption 1 and $\mathcal{H}_1, \mathcal{H}_2$ be reproducing kernel Hilbert spaces associated with positive definite kernels $k_1 : \mathcal{X}_1^2 \rightarrow \mathbb{R}$, $k_2 : \mathcal{X}_2^2 \rightarrow \mathbb{R}$ that satisfy Assumption 2. Additionally, suppose $(\lambda_{1,i}, \phi_{1,i})_{i \in \mathbb{N}}$, $(\lambda_{2,i}, \phi_{2,i})_{i \in \mathbb{N}}$ are eigendecompositions of the operators $\mathcal{T}_1, \mathcal{T}_2 : L_2(\mu) \rightarrow L_2(\mu)$, $\mathcal{T}_i : \varphi \mapsto \int_{\mathcal{X}_i} k_i(\cdot, x)\varphi(x)d\mu(x)$ for $i = 1, 2$, that satisfy Assumption 3. Then, we have the equality*

$$\mathcal{H}_1 \otimes \mathcal{H}_2 = \left\{ \sum_{(i,j) \in \mathbb{N}^2} a_{ij} \lambda_{1,i}^{\frac{1}{2}} \lambda_{2,i}^{\frac{1}{2}} (\phi_{1,i} \otimes \phi_{2,i}) : \sum_{(i,j) \in \mathbb{N}^2} a_{i,j}^2 < \infty \right\} \quad (60)$$

is the RKHS of kernel $k_1 \otimes k_2$

Proof. By Proposition 1 and Theorem 3 in (Sun, 2005), the continuity and boundedness of k_1, k_2 and σ -compactness of $\mathcal{X}_1, \mathcal{X}_2$ implies that $(\lambda_{1,i}^{\frac{1}{2}} \phi_{1,i})_{i \in \mathbb{N}}$, $(\lambda_{2,i}^{\frac{1}{2}} \phi_{2,i})_{i \in \mathbb{N}}$ are ONBs of $\mathcal{H}_1, \mathcal{H}_2$ respectively. Therefore, $(\lambda_{1,i}^{\frac{1}{2}} \lambda_{2,j}^{\frac{1}{2}} (\phi_{1,i} \otimes \phi_{2,j}))_{(i,j) \in \mathbb{N}^2}$ is an ONB of $\mathcal{H}_1 \otimes \mathcal{H}_2$, which implies the result. \square

Proposition 1. *Let $X_1 \in \mathcal{X}_1, X_2 \in \mathcal{X}_2, X_3 \in \mathcal{X}_3$ be random variables, $\mathcal{X}_1, \mathcal{X}_2, \mathcal{X}_3$ satisfy Assumption 1 and $\mathcal{H}_1, \mathcal{H}_2, \mathcal{H}_3$ be reproducing kernel Hilbert spaces associated with positive definite kernels $k_1 : \mathcal{X}_1^2 \rightarrow \mathbb{R}$, $k_2 : \mathcal{X}_2^2 \rightarrow \mathbb{R}$, $k_3 : \mathcal{X}_3^2 \rightarrow \mathbb{R}$ that satisfy Assumption 2. Additionally, suppose $(\lambda_{1,i}, \phi_{1,i})_{i \in \mathbb{N}}$, $(\lambda_{2,i}, \phi_{2,i})_{i \in \mathbb{N}}$ and $(\lambda_{3,i}, \phi_{3,i})_{i \in \mathbb{N}}$ are eigendecompositions of the operators $\mathcal{T}_1, \mathcal{T}_2, \mathcal{T}_3 : L_2(\mu) \rightarrow L_2(\mu)$, $\mathcal{T}_i : \varphi \mapsto \int_{\mathcal{X}_i} k_i(\cdot, x)\varphi(x)d\mu(x)$ for $i = 1, 2, 3$, that satisfy Assumption 3. Then, for any $Y \in \mathbb{R}$ with $\mathbb{E}[Y^2] < \infty$ we have*

$$\mathbb{E}[Y|(X_1, X_2) = \bullet] \in \mathcal{H}_1 \otimes \mathcal{H}_2 \quad \Leftrightarrow \quad \mathbb{E}[Y|(X_1, X_2) = \bullet] \in \left\{ f = \sum_{(i,j) \in \mathbb{N}^2} a_{ij} (\tilde{\phi}_{1,i} \otimes \tilde{\phi}_{2,j}) : \sum_{(i,j) \in \mathbb{N}^2} a_{i,j}^2 < \infty \right\} \quad (61)$$

$$\mathbb{E}[k_2(X_2, \bullet)|X_3 = \bullet] \in HS(\mathcal{H}_3, \mathcal{H}_2) \quad \Leftrightarrow \quad \mathbb{E}[\phi_i(X_2)|X_3 = \bullet] \in \left\{ f = \sum_{j \in \mathbb{N}^2} a_{ij} \tilde{\phi}_{3,j} : \sum_{j \in \mathbb{N}} a_{i,j}^2 < \infty \right\} \quad \forall i \in \mathbb{N} \quad (62)$$

Proof. The first equivalence Eq. (61) is immediately implied by Lemma 1. For the second equivalence Eq. (62) we show ‘ \Leftarrow ’ first. To start, note that the RHS of Eq. (62) implies that there exists $(a_{ij})_{(i,j) \in \mathbb{N}^2} \in \mathbb{R}^\infty \times \ell_2(\mathbb{N})$ such that

$$\mathbb{E}[\phi_i(X_2)|X_3] = \sum_{j \in \mathbb{N}^2} a_{i,j} \tilde{\phi}_{3,j}(X_3), \quad \forall i \in \mathbb{N} \quad (63)$$

This immediately implies that

$$\mathbb{E}[\tilde{\phi}_i(X_2)|X_3] = \lambda_{2,i}^{\frac{1}{2}} \sum_{j \in \mathbb{N}^2} a_{i,j} \tilde{\phi}_{3,j}(X_3), \quad \forall i \in \mathbb{N} \quad (64)$$

Since $\sum_{j \in \mathbb{N}} a_{ij}^2 < \infty$ for every $i \in \mathbb{N}$, by Mercer’s theorem (Sun, 2005) the RHS can be expressed as

$$\mathbb{E}[\tilde{\phi}_i(X_2)|X_3] = \lambda_{2,i}^{\frac{1}{2}} \langle \hat{a}_i, k_3(X_3, \bullet) \rangle_{\mathcal{H}_3} \quad \forall i \in \mathbb{N} \quad (65)$$

where $\hat{a}_i \in \mathcal{H}_3 \forall i \in \mathbb{N}$. Since $k_2(X_2, \bullet) = \sum_{j \in \mathbb{N}} \tilde{\phi}_{2,j}(X_2) \tilde{\phi}_{2,j}$, using the above result for $\mathbb{E}[\tilde{\phi}_i(X_2)|X_3]$ we can

write

$$\mathbb{E}[k_2(X_2, \bullet)|X_3] = \mathbb{E}\left[\sum_{j \in \mathbb{N}} \tilde{\phi}_{2,j}(X_2) \tilde{\phi}_{2,j} \middle| X_3\right] \quad (66)$$

$$= \sum_{j \in \mathbb{N}} \mathbb{E}[\tilde{\phi}_{2,j}(X_2)|X_3] \tilde{\phi}_{2,j} \quad (67)$$

$$= \sum_{j \in \mathbb{N}} \lambda_{2,j}^{\frac{1}{2}} \langle \hat{a}_j, k_3(X_3, \bullet) \rangle_{\mathcal{H}_3} \tilde{\phi}_{2,j} \quad (68)$$

Where the expectation can be exchanged with the summation using the Dominated Convergence Theorem (DCT). In particular, recall that a random element H in a Hilbert space \mathcal{H} has mean $\mathbb{E}[H] \in \mathcal{H}$ if $\mathbb{E}\langle h, H \rangle_{\mathcal{H}} = \langle h, \mathbb{E}[H] \rangle_{\mathcal{H}}$ for any $h \in \mathcal{H}$. In our situation it therefore suffices to show that

$$\mathbb{E}\left[\sum_{j \in \mathbb{N}} \tilde{\phi}_{2,j}(X_2) \langle h, \tilde{\phi}_{2,j} \rangle_{\mathcal{H}_2} \middle| X_3\right] = \sum_{j \in \mathbb{N}} \mathbb{E}\left[\tilde{\phi}_{2,j}(X_2)|X_3\right] \langle h, \tilde{\phi}_{2,j} \rangle_{\mathcal{H}_2}, \quad \forall h \in \mathcal{H}_2 \quad (69)$$

By the Cauchy-Schwartz inequality, we have

$$\sum_{j \in \mathbb{N}} \tilde{\phi}_{2,j}(X_2) \langle h, \tilde{\phi}_{2,j} \rangle_{\mathcal{H}_2} \leq \|\tilde{\phi}_2(X_2)\|_{\ell_2} \left(\sum_{j \in \mathbb{N}} \langle h, \tilde{\phi}_{2,j} \rangle_{\mathcal{H}_2}^2 \right)^{\frac{1}{2}} \quad (70)$$

$$= k_2(X_2, X_2)^{\frac{1}{2}} \|h\|_{\mathcal{H}_2} \leq B \quad (71)$$

Where the last inequality uses the fact that k_2 is bounded. Therefore, by the DCT Eq. (69) holds, which in turn implies (68) holds.

Now, since each $\hat{a}_j \in \mathcal{H}_3$ it can be expressed as $\hat{a}_j = \sum_{i \in \mathbb{N}} \hat{b}_{i,j} \tilde{\phi}_{3,i}$ for some $(\hat{b}_{i,j})_{i \in \mathbb{N}} \in \ell_2(\mathbb{N})$. Substituting this into the above, gives

$$\mathbb{E}[k_2(X_2, \bullet)|X_3] = \sum_{j \in \mathbb{N}} \lambda_{2,j}^{\frac{1}{2}} \left\langle \sum_{i \in \mathbb{N}} \hat{b}_{i,j} \tilde{\phi}_{3,i}, k_3(X_3, \bullet) \right\rangle_{\mathcal{H}_3} \tilde{\phi}_{2,j} \quad (72)$$

$$= \sum_{j \in \mathbb{N}} \sum_{i \in \mathbb{N}} \lambda_{2,j}^{\frac{1}{2}} \hat{b}_{i,j} \left\langle \tilde{\phi}_{3,i}, k_3(X_3, \bullet) \right\rangle_{\mathcal{H}_3} \tilde{\phi}_{2,j} \quad (73)$$

$$= \sum_{j \in \mathbb{N}} \sum_{i \in \mathbb{N}} \lambda_{2,j}^{\frac{1}{2}} \hat{b}_{i,j} (\tilde{\phi}_{2,j} \otimes \tilde{\phi}_{3,i}) [k_3(X_3, \bullet)] \quad (74)$$

$$= \sum_{j \in \mathbb{N}} \sum_{i \in \mathbb{N}} b_{i,j} (\tilde{\phi}_{2,j} \otimes \tilde{\phi}_{3,i}) [k_3(X_3, \bullet)] \quad (75)$$

where $b_{i,j} := \lambda_{2,j}^{\frac{1}{2}} \hat{b}_{i,j}$. Therefore, we have

$$\mathbb{E}[k_2(X_2, \bullet)|X_3 = \bullet] = \underbrace{\sum_{j \in \mathbb{N}} \sum_{i \in \mathbb{N}} b_{i,j} (\tilde{\phi}_{2,j} \otimes \tilde{\phi}_{3,i})}_{:=\tilde{L}} = \underbrace{\sum_{(i,j) \in \mathbb{N}^2} b_{i,j} (\tilde{\phi}_{2,j} \otimes \tilde{\phi}_{3,i})}_{:=L} : \sum_{(i,j) \in \mathbb{N}^2} b_{i,j}^2 < \infty \quad (76)$$

Note, the last equality follows from the fact that $L = \tilde{L}$ in Hilbert-Schmidt norm due to the orthogonality of the series elements

$$\|L - \tilde{L}\|_{\text{HS}(\mathcal{H}_3, \mathcal{H}_2)} = \sum_{l \in \mathbb{N}} \left\| \sum_{(i,j) \in \mathbb{N}^2} b_{i,j} \tilde{\phi}_{2,j} \langle \tilde{\phi}_{3,i}, \tilde{\phi}_{3,l} \rangle_{\mathcal{H}_3} - \sum_{j \in \mathbb{N}} \sum_{i \in \mathbb{N}} b_{i,j} \tilde{\phi}_{2,j} \langle \tilde{\phi}_{3,i}, \tilde{\phi}_{3,l} \rangle_{\mathcal{H}_3} \right\|_{\mathcal{H}_2} \quad (77)$$

$$= \sum_{l \in \mathbb{N}} \left\| \sum_{j \in \mathbb{N}} b_{l,j} (\tilde{\phi}_{2,l} - \tilde{\phi}_{2,j}) \right\|_{\mathcal{H}_2} = 0 \quad (78)$$

As a result $\mathbb{E}[k_2(X_2, \bullet)|X_3 = \bullet] \in \text{HS}(\mathcal{H}_3, \mathcal{H}_2)$, which implies the first direction. The reverse direction holds by noting that every $\mathbb{E}[k_2(X_2, \bullet)|X_3 = \bullet] \in \text{HS}(\mathcal{H}_3, \mathcal{H}_2)$ has a representation of form Eq. (76) and following the same steps in reverse. \square

Proposition 2 (Spectral process GP equivalence). *Assume the model Eq. (12)-Eq. (14) in the main text and that (i) $\mathcal{X}, \mathcal{V}, \mathcal{Z}$ satisfy Assumption 1, (ii) k_V, k_W, k_Z satisfy Assumption 2 and Assumption 3 with eigendecomposition $(\lambda_i, \phi_i)_{i \in \mathbb{N}}$, and (iii) $Y \in \mathbb{R}, W \in \mathcal{W}, V \in \mathcal{V}, Z \in \mathcal{Z}$ are random variables with $\mathbb{E}[Y^2] < \infty$. Then,*

$$\mathbb{E}[Y|W = \bullet, V = \bullet] \sim \mathcal{GP}(0, k_W \otimes k_V) \quad (79)$$

$$\mathbb{E}[\phi_i(V)|Z = \bullet] \sim \mathcal{GP}(0, k_Z), \quad \forall i \in \mathbb{N} \quad (80)$$

Proof. We prove the result for Eq. (79) only, since the proof for Eq. (80) is identical (and moreover is already implied by the Karhunen-Loeve Theorem). For $(\mathbb{E}[Y|W = w, V = v] : (w, v) \in \mathcal{W} \times \mathcal{V})$ to be a centered Gaussian process with covariance function $k_W \otimes k_V$, we require that (i) $\mathbb{E}[Y|W = w, V = v]$ is Borel measurable for every $(w, v) \in \mathcal{W} \times \mathcal{V}$ and (ii) any finite subcollection of $(\mathbb{E}[Y|W = w, V = v] : (w, v) \in \mathcal{W} \times \mathcal{V})$ is Gaussian with the required moments, since these conditions define a Gaussian process (Le Gall, 2016). For (i), note first that $\mathbb{E}[Y|W = w, V = v]$ can be expressed as the double sum

$$\mathbb{E}[Y|W = w, V = v] = \sum_{(i,j) \in \mathbb{N}^2} \tilde{Z}_{i,j}(w, v) \quad (81)$$

where summands are independent normal variables $\tilde{Z}_{i,j}(w, v) \sim \mathcal{N}(0, \phi_i(w)^2 \phi_j(v)^2 \lambda_i \lambda_j)$. By Kolmogorov's two series criterion for multi-series (see Corollary 2 in Klesov (1996)), since $\sum_{(i,j) \in \mathbb{N}^2} \phi_i(w)^2 \phi_j(v)^2 \lambda_i \lambda_j = k(w, w)k(v, v) < \infty$, the series $\sum_{(i,j) \in \mathbb{N}^2} \tilde{Z}_{i,j}(w, v)$ converges for all $\omega \notin N \subseteq \Omega : \mathbb{P}(N) = 0$ (where Ω is the sample space). Now, for each $(w, v) \in \mathcal{W} \times \mathcal{V}$ and $n \in \mathbb{N}$, define the random variable $S_n(w, v)$ as

$$S_n(w, v)(\omega) := \begin{cases} \sum_{i,j=1}^n \tilde{Z}_{i,j}(w, v)(\omega) & : \omega \notin N \\ 0 & : \omega \in N \end{cases} \quad (82)$$

Clearly each $S_n(w, v)$ is Borel measurable and moreover $S(w, v) := \lim_{n \rightarrow \infty} S_n(w, v)$ exists for all $\omega \in \Omega$. Since the pointwise limit of measurable maps is measurable under our topological assumptions, $S(w, v)$ is measurable. Moreover, since $\mathbb{E}[Y|W = w, V = v] =_{a.s.} S(w, v)$, then $\mathbb{E}[Y|W = w, V = v] : \Omega \rightarrow \mathbb{R}$ is also Borel measurable. For (ii), it suffices to show that the finite dimensional marginals of S agree with those of $\mathcal{GP}(0, k_W \otimes k_V)$. To that end fix any $m \in \mathbb{N}$ and $\{(w_1, v_1), \dots, (w_m, v_m)\} \subset \mathcal{W} \times \mathcal{V}$. Note that $\mathbf{S}_n := (S_n(w_1, v_1), \dots, S_n(w_m, v_m)) \sim \mathcal{N}(\mathbf{0}, C_n)$ by definition, where $C_n = \sum_{i,j} C_{i,j}$ and $[C_{i,j}]_{s,t} = \phi_i(w_s) \phi_j(v_t)$ for every $s, t \in [m]$. Now, let $\psi_n : \mathbb{R}^k \rightarrow \mathbb{C}$ be the characteristic function of \mathbf{S}_n . By Levy's continuity theorem (Kallenberg, 1997), if $\psi_n(\mathbf{t}) \rightarrow \psi(\mathbf{t})$ for every $\mathbf{t} \in \mathbb{R}^k$ and ψ is the characteristic function of $\mathcal{N}(\mathbf{0}, C)$, then $\mathbf{S}_n \rightarrow_d \mathcal{N}(\mathbf{0}, C)$. This is straightforward to see since

$$\lim_{n \rightarrow \infty} \psi_n(\mathbf{t}) = \lim_{n \rightarrow \infty} \exp\left(-\frac{1}{2} \mathbf{t}^T C_n \mathbf{t}\right) = \exp\left(-\frac{1}{2} \mathbf{t}^T C \mathbf{t}\right), \quad \forall \mathbf{t} \in \mathbb{R}^k \quad (83)$$

where $C := \lim_{n \rightarrow \infty} C_n = K_{WW} \odot K_{VV}$ and $[K_{WW}]_{s,t} = k(w_s, w_t) = \sum_{i \in \mathbb{N}} \tilde{\phi}_i(w_s) \tilde{\phi}_i(w_t)$, $[K_{VV}]_{s,t} = k(v_s, v_t) = \sum_{i \in \mathbb{N}} \tilde{\phi}_i(v_s) \tilde{\phi}_i(v_t)$ by Mercer's Theorem. Since $\mathbf{S}_n \rightarrow_d \mathbf{S}$ and the choice of m and $\{(w_1, v_1), \dots, (w_m, v_m)\}$ was arbitrary, we are done. \square

Proposition 3 (Gaussian process posteriors for spectral processes). *Assume the model Eq. (12)-Eq. (14) and Eq. (19)- Eq. (20) in the main text and that (i) $\mathcal{X}, \mathcal{V}, \mathcal{Z}$ satisfy Assumption 1, (ii) k_V, k_W, k_Z satisfy Assumption 2 and Assumption 3 with eigendecomposition $(\lambda_i, \phi_i)_{i \in \mathbb{N}}$, and (iii) $\mathcal{X}^n = \{Y_i, W_i, V_i, Z_i\}_{i=1}^n$ is a dataset of i.i.d. tuples (Y_i, W_i, V_i, Z_i) , where $Y_i \in \mathbb{R}, W_i \in \mathcal{W}, V_i \in \mathcal{V}, Z_i \in \mathcal{Z}$ and $\mathbb{E}[Y_i^2]$ for every $i = \{1, \dots, n\}$. Then, we have that*

$$\mathbb{E}[Y|W = \bullet, V = \bullet] \sim \mathcal{GP}(\hat{m}, \hat{k}) \quad (84)$$

$$\mathbb{E}[\tilde{\phi}_i(V)|Z = \bullet] \sim \mathcal{GP}(\hat{m}_i, \hat{k}_i), \quad \forall i \in \mathbb{N} \quad (85)$$

where

$$\hat{m}(w, v) := \mathbf{k}_{W,V}(w, v)^T (K_{WW} \odot K_{VV} + \sigma^2 I)^{-1} \mathbf{Y} \quad (86)$$

$$\hat{k}((w, v), (w', v')) := k_{w,v}((w, v), (w', v')) - \mathbf{k}_{W,V}(w, v)^T (K_{WW} \odot K_{VV} + \sigma^2 I)^{-1} \mathbf{k}_{W,V}(w, v) \quad (87)$$

$$\hat{m}_i(z) := \mathbf{k}_Z(z)^T (K_{ZZ} + \eta^2 I)^{-1} \tilde{\Phi}_{V,i} \quad (88)$$

$$\hat{k}_i(z, z') := \lambda_i (k_Z(z, z') - \mathbf{k}_Z(z)^T (K_{ZZ} + \eta^2 I)^{-1} \mathbf{k}_Z(z)) \quad (89)$$

Proof. The proof proceeds using similar steps for the result for the priors in Proposition 2. We again prove the result only for $\mathbb{E}[Y|W = \bullet, V = \bullet]$, since the proof is identical for $\mathbb{E}[\phi_i(V)|Z = \bullet]$ and follows analogously. As in Proposition 2 we show that (i) $\mathbb{E}[Y|W = w, V = v]$ is Borel measurable for every $(w, v) \in \mathcal{W} \times \mathcal{V}$ and (ii) any finite subcollection of $(\mathbb{E}[Y|W = w, V = v] : (w, v) \in \mathcal{W} \times \mathcal{V})$ is Gaussian with the required moments.

From Theorem 2, we know that

$$\tilde{f}|\mathcal{X}^n \sim \mathcal{N}(\mu_{\tilde{f}}, \Sigma_{\tilde{f}}) \quad (90)$$

$$\mu_{\tilde{f}} = \Lambda^{\frac{1}{2}} \tilde{\Phi}_{W,V}^* (K_{WW} \odot K_{VV} + I\sigma^2)^{-1} \mathbf{Y} \quad (91)$$

$$\Sigma_{\tilde{f}} = \Lambda - \Lambda^{\frac{1}{2}} \tilde{\Phi}_{W,V}^* (K_{WW} \odot K_{VV} + I\sigma^2)^{-1} \tilde{\Phi}_{W,V} \Lambda^{\frac{1}{2}} \quad (92)$$

where recall $\tilde{f} := (\tilde{f}_{i,j})_{(i,j) \in \mathbb{N}^2} = (\lambda_i^{\frac{1}{2}} \lambda_j^{\frac{1}{2}} f_{i,j})_{(i,j) \in \mathbb{N}^2}$, $\Lambda : (h_{i,j})_{(i,j) \in \mathbb{N}^2} \mapsto (\lambda_i \lambda_j h_{i,j})_{(i,j) \in \mathbb{N}^2}$, $\Lambda^{\frac{1}{2}} : (h_{i,j})_{(i,j) \in \mathbb{N}^2} \mapsto (\lambda_i^{\frac{1}{2}} \lambda_j^{\frac{1}{2}} h_{i,j})_{(i,j) \in \mathbb{N}^2}$ for any $(h_{i,j})_{(i,j) \in \mathbb{N}^2} \in \ell_2(\mathbb{N}^2)$, and $\tilde{\Phi}_{W,V} = [\tilde{\phi}(W_1) \otimes \tilde{\phi}(V_1), \dots, \tilde{\phi}(W_n) \otimes \tilde{\phi}(V_n)] \in \ell_2(\mathbb{N}^2)^n$. Now, recall from the proof of Proposition 2 that $\sum_{(i,j) \in \mathbb{N}^2} \tilde{f}_{i,j} \phi_i(w) \phi_j(v)$ converges for all $\omega \notin N \subseteq \Omega : \mathbb{P}(N) = 0$. Since Theorem 2 is an application of Theorem 1, we also know the posterior distribution $\mathbb{P}_{\tilde{f}|\mathcal{X}^n}$ is equivalent to the prior $\mathbb{P}_{\tilde{f}}$. This means that $\mathbb{P}(N|\mathcal{X}^n) = 0$ as well.

Now, for each $(w, v) \in \mathcal{W} \times \mathcal{V}$ and $n \in \mathbb{N}$, define the random variable $S_m(w, v)$ as

$$S_m(w, v)(\omega) := \begin{cases} \sum_{i,j=1}^m \tilde{f}_{i,j}(\omega) \phi_i(w) \phi_j(v) & : \omega \notin N \\ 0 & : \omega \in N \end{cases} \quad (93)$$

Clearly each $S_m(w, v)$ is Borel measurable and moreover $S(w, v) := \lim_{m \rightarrow \infty} S_m(w, v)$ exists for all $\omega \in \Omega$. Since the pointwise limit of measurable maps is measurable under our topological assumptions, $S(w, v)$ is measurable. Moreover, since $\mathbb{E}[Y|W = w, V = v] =_{a.s.} S(w, v)$, then $\mathbb{E}[Y|W = w, V = v] : \Omega \rightarrow \mathbb{R}$ is also Borel measurable.

For (ii), it suffices to show that the finite dimensional marginals of $S|\mathcal{X}^n$ agree with those of $\mathcal{GP}(\hat{m}, \hat{k})$, since $\mathbb{E}[Y|W = w, V = v] = S(w, v)$ $\mathbb{P}_{\tilde{f}|\mathcal{X}^n}$ -a.e. also. To that end, fix any $p \in \mathbb{N}$ and $\{(w_1, v_1), \dots, (w_p, v_p)\} \subset \mathcal{W} \times \mathcal{V}$. Using the form of the posterior on $\tilde{f}|\mathcal{X}^n$, we have that $\mathcal{S}_n|\mathcal{X}^n := (S_m(w_1, v_1), \dots, S_m(w_p, v_p))|\mathcal{X}^n \sim \mathcal{N}(\mathbf{m}_m, \mathbf{C}_m)$, where by Mercers' Theorem (Sun, 2005)

$$[\mathbf{m}_m]_t = \sum_{j=1}^m \sum_{l=1}^m \phi_j(w_t) \phi_l(v_t) \lambda_j^{\frac{1}{2}} \lambda_l^{\frac{1}{2}} \left(\sum_{i=1}^n \alpha_i \phi_j(w_i) \phi_l(v_i) \right) \xrightarrow{m \rightarrow \infty} \sum_{i=1}^n k_{W,V}((w_t, v_t), (w_i, v_i)) \alpha_i = \hat{m}(w_t, v_t) \quad (94)$$

$$\begin{aligned} [\mathbf{C}_m]_{t,s} &= \sum_{j=1}^m \sum_{l=1}^m \phi_j(w_t) \phi_l(v_t) \lambda_j^{\frac{1}{2}} \lambda_l^{\frac{1}{2}} \phi_j(w_s) \phi_l(v_s) \\ &\quad - \sum_{i,i'=1}^n A_{i,i'} \left(\sum_{j=1}^m \sum_{l=1}^m \phi_j(w_t) \phi_l(v_t) \lambda_j^{\frac{1}{2}} \lambda_l^{\frac{1}{2}} \phi_j(w_i) \phi_l(v_i) \right) \left(\sum_{j=1}^m \sum_{l=1}^m \phi_j(w_s) \phi_l(v_s) \lambda_j^{\frac{1}{2}} \lambda_l^{\frac{1}{2}} \phi_j(w_{i'}) \phi_l(v_{i'}) \right) \\ &\xrightarrow{m \rightarrow \infty} \sum_{i,i'=1}^n k_{W,V}((w_t, v_t), (w_i, v_i)) A_{i,i'} k_{W,V}((w_s, v_s), (w_{i'}, v_{i'})) = \hat{k}((w_t, v_t), (w_s, v_s)) \end{aligned} \quad (95)$$

Note $\alpha_i = [(K_{WW} \odot K_{VV} + I\sigma^2)^{-1} \mathbf{Y}]_i$ and $A_{i,i'} = [(K_{WW} \odot K_{VV} + I\sigma^2)^{-1}]_{i,i'}$ in the above equations.

Therefore, by Levy's continuity theorem (Kallenberg, 1997), since $\mathcal{S}_m \rightarrow_d \mathcal{S}$ and the choice of p and $\{(w_1, v_1), \dots, (w_p, v_p)\}$ was arbitrary, we are done. \square

Remark 3. The result holds analogously for the causal data fusion setting, and for the case where $W = \emptyset$

C Proofs of Main Results and Extensions of Results

C.1 Proof of Theorem 1

Theorem 1. Let \mathcal{H}_W be a real, separable Hilbert space with Borel σ -algebra $\mathcal{B}(\mathcal{H}_W)$. Let $W \sim \mathcal{N}(0, \Lambda)$ and $\xi \sim \mathcal{N}(0, \Omega)$ be Gaussian elements in \mathcal{H}_W and \mathbb{R}^n respectively, with trace-class, positive, and injective covariance operators. Let $L : \mathcal{H}_W \rightarrow \mathbb{R}^n$ be a $\mathcal{N}(0, \Lambda)$ -mlt. Then the posterior distribution of $W | (Y := LW + \xi)$ is $\mathcal{N}(BY, S)$. The posterior is proper and equivalent to $\mathcal{N}(0, \Lambda)$. Additionally, $B : \mathbb{R}^n \rightarrow \mathcal{H}_W$ is continuous and linear, $S : \mathcal{H}_W \rightarrow \mathcal{H}_W$ is positive and trace class and

$$B = (L\Lambda)^* \left((L\Lambda^{\frac{1}{2}})(L\Lambda^{\frac{1}{2}})^* + \Omega \right)^{-1} \quad (17)$$

$$S = \Lambda - (L\Lambda)^* \left((L\Lambda^{\frac{1}{2}})(L\Lambda^{\frac{1}{2}})^* + \Omega \right)^{-1} (L\Lambda) \quad (18)$$

Proof. Since L is $\mathcal{N}(0, \Lambda)$ measurable, there exists a sequence of continuous linear transformations $(L_m)_{m \geq 1}$ such that $Lh = L_m h$ for $\mathcal{N}(0, \Lambda)$ -almost all $h \in \mathcal{H}_W$. Define $Y_m = L_m W + \xi$. It is well known (e.g. see Proposition 3.1 in [Knapik et al. \(2011\)](#) and Theorem 6.3.5 in [Grenander \(1963\)](#)) that the joint distribution on $(Y_m, W) \in \mathbb{R}^n \times \mathcal{H}_W$ endowed with the product σ -algebra $\mathcal{B}(\mathcal{H}_W \times \mathbb{R}^n)$, is:

$$(Y_m, W) \sim \mathcal{N} \left(0, \begin{bmatrix} C_{m,Y} & C_{m,YW} \\ C_{m,YW}^* & C_W \end{bmatrix} \right) \quad (96)$$

Where $C_{m,Y} : \mathbb{R}^n \rightarrow \mathbb{R}^n, g \mapsto (L_m \Lambda^{\frac{1}{2}})(L_m \Lambda^{\frac{1}{2}})^*[g] + \Omega[g]$ is the covariance operator on Y , $C_{m,YW} : \mathcal{H}_W \rightarrow \mathbb{R}^n, h \mapsto (L_m \Lambda)[h]$ is the cross-covariance operator, $C_W : \mathcal{H}_W \rightarrow \mathcal{H}_W, h \mapsto \Lambda[h]$ is the covariance operator on W . Following ([Baker, 1973](#)), if we endow $\mathbb{R}^n \times \mathcal{H}_W$ with its direct sum inner product $\langle (g_1, h_1), (g_2, h_2) \rangle_{\mathbb{R}^n \times \mathcal{H}_W} = \langle g_1, g_2 \rangle_{\mathbb{R}^n} + \langle h_1, h_2 \rangle_{\mathcal{H}_W}$ we can say that (Y_m, W) is distributed according to the (joint) Gaussian measure $\mu_{m,YW} = \mathcal{N}(0, C_m)$ on the direct sum space $\mathbb{R}^n \oplus \mathcal{H}_W$, where:

$$C_m : \mathbb{R}^n \oplus \mathcal{H}_W \rightarrow \mathbb{R}^n \oplus \mathcal{H}_W, \quad (h, g) \mapsto (C_{m,Y}[g] + C_{m,YW}[h], C_{m,YW}^*[g] + C_W[h]) \quad (97)$$

Now, by Theorem 6.3.6 in [Grenander \(1963\)](#), if:

- (i) $\langle (g, h), C[(g, h)] \rangle_{\mathbb{R}^n \oplus \mathcal{H}_W} = \lim_{m \rightarrow \infty} \langle (g, h), C_m[(g, h)] \rangle_{\mathbb{R}^n \oplus \mathcal{H}_W}, \quad \forall (g, h) \in \mathbb{R}^n \oplus \mathcal{H}_W$
- (ii) C is an S-operator (i.e. linear, self-adjoint, positive, trace class)

then $(Y_m, W) \xrightarrow{d} \mathcal{N}(0, C)$. For (i), since the inner product with C_m is

$$\langle (g, h), C_m[(g, h)] \rangle_{\mathbb{R}^n \oplus \mathcal{H}_W} = \langle g, C_{m,Y}[g] + C_{m,YW}[h] \rangle_{\mathbb{R}^n} + \langle h, C_{m,YW}^*[g] + C_W[h] \rangle_{\mathcal{H}_W} \quad (98)$$

we require that the following holds $\forall (g, h) \in \mathbb{R}^n \oplus \mathcal{H}_W$:

$$\langle g, (L_m \Lambda^{\frac{1}{2}})(L_m \Lambda^{\frac{1}{2}})^*[g] \rangle_{\mathbb{R}^n} \rightarrow \langle g, (L\Lambda^{\frac{1}{2}})(L\Lambda^{\frac{1}{2}})^*[g] \rangle_{\mathbb{R}^n} \quad (99)$$

$$\langle g, (L_m \Lambda^{\frac{1}{2}})[h] \rangle_{\mathbb{R}^n} \rightarrow \langle g, (L\Lambda^{\frac{1}{2}})[h] \rangle_{\mathbb{R}^n} \quad (100)$$

It is therefore sufficient to show that $L_m \Lambda^{\frac{1}{2}}[h] \rightarrow L\Lambda^{\frac{1}{2}}[h], \forall h \in \mathcal{H}_W$ ⁴. We show this following the same arguments as in ([Knapik et al., 2011](#)). In particular, let $V = \{h \in \mathcal{H}_W : L_m h \rightarrow Lh\}$. Let $h_0 \notin V$. Then $V_1 := V + h_0$ and V are disjoint, measurable, affine subspaces of \mathcal{H}_W , where $\mathcal{N}(0, \Lambda)(V) = 1$. Suppose

⁴Suppose $L_m \Lambda^{\frac{1}{2}} \rightarrow L\Lambda^{\frac{1}{2}}$ weakly. Since $L_m \Lambda^{\frac{1}{2}}, L\Lambda^{\frac{1}{2}}$ are finite-rank, we have the representation $L_m \Lambda^{\frac{1}{2}} = \sum_{i=1}^n b_{i,m} \langle \cdot, f_i \rangle_{\mathcal{H}_W} e_i$, $L\Lambda^{\frac{1}{2}} = \sum_{i=1}^n b_i \langle \cdot, f_i \rangle_{\mathcal{H}_W} e_i$. Weak convergence implies strong convergence as: $b_{i,m} \rightarrow b_i, \forall i \in [N] \implies \sup_i (|b_{i,m} - b_i|) \rightarrow 0$. By the properties of limits, $\sup_i (|b_{i,m} - b_i|) \rightarrow 0 \implies \sup_i (|b_{i,m}^2 - b_i^2|) \rightarrow 0$. Since $(L_m \Lambda^{\frac{1}{2}})(L_m \Lambda^{\frac{1}{2}})^* = \sum_{i=1}^n b_{i,m}^2 \langle \cdot, e_i \rangle_{\mathbb{R}^n} e_i$, and $(L\Lambda^{\frac{1}{2}})(L\Lambda^{\frac{1}{2}})^* = \sum_{i=1}^n b_i^2 \langle \cdot, e_i \rangle_{\mathbb{R}^n} e_i$ then $(L_m \Lambda^{\frac{1}{2}})(L_m \Lambda^{\frac{1}{2}})^* \rightarrow (L\Lambda^{\frac{1}{2}})(L\Lambda^{\frac{1}{2}})^*$ strongly.

h_0 is in the range of $\Lambda^{\frac{1}{2}}$, then $\mathcal{N}(0, \Lambda) \gg \mathcal{N}(h_0, \Lambda)$ and $\mathcal{N}(0, \Lambda) \ll \mathcal{N}(h_0, \Lambda)$. Thus $\mathcal{N}(0, \Lambda)(V) = 1 \implies \mathcal{N}(g, \Lambda)(V_1) = 1 \implies \mathcal{N}(0, \Lambda)(V_1) > 0$ (Ryabov, 2008). However then V and V_1 must not be disjoint.

For (ii) linearity and self-adjointness is trivial. To show C is trace class, note that if $(e_i)_{i \in I}$ is a complete ONB in \mathcal{H}_W , and $(f_i)_{i \in J}$ is a complete ONB of \mathbb{R}^n , then $\{(e_i, 0)_{i \in I}\} \cup \{(0, f_i)_{i \in J}\}$ is a ONB of $\mathcal{H}_W \oplus \mathbb{R}^n$ (Baker, 1973). Since,

$$\text{Tr}[C] = \sum_{i \in I} \langle (e_i, 0), C(e_i, 0) \rangle_{\mathcal{H}_W \oplus \mathbb{R}^n} + \sum_{i \in J} \langle (0, f_i), C(0, f_i) \rangle_{\mathcal{H}_W \oplus \mathbb{R}^n} = \text{Tr}[C_Y] + \text{Tr}[C_W] \quad (101)$$

and both $\text{Tr}[C_W]$, $\text{Tr}[C_Y]$ are trace class by assumption, we are done. Lastly, for positiveness we show that C_m is positive for all $m \in \mathbb{N}$, since weak convergence of positive $C_m \rightarrow C$ implies positiveness of C ⁵. To see that C_m is positive, recall from Baker (1973) that the cross-covariance operator $C_{m, YW} = C_{m, Y}^{\frac{1}{2}} V_m C_W^{\frac{1}{2}}$. Where $V : \mathcal{H}_W \rightarrow \mathbb{R}^n$ is a bounded linear operator with $\|V_m\| \leq 1$. From this it follows that:

$$\langle (u, v), C_m(u, v) \rangle_{\mathcal{H}_W \oplus \mathbb{R}^n} = \langle C_W u, u \rangle_{\mathcal{H}_W} + \langle C_{m, Y} v, v \rangle_{\mathbb{R}^n} + 2 \langle C_{m, WY} v, u \rangle_{\mathcal{H}_W} \quad (102)$$

$$= \|C_W^{\frac{1}{2}} u\|_{\mathcal{H}_W}^2 + \|C_Y^{\frac{1}{2}} v\|_{\mathbb{R}^n}^2 + 2 \langle V_m C_{m, Y}^{\frac{1}{2}} v, C_W^{\frac{1}{2}} u \rangle_{\mathcal{H}_W} \quad (103)$$

$$\geq \|C_W^{\frac{1}{2}} u\|_{\mathcal{H}_W}^2 + \|C_Y^{\frac{1}{2}} v\|_{\mathbb{R}^n}^2 - 2 \|C_{m, Y}^{\frac{1}{2}} v\|_{\mathbb{R}^n} \|C_W^{\frac{1}{2}} u\|_{\mathcal{H}_W} \quad (104)$$

$$= (\|C_W^{\frac{1}{2}} u\|_{\mathcal{H}_W} - \|C_{m, Y}^{\frac{1}{2}} v\|_{\mathbb{R}^n})^2 \geq 0 \quad (105)$$

Additionally, $C_Y = (L\Lambda^{\frac{1}{2}})(L\Lambda^{\frac{1}{2}})^* + \Omega$ is self-adjoint, finite-dimensional with full rank, and is strictly positive by strict positivity of Ω and positivity of $(L\Lambda^{\frac{1}{2}})(L\Lambda^{\frac{1}{2}})^*$, so is invertible. Since $(Y, W) =_{a.s.} \lim_{m \rightarrow \infty} (Y_m, W)$ by the definition of L_m and Y_m , this implies $(Y, W) =_d \mathcal{N}(0, C)$. From here, we can follow the same steps in Proposition 3.1 of Knapik et al. (2011) or use Theorem 3.1 in Steinwart (2024), to recover the form of the conditional posterior distribution $\mu_{W|Y}$ in the theorem. Properness of $C_{W|Y}$ is inferred by $0 \leq C_{W|Y} \leq \Lambda$, where Λ is trace class by assumption. For $\mu_{W|Y}$ to be equivalent to μ_W , we require the existence of some linear operator $U : \mathcal{H}_W \rightarrow \mathcal{H}_W$ with the following properties (Ryabov, 2008):

(i) $C_W^{\frac{1}{2}}(1 + U)C_W^{\frac{1}{2}} = C_{W|Y}$

(ii) U is Hilbert-Schmidt and symmetric

(iii) $I + U$ is invertible

For (i) we require $U = -(L\Lambda^{\frac{1}{2}})^* \left((L\Lambda^{\frac{1}{2}})(L\Lambda^{\frac{1}{2}})^* + \Omega \right)^{-1} (L\Lambda^{\frac{1}{2}})$. For (ii), since U is a product of finite rank operators it is therefore Hilbert-Schmidt. For (iii) it suffices to show that $\|T\| < 1$, where $T = -U$, as then $I - T$ is invertible⁶. Since $\dim(\mathbb{R}^n) = n$, the finite rank operator $B = L\Lambda^{\frac{1}{2}}$ has canonical representation $B[\cdot] = \sum_{i=1}^n \lambda_i e_i \langle f_i, \cdot \rangle_{\mathcal{H}_W}$, where $(e_i)_{i=1}^n, (f_i)_{i \in I}$ are c.o.n.b.'s of $\mathbb{R}^n, \mathcal{H}_W$ respectively, and $(\lambda_i) \in \mathbb{R}^n$. Similarly, $\Omega = \sum_{i=1}^N e_i s_i \langle e_i, \cdot \rangle_{\mathbb{R}^n}$, where $(s_i) \in (0, \infty)^n$. Thus, after some algebra is clear that:

$$T = B^*(BB^* + \Omega)^{-1}B = \sum_{i=1}^n t_i f_i \langle f_i, \cdot \rangle_{\mathcal{H}_W} : t_i = \frac{\lambda_i^2}{\lambda_i^2 + s_i} \in (0, 1) \quad (106)$$

T is a strict contraction since $\|Tx\| = \sum_{i=1}^n \langle f_i, x \rangle_{\mathcal{H}_x}^2 t_i^2 < \sum_{i=1}^n \langle f_i, x \rangle_{\mathcal{H}_x}^2 \leq \|x\|, \forall x \in \mathcal{H}_W$. This completes the proof. \square

C.2 Proof of Theorem 2

Theorem 2. Assume the model Eq. (12)-Eq. (14) and Eq. (19)-Eq. (20) in the main text and that (i) $\mathcal{X}, \mathcal{V}, \mathcal{Z}$ satisfy Assumption 1, (ii) k_V, k_W, k_Z satisfy Assumption 2 and Assumption 3 with eigendecomposition $(\lambda_i, \phi_i)_{i \in \mathbb{N}}$, and (iii) $\mathcal{X}^n = \{Y_i, W_i, V_i, Z_i\}_{i=1}^n$ is a dataset of i.i.d. tuples (Y_i, W_i, V_i, Z_i) , where $Y_i \in \mathbb{R}, W_i \in$

⁵Suppose by contradiction that for some $f \in \mathcal{H}_W \oplus \mathbb{R}^n, \langle f, Cf \rangle = -\epsilon, \epsilon > 0$. However, we know that for large enough $m: |\langle f, Cf \rangle - \langle f, C_m f \rangle| < \epsilon \implies \langle f, C_m f \rangle + \epsilon < \epsilon \implies \langle f, C_m f \rangle < 0$, which is a contradiction. Since (ϵ, f) were arbitrary, we must have $\langle f, Cf \rangle \geq 0, \forall f \in \mathcal{H}_W \oplus \mathbb{R}^n$.

⁶Write $T = -U, C = \sum_{n=0}^{\infty} B^n$. This converges everywhere since $\|T\| < 1$. Thus, $C(I - T) = \lim_{N \rightarrow \infty} (I - T^N) = I$.

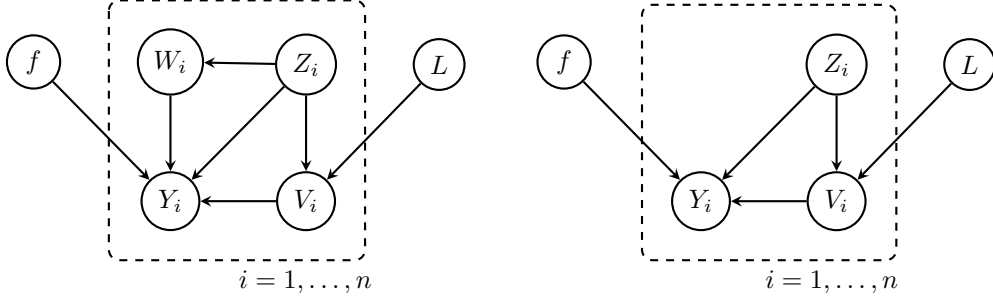


Figure 7: LHS: DAG showing one factorisation of (\mathcal{X}^n, f, L) when $W \neq \emptyset$. RHS: DAG showing one factorisation of (\mathcal{X}^n, f, L) when $W = \emptyset$. Note that not all edges represent causal directions.

$W, V_i \in \mathcal{W}, Z_i \in \mathcal{Z}$ and $\mathbb{E}[Y_i^2]$ for every $i = \{1, \dots, n\}$. Additionally, define $\tilde{\Phi}_{W,V} = [\tilde{\phi}(W_1) \otimes \tilde{\phi}(V_1), \dots, \tilde{\phi}(W_n) \otimes \tilde{\phi}(V_n)] \in \ell_2(\mathbb{N}^2)^n$, $\tilde{\Phi}_Z = [\tilde{\phi}(Z_1), \dots, \tilde{\phi}(Z_n)] \in \ell_2(\mathbb{N})^n$, where $\tilde{\phi}_i = \lambda_i^{\frac{1}{2}} \phi_i$ for each $i \in \mathbb{N}$ and $\Lambda : (h_{ij})_{(i,j) \in \mathbb{N}^2} \mapsto (\lambda_i \lambda_j h_{ij})_{(i,j) \in \mathbb{N}^2}$, $\Lambda^{\frac{1}{2}} : (h_{ij})_{(i,j) \in \mathbb{N}^2} \mapsto (\lambda_i^{\frac{1}{2}} \lambda_j^{\frac{1}{2}} h_{ij})_{(i,j) \in \mathbb{N}^2}$. Then, we have the following posteriors on $\tilde{f} := (\lambda_i^{\frac{1}{2}} \lambda_j^{\frac{1}{2}} f_{i,j})_{(i,j) \in \mathbb{N}^2}$ and $\tilde{L}_i := (\lambda_i^{\frac{1}{2}} \lambda_j^{\frac{1}{2}} L_{i,j})_{j \in \mathbb{N}}$ for each $i \in \mathbb{N}$,

$$\mathbb{P}_{\tilde{f}|\mathcal{X}^n} = \mathcal{N}(\mu_{\tilde{f}}, \Sigma_{\tilde{f}}) \quad (107)$$

$$\mathbb{P}_{\tilde{L}_i|\mathcal{X}^n} = \mathcal{N}(\mu_{\tilde{L}_i}, \lambda_i \Sigma_{\tilde{L}_i}) : i \in \mathbb{N} \quad (108)$$

$$\mu_{\tilde{f}} = (\tilde{\Phi}_{W,V} \Lambda^{\frac{1}{2}})^* \left(\tilde{\Phi}_{W,V} \tilde{\Phi}_{W,V}^* + I\sigma^2 \right)^{-1} \mathbf{Y} \quad (109)$$

$$\Sigma_{\tilde{f}} = \Lambda - (\tilde{\Phi}_{W,V} \Lambda^{\frac{1}{2}})^* \left(\tilde{\Phi}_{W,V} \tilde{\Phi}_{W,V}^* + I\sigma^2 \right)^{-1} (\tilde{\Phi}_{W,V} \Lambda^{\frac{1}{2}}) \quad (110)$$

$$\mu_{\tilde{L}_i} = (\tilde{\Phi}_Z \Lambda^{\frac{1}{2}})^* \left(\tilde{\Phi}_Z \tilde{\Phi}_Z^* + I\eta^2 \right)^{-1} \tilde{\Phi}_{V,i} \quad (111)$$

$$\Sigma_{\tilde{L}_i} = \Lambda - (\tilde{\Phi}_Z \Lambda^{\frac{1}{2}})^* \left(\tilde{\Phi}_Z \tilde{\Phi}_Z^* + I\eta^2 \right)^{-1} (\tilde{\Phi}_Z \Lambda^{\frac{1}{2}}) \quad (112)$$

Proof. We first verify that $f \perp\!\!\!\perp L | \mathcal{X}^n$ and that $(L_{i,j})_{j \in \mathbb{N}} \perp\!\!\!\perp (L_{k,j})_{j \in \mathbb{N}} | \mathcal{X}^n \forall i, k \in \mathbb{N}$ given our specified model Eq. (12)-Eq. (14), where $\mathcal{X}^n = \{Y_i, W_i, V_i, Z_i\}$ and we note that we may have $W_i \cap Z_i \neq \emptyset$. We show $f \perp\!\!\!\perp L | \mathcal{X}^n$ using the D-separation criteria (Geiger et al., 1990) on the mixed DAG that corresponds to a factorisation implied by this model⁷, which is displayed on the LHS of Fig. 7. Clearly, all paths between $f - L$ must either go through $Y_i - V_i$ or $Z_i - V_i$. Any path which goes through $Y_i - V_i$ is blocked by V_i and any path which goes through $Z_i - V_i$ is blocked by Z_i . Therefore, we conclude that $f \in L | \mathcal{X}^n$.

Now we derive the posterior on $\tilde{f} := (\lambda_i^{\frac{1}{2}} \lambda_j^{\frac{1}{2}} f_{i,j})_{(i,j) \in \mathbb{N}^2}$. We note the model Eq. (19) implies that

$$\mathbf{Y} = \mathbf{F} + \mathbf{U} \quad (113)$$

Where $\mathbf{U} \sim \mathcal{N}(0, I_n \sigma^2)$, $\mathbf{F} = L_\phi(\tilde{f}) := \sum_{(i,j) \in \mathbb{N}^2} \Phi_{i,j} \tilde{f}_{i,j}$ and $\Phi_{i,j} = [\phi_i(W_1) \phi_j(V_1), \dots, \phi_i(W_n) \phi_j(V_n)]^T \in \mathbb{R}^n$. We now claim that L_ϕ is a $\mathcal{N}(0, \Lambda)$ -mlt, where $\Lambda : (h_{ij})_{(i,j) \in \mathbb{N}^2} \mapsto (\lambda_i \lambda_j h_{ij})_{(i,j) \in \mathbb{N}^2}$. By definition, it suffices to construct a series $(L_m)_{m \in \mathbb{N}}$ of continuous linear transformations with $L_m : \ell_2(\mathbb{N}^2) \rightarrow \mathbb{R}^n$, such that

$$L_\phi(\tilde{f}) = \text{a.s.} \lim_{m \rightarrow \infty} L_m(\tilde{f}) \quad (114)$$

To that end, choose the continuous linear transformation $L_m : \tilde{f} \mapsto \sum_{i,j=1}^m \Phi_{i,j} \tilde{f}_{i,j}$ and note that $L_m(\tilde{f}) \sim \mathcal{N}(0, \sum_{i,j=1}^m \tilde{\Phi}_{i,j} \tilde{\Phi}_{i,j}^*)$, where $\tilde{\Phi}_{i,j} = [\tilde{\phi}_i(W_1) \tilde{\phi}_j(V_1), \dots, \tilde{\phi}_i(W_n) \tilde{\phi}_j(V_n)]^T \in \mathbb{R}^n$. Applying Levy's continuity theorem equivalently to the proof of Proposition 2, we have that $L_m(\tilde{f}) \rightarrow_d \mathcal{N}(0, K)$ as $m \rightarrow \infty$ iff $\lim_{m \rightarrow \infty} \sum_{i,j=1}^m \tilde{\Phi}_{i,j} \tilde{\Phi}_{i,j}^* = K$. By Mercer's Theorem (Steinwart and Christmann, 2008), $\lim_{m \rightarrow \infty} \sum_{i,j=1}^m \tilde{\Phi}_{i,j} \tilde{\Phi}_{i,j}^* = K_{WW} \odot K_{VV}$, where $[K_{WW} \odot K_{VV}]_{l,l'} = k(W_l, W_{l'}) k(V_l, V_{l'})$, $\forall l, l' \in \{1, \dots, n\}$. This means we indeed have $L_m(\tilde{f}) \rightarrow_d \mathcal{N}(0, K)$ as $m \rightarrow \infty$. By the two series criterion extended to double

⁷We emphasise that this is *not* necessarily a causal DAG, and just represents one factorisation of $\mathbb{P}_{Y,W,V,Z,f,L}$

series in Klesov (1996) Corollary 2, $L_m(\tilde{f})$ also converges almost surely, which implies Eq. (114). By an application of Theorem 1, we then get the posterior distribution

$$\tilde{f}|\mathcal{X}^n \sim \mathcal{N}(\mu_{\tilde{f}}, \Sigma_{\tilde{f}}) \quad (115)$$

$$\tilde{\mu}_n = \Lambda^{\frac{1}{2}} \tilde{\Phi}_{W,V}^* \left(\tilde{\Phi}_{W,V} \tilde{\Phi}_{W,V}^* + I\sigma^2 \right)^{-1} \mathbf{Y} \quad (116)$$

$$\tilde{\Sigma}_n = \Lambda - \Lambda^{\frac{1}{2}} \tilde{\Phi}_{W,V}^* \left(\tilde{\Phi}_{W,V} \tilde{\Phi}_{W,V}^* + I\sigma^2 \right)^{-1} \tilde{\Phi}_{W,V} \Lambda^{\frac{1}{2}} \quad (117)$$

Where $\Lambda^{\frac{1}{2}} : (h_{ij})_{(i,j) \in \mathbb{N}^2} \mapsto (\lambda_i^{\frac{1}{2}} \lambda_j^{\frac{1}{2}} h_{ij})_{(i,j) \in \mathbb{N}^2}$. The result for the posterior on $\tilde{L}_i|\mathcal{X}^n$ follows from applying exactly the same steps where now instead of $\mathbf{Y} = \mathbf{F} + \mathbf{U}$, we have $\tilde{\Phi}_{V,i} = \mathbf{G}_i + \boldsymbol{\xi}_i$, where $\tilde{\Phi}_{V,i} = [\tilde{\phi}_i(V_1), \dots, \tilde{\phi}_i(V_n)]^T$, $\mathbf{G}_i = \sum_{j \in \mathbb{N}} \Phi_{Z,j} \tilde{L}_{i,j}$, $\Phi_{Z,j} = [\phi_j(Z_1), \dots, \phi_j(Z_n)]^T$ and $\boldsymbol{\xi}_i \sim \mathcal{N}(0, \lambda_i \eta^2 I_n)$. \square

Corollary 1 (Theorem 2 for causal data fusion). *Assume the conditions in Theorem 2 hold but now $\mathcal{X}^n = \mathcal{D}_1 \cup \mathcal{D}_2$, where $\mathcal{D}_1 = \{Y_i^{(1)}, W_i^{(1)}, V_i^{(1)}\}_{i=1}^{m_1}$ and $\mathcal{D}_2 = \{V_i^{(2)}, Z_i^{(2)}\}_{i=1}^{m_2}$ are two independent datasets of i.i.d. observations and $n = m_1 + m_2$. Then, we have the posteriors.*

$$\mathbb{P}_{\tilde{f}|\mathcal{X}^n} = \mathbb{P}_{\tilde{f}|\mathcal{D}_1} = \mathcal{N}(\mu_{\tilde{f}}, \Sigma_{\tilde{f}}) \quad (118)$$

$$\mathbb{P}_{\tilde{L}_i|\mathcal{X}^n} = \mathbb{P}_{\tilde{L}_i|\mathcal{D}_2} = \mathcal{N}(\mu_{\tilde{L}_i}, \lambda_i \Sigma_{\tilde{L}_i}) : i \in \mathbb{N} \quad (119)$$

where

$$\mu_{\tilde{f}} = (\tilde{\Phi}_{W,V}^{(1)} \Lambda^{\frac{1}{2}})^* \left(\tilde{\Phi}_{W,V}^{(1)} \tilde{\Phi}_{W,V}^{(1)*} + I\sigma^2 \right)^{-1} \mathbf{Y}^{(1)} \quad (120)$$

$$\Sigma_{\tilde{f}} = \Lambda - (\tilde{\Phi}_{W,V}^{(1)} \Lambda^{\frac{1}{2}})^* \left(\tilde{\Phi}_{W,V}^{(1)} \tilde{\Phi}_{W,V}^{(1)*} + I\sigma^2 \right)^{-1} (\tilde{\Phi}_{W,V}^{(1)} \Lambda^{\frac{1}{2}}) \quad (121)$$

$$\mu_{\tilde{L}_i} = (\tilde{\Phi}_Z^{(2)} \Lambda^{\frac{1}{2}})^* \left(\tilde{\Phi}_Z^{(2)} \tilde{\Phi}_Z^{(2)*} + I\eta^2 \right)^{-1} \tilde{\Phi}_{V,i}^{(2)} \quad (122)$$

$$\Sigma_{\tilde{L}_i} = \Lambda - (\tilde{\Phi}_Z^{(2)} \Lambda^{\frac{1}{2}})^* \left(\tilde{\Phi}_Z^{(2)} \tilde{\Phi}_Z^{(2)*} + I\eta^2 \right)^{-1} (\tilde{\Phi}_Z^{(2)} \Lambda^{\frac{1}{2}}) \quad (123)$$

Proof. In the causal data fusion setting, one only specifies the model $V, W \rightarrow Y$ for \mathcal{D}_1 and the model $Z \rightarrow W$ for \mathcal{D}_2 (e.g. see (Chau et al., 2021b)). We therefore immediately have $f \perp\!\!\!\perp \mathcal{D}_2, L|\mathcal{D}_1$, and $L \perp\!\!\!\perp f, \mathcal{D}_1|\mathcal{D}_2$. The result then follows by deriving the posteriors on $\tilde{f}|\mathcal{D}_1$ and $\tilde{L}|\mathcal{D}_2$ using the same steps as in Theorem 2. The independence $(L_{i,j})_{j \in \mathbb{N}} \perp\!\!\!\perp (L_{k,j})_{j \in \mathbb{N}}|\mathcal{D}_2$ still trivially holds given our prior Eq. (14). \square

Corollary 2 (Theorem 2 and Corollary 1 for $W = \emptyset$). *Assume the conditions in Theorem 2 hold but now $W = \emptyset$, so that Eq. (12) becomes $\mathbb{E}[Y|V] = \sum_{i \in \mathbb{N}} f_i \lambda_i^{\frac{1}{2}} \phi_i(V)$ and $f_i \sim \mathcal{N}(0, 1)$. Then, the posteriors in Theorem 2 and Corollary 1 are identical but with $\tilde{\Phi}_{W,V}$ replaced by $\tilde{\Phi}_V$ and with $\Lambda : (h_i)_{i \in \mathbb{N}} \mapsto (\lambda_i^{\frac{1}{2}} h_i)_{i \in \mathbb{N}}$.*

Proof. In the single dataset case, note that we still have $f \perp\!\!\!\perp L|\mathcal{X}^n$ using the D-separation criteria (Geiger et al., 1990) on the mixed DAG that corresponds to a factorisation implied by this model, which is displayed on the RHS of Fig. 7. Clearly, all paths between $f - L$ must go through $Y_i - V_i$ or $Z_i - V_i$. Any path which goes through $Y_i - V_i$ is blocked by V_i and any path which goes through $Z_i - V_i$ is blocked by Z_i . Therefore, we conclude that $f \perp\!\!\!\perp L|\mathcal{X}^n$. From here, the result follows by following the proof of Theorem 2 for the posterior on \tilde{f} , but where now $\mathbf{F} := L_\phi(\tilde{f}) := \sum_{i \in \mathbb{N}} \Phi_i \tilde{f}_i$ and $\Phi_i = [\phi_i(V_1), \dots, \phi_i(V_n)]^T \in \mathbb{R}^n$. For the causal data fusion setting, we also trivially still have $f \perp\!\!\!\perp L|\mathcal{X}^n$. Therefore, the result in this case similarly follows by deriving the posteriors on $\tilde{f}|\mathcal{D}_1$ and $\tilde{L}|\mathcal{D}_2$ using the same steps as in Theorem 2, with the updated definition of \mathbf{F} to reflect $W = \emptyset$. \square

C.3 Proof of Theorem 3

Theorem 3. *Under the conditions in Theorem 2, we have the posterior moments*

$$\mathbb{E}[\gamma(w, z)|\mathcal{X}^n] = \boldsymbol{\beta}(z)^T K_{V,V} \boldsymbol{\alpha}(w) \quad (124)$$

$$\text{Var}[\gamma(w, z)|\mathcal{X}^n] = S_1 + S_2 + S_3 \quad (125)$$

$$S_1 = \boldsymbol{\beta}(z)^T K_{VV} (Ik(w, w) - A(w)K_{VV}) \boldsymbol{\beta}(z) \quad (126)$$

$$S_2 = \hat{k}(z, z) (\text{Tr}[\tilde{K}_{VV}(\boldsymbol{\alpha}(w)\boldsymbol{\alpha}(w)^T - A(w))] \quad (127)$$

$$S_3 = \left(\sum_{i \in \mathbb{N}} \lambda_i \right) \hat{k}(z, z) k(w, w) \quad (128)$$

$\boldsymbol{\alpha}(w) = D(w)(K_{WW} \odot K_{VV} + \sigma^2 I)^{-1} \mathbf{Y}$, $A(w) = D(w)(K_{WW} \odot K_{VV} + \sigma^2 I)^{-1} D(w)$, $D(w) = \text{diag}(\mathbf{k}(w))$, $\boldsymbol{\beta}(z) = (K_{ZZ} + \eta^2 I)^{-1} \mathbf{k}(z)$, $\hat{k}(z, z) = k(z, z) - \mathbf{k}(z)^T \boldsymbol{\beta}(z)$, $\tilde{K}_{V,V} = \int \mathbf{k}(v) \mathbf{k}(v)^T d\mu(v)$.

Proof. To avoid confusion when taking posterior moments of models for conditional expectations, we will use the definitions

$$f[\tilde{\phi}(w) \otimes \tilde{\phi}(v)] := \sum_{(i,j) \in \mathbb{N}^2} f_{i,j} \lambda_i^{\frac{1}{2}} \lambda_j^{\frac{1}{2}} \phi_i(w) \phi_j(v) \quad (129)$$

$$L_i[\tilde{\phi}(z)] := \lambda_i^{\frac{1}{2}} \sum_{j \in \mathbb{N}} L_{i,j} \lambda_j^{\frac{1}{2}} \phi_j(z), \quad \forall i \in \mathbb{N} \quad (130)$$

to denote the models specified for $\mathbb{E}[Y|W = w, V = v]$, $\mathbb{E}[\tilde{\phi}_i(V)|Z]$, respectively. Now, note from Proposition 3 we have that $(f[\tilde{\phi}(w) \otimes \tilde{\phi}(v)] : w, v \in \mathcal{W} \times \mathcal{V}) | \mathcal{X}^n \sim \mathcal{GP}(\hat{m}, \hat{k})$ with \hat{m}, \hat{k} defined in that result. By Proposition 3.2 in Chau et al. (2021a), as long as $\mathbb{E}[\|\hat{m}(w, V)\| | \mathcal{X}^n] < \infty$ and $\mathbb{E}[\|\hat{k}((w, V), \bullet)\|_{\mathcal{H}_W \otimes \mathcal{H}_V} | \mathcal{X}^n] < \infty$, we have

$$\mathbb{E}[f[\tilde{\phi}(\bullet) \otimes \tilde{\phi}(V)] | \mathcal{X}^n, L = \hat{L}, Z = \bullet] \sim \mathcal{GP}(\nu, q) \quad (131)$$

where $\nu(w, z, \hat{L}) := \mathbb{E}[\hat{m}(w, V) | \mathcal{X}^n, Z = z, L = \hat{L}]$, $q((w, z, \hat{L}), (w', z', \hat{L}')) = \mathbb{E}[\hat{k}((w, V), (w', V')) | \mathcal{X}^n, Z = z, Z' = z', L = \hat{L}, L' = \hat{L}']$, with (V', Z', L') as independent copies of (V, Z, L) . We first show $\mathbb{E}[\|\hat{m}(w, V)\| | \mathcal{X}^n] < \infty$. Since we can express $\hat{m}(w, V) = \sum_{i \in \mathbb{N}} \tilde{\phi}_i(V) \tilde{\Phi}_{V,i} \boldsymbol{\alpha}(z)$ for $\boldsymbol{\alpha}(z) \in \mathbb{R}^n$, we know $|\hat{m}(w, V)| \leq \|\tilde{\phi}(V)\|_{\ell_2} \|\tilde{\Phi}_V \boldsymbol{\alpha}(w)\|_{\ell_2}$. Therefore, one only needs to check that $\mathbb{E}[\|\tilde{\phi}(V)\|_{\ell_2}^2 | \mathcal{X}^n, Z = z] < \infty$ \mathbb{P}_Z -a.e. as this implies that $\mathbb{E}[\|\tilde{\phi}(V)\|_{\ell_2}^2 | \mathcal{X}^n] < \infty$, which in turn implies the result. Since the series terms are positive, we can write

$$\mathbb{E}[\|\tilde{\phi}(V)\|_{\ell_2}^2 | \mathcal{X}^n, Z = z] = \sum_{i \in \mathbb{N}} \mathbb{E}[\tilde{\phi}_i(V)^2 | \mathcal{X}^n, Z = z] \quad (132)$$

$$= \sum_{i \in \mathbb{N}} \hat{m}_i(z)^2 + \sum_{i \in \mathbb{N}} \hat{k}_i(z, z) + \eta^2 \sum_{i \in \mathbb{N}} \lambda_i \quad (133)$$

Where $\hat{m}_i(z)^2 = (\boldsymbol{\beta}(z) \tilde{\Phi}_i)^2 = \sum_{l,m=1}^n \beta_l(z) \beta_m(z) \tilde{\phi}_i(V_m) \tilde{\phi}_i(V_l)$ and $\hat{k}_i(z, z) \leq \lambda_i k_Z(z, z)$. Substituting these terms in, we get

$$\mathbb{E}[\|\tilde{\phi}(V)\|_{\ell_2}^2 | \mathcal{X}^n, Z = z] = \boldsymbol{\beta}(z)^T K_{VV} \boldsymbol{\beta}(z) + \left(\sum_{i \in \mathbb{N}} \lambda_i \right) (\|k_Z\|_0 + \eta^2) < \infty \quad \forall z \in \mathcal{Z} \quad (134)$$

Where the last inequality follows from the fact that $\boldsymbol{\beta}(z) = (K_{ZZ} + \eta^2 I)^{-1} \mathbf{k}_Z(z) \in \mathbb{R}^n$ for every $z \in \mathcal{Z}$ and Assumption 2 and Assumption 3. For the variance condition, note that $\|\hat{k}((w, V), \bullet)\|_{\mathcal{H}_W \otimes \mathcal{H}_V} \leq k_W(w, w)^{\frac{1}{2}} \left(\sum_{i \in \mathbb{N}} \tilde{\phi}_i(V)^2 \right)$. Since we already showed $\mathbb{E}[\|\tilde{\phi}(V)\|_{\ell_2}^2 | \mathcal{X}^n] < \infty$ and k_W is bounded, this implies $\mathbb{E}[\|\hat{k}((w, V), \bullet)\|_{\mathcal{H}_W \otimes \mathcal{H}_V} | \mathcal{X}^n] < \infty$.

Using this result we can now derive the posterior moments of $(\gamma(w, z) | \mathcal{X}^n)$. For the mean we have

$$\mathbb{E}[\gamma(w, z) | \mathcal{X}^n] = \mathbb{E}[\mathbb{E}[\gamma(w, z) | \mathcal{X}^n, L] | \mathcal{X}^n] \quad (135)$$

$$= \mathbb{E}[\mathbb{E}[\hat{m}(w, V) | \mathcal{X}^n, Z = z, L] | \mathcal{X}^n] \quad (136)$$

$$= \mathbb{E}[(L \tilde{\phi}(z))^* | \mathcal{X}^n]^* \tilde{\Phi}_V^* \boldsymbol{\alpha}(w) \quad (137)$$

where $\boldsymbol{\alpha}(w) := D(w)(K_{WW} \odot K_{VV} + I\sigma^2)^{-1} \mathbf{Y}$ and the last equality follows from the DCT, because $\sum_{i \in \mathbb{N}} L_i[\tilde{\phi}(z)] \tilde{\phi}_i(v) \leq \|L[\tilde{\phi}(z)]\|_{\ell_2} k_V(v, v)^{\frac{1}{2}}$ and $\mathbb{E}[\|L[\tilde{\phi}(z)]\|_{\ell_2}^2 | \mathcal{X}^n] \leq \mathbb{E}[\|\tilde{\phi}(V)\|_{\ell_2}^2 | \mathcal{X}^n, Z = z] < \infty$. From Proposition 3 we know that $L_i[\tilde{\phi}(z)] | \mathcal{X}^n \sim \mathcal{N}(\hat{m}_i(z), \hat{k}_i(z, z))$, where the moments are

$$\hat{m}_i(z) := \tilde{\Phi}_{V,i}^T (K_{ZZ} + I\eta^2)^{-1} \mathbf{k}_Z(z) \quad (138)$$

$$\hat{k}_i(z, z) := \lambda_i (k_Z(z, z) - \mathbf{k}_Z(z)^T (K_{ZZ} + \eta^2 I)^{-1} \mathbf{k}_Z(z)) \quad (139)$$

Substituting this into Eq. (137), we get

$$\mathbb{E}[\gamma(w, z)|\mathcal{X}^n] = \mathbf{k}_Z(z)^T (K_{ZZ} + I\eta^2)^{-1} \tilde{\Phi}_V \tilde{\Phi}_V^* \boldsymbol{\alpha}(w) \quad (140)$$

$$= \boldsymbol{\beta}(z)^T K_{VV} \boldsymbol{\alpha}(w) \quad (141)$$

Which is the form of the expectation in the theorem.

For the variance we use the law of total variance, which states

$$\text{Var}[\gamma(w, z)|\mathcal{X}^n] = \text{Var}[\mathbb{E}[\gamma(w, z)|\mathcal{X}^n, L]|\mathcal{X}^n] + \mathbb{E}[\text{Var}[\gamma(w, z)|\mathcal{X}^n, L]|\mathcal{X}^n] \quad (142)$$

all that remains is to take the required moments of these expressions. For the first term, we have

$$\text{Var}[\mathbb{E}[\gamma(w, z)|\mathcal{X}^n, L]|\mathcal{X}^n] = \text{Var}[\mathbb{E}[\hat{m}(w, V)|\mathcal{X}^n, Z = z, L]|\mathcal{X}^n] \quad (143)$$

$$= \underbrace{\mathbb{E}[\mathbb{E}[\hat{m}(w, V)|\mathcal{X}^n, Z = z, L]^2|\mathcal{X}^n]}_{I_1} - \underbrace{\mathbb{E}[\hat{m}(w, V)|Z = z, \mathcal{X}^n]^2}_{I_2} \quad (144)$$

Using the properties of expectations and tensor product Hilbert spaces, we can expand I_1 as follows

$$I_1 = \mathbb{E}[L[\tilde{\phi}(z)]^* \tilde{\Phi}_V^* \boldsymbol{\alpha}(w) \boldsymbol{\alpha}(w)^T \tilde{\Phi}_V L[\tilde{\phi}(z)]|\mathcal{X}^n] \quad (145)$$

$$= \sum_{l,m=1}^n a_{n,m}(w) \mathbb{E}[\langle L[\tilde{\phi}(z)], \tilde{\phi}(V_l) \rangle_{\ell_2} \langle L[\tilde{\phi}(z)], \tilde{\phi}(V_m) \rangle_{\ell_2} |\mathcal{X}^n] \quad (146)$$

$$= \sum_{l,m=1}^n a_{n,m}(w) \mathbb{E}[\langle L[\tilde{\phi}(z)] \otimes L[\tilde{\phi}(z)], \tilde{\phi}(V_l) \otimes \tilde{\phi}(V_m) \rangle_{HS(\ell_2, \ell_2)} |\mathcal{X}^n] \quad (147)$$

$$= \sum_{l,m=1}^n a_{n,m}(w) \langle \mathbb{E}[L[\tilde{\phi}(z)] \otimes L[\tilde{\phi}(z)]|\mathcal{X}^n], \tilde{\phi}(V_l) \otimes \tilde{\phi}(V_m) \rangle_{HS(\ell_2, \ell_2)} \quad (148)$$

$$= \sum_{l,m=1}^n a_{n,m}(w) \langle \mathbb{E}[L[\tilde{\phi}(z)]|\mathcal{X}^n] \otimes \mathbb{E}[L[\tilde{\phi}(z)]|\mathcal{X}^n] + \text{Cov}[L[\tilde{\phi}(z)]|\mathcal{X}^n], \tilde{\phi}(V_l) \otimes \tilde{\phi}(V_m) \rangle_{HS(\ell_2, \ell_2)} \quad (149)$$

$$= \sum_{l,m=1}^n a_{n,m}(w) \left(\langle \mathbb{E}[L[\tilde{\phi}(z)]|\mathcal{X}^n], \tilde{\phi}(V_l) \rangle_{\ell_2} \langle \mathbb{E}[L[\tilde{\phi}(z)]|\mathcal{X}^n], \tilde{\phi}(V_m) \rangle_{\ell_2} + \langle \tilde{\phi}(V_l), \text{Cov}[L[\tilde{\phi}(z)]|\mathcal{X}^n] \tilde{\phi}(V_m) \rangle_{\ell_2} \right) \quad (150)$$

$$= \underbrace{\mathbb{E}[(L[\tilde{\phi}(z)]|\mathcal{X}^n)^* \tilde{\Phi}_V^* \boldsymbol{\alpha}(w) \boldsymbol{\alpha}(w)^T \tilde{\Phi}_V \mathbb{E}[L[\tilde{\phi}(z)]|\mathcal{X}^n, Z]}_{I_{11}} + \underbrace{\text{Tr}[\tilde{\Phi}_V^* \boldsymbol{\alpha}(w) \boldsymbol{\alpha}(w)^T \tilde{\Phi}_V \text{Cov}[L[\tilde{\phi}(z)]|\mathcal{X}^n]}_{I_{12}} \quad (151)$$

Note, we are able to pass the expectation inside the inner product in Eq. (148) because the operator $A \mapsto \mathbb{E}[\langle L[\tilde{\phi}(z)] \otimes L[\tilde{\phi}(z)], A \rangle_{HS(\ell_2, \ell_2)} |\mathcal{X}^n]$ is bounded. To see that this is true, note by Cauchy Schartz and Jensen's inequality,

$$\mathbb{E}[\langle L[\tilde{\phi}(z)] \otimes L[\tilde{\phi}(z)], A \rangle_{HS(\ell_2, \ell_2)} |\mathcal{X}^n] \leq \sqrt{\mathbb{E}[\|L[\tilde{\phi}(z)] \otimes L[\tilde{\phi}(z)]\|_{HS(\ell_2, \ell_2)}^2 |\mathcal{X}^n]} \|A\|_{HS(\ell_2, \ell_2)} \quad (152)$$

$$= \sqrt{\mathbb{E} \left[\sum_{i \in \mathbb{N}} \langle e_i, L[\tilde{\phi}(z)] \rangle_{\ell_2}^2 \middle| \mathcal{X}^n \right]} \|A\|_{HS(\ell_2, \ell_2)} \quad (153)$$

$$= \sqrt{\mathbb{E} \left[\sum_{i \in \mathbb{N}} L_i[\tilde{\phi}(z)]^2 \middle| \mathcal{X}^n \right]} \|A\|_{HS(\ell_2, \ell_2)} \quad (154)$$

$$\leq \sqrt{\sum_{i \in \mathbb{N}} (\hat{m}_i(z)^2 + \lambda_i k_Z(z, z))} \|A\|_{HS(\ell_2, \ell_2)} \quad (155)$$

$$= \sqrt{\boldsymbol{\beta}(z)^T K_{VV} \boldsymbol{\beta}(z) + \left(\sum_{i \in \mathbb{N}} \lambda_i \right) k_Z(z, z)} \|A\|_{HS(\ell_2, \ell_2)} \quad (156)$$

$$\leq C \|A\|_{HS(\ell_2, \ell_2)} \quad (157)$$

where $C < \infty$ is implied by Assumption 2 and Assumption 3.

Now, since $I_{11} = I_2$, we have $\text{Var}[\mathbb{E}[\gamma(w, z)|\mathcal{X}^n, L]|\mathcal{X}^n] = I_{12}$. Since $\text{Cov}[L[\tilde{\phi}(z)]] = \Lambda \hat{k}(z, z)$ (where now we define $\Lambda : \ell_2 \rightarrow \ell_2$ by $\langle e_i, \Lambda e_j \rangle_{\ell_2} = \lambda_i \delta(i = j)$ and $\hat{k} = \lambda_i^{-1} \hat{k}_i$), this simplifies to

$$\text{Var}[\mathbb{E}[\gamma(w, z)|\mathcal{X}^n, L]|\mathcal{X}^n] = \text{Tr}[\tilde{\Phi}_V^* \alpha(w) \alpha(w)^T \tilde{\Phi}_V \Lambda] \hat{k}(z, z) \quad (158)$$

$$= \text{Tr}[\alpha(w) \alpha(w)^T \tilde{K}_{VV}] \hat{k}(z, z) \quad (159)$$

Where $[\tilde{K}_{VV}]_{i,j} = \sum_{l \in \mathbb{N}} \lambda_l^2 \phi_l(V_i) \phi_l(V_j) = \int_{\mathcal{Y}} k(V_i, t) k(t, V_j) d\mu(t)$. This is the first part of S_2 . Now for the second term, we have

$$\mathbb{E}[\text{Var}[\gamma(w, z)|\mathcal{X}^n, L]|\mathcal{X}^n] = \mathbb{E}[\text{Tr}[BL[\tilde{\phi}(z)] \otimes L[\tilde{\phi}(z)]^*]|\mathcal{X}^n] \quad (160)$$

$$(161)$$

where $B = Ik(w, w) - \tilde{\Phi}_V^* A(w) \tilde{\Phi}_V$ and $A(w) = D(w) (K_{WW} \odot K_{VV} + I\sigma^2)^{-1} D(w)$. Now, recall that for any random element $X \in \mathcal{H}$ (where \mathcal{H} is a Hilbert space) and bounded linear $A : \mathcal{H} \rightarrow \mathcal{H}$ we have $\mathbb{E}[AX] = A\mathbb{E}[X]$ whenever $\mathbb{E}\|X\|_{\mathcal{H}} < \infty$. Therefore, in our case we can exchange the expectation with $\text{Tr} \circ B$ as long as (i) $A \mapsto \text{Tr}[BA]$ is bounded and (ii) $\mathbb{E}[\|L[\tilde{\phi}(z)] \otimes L[\tilde{\phi}(z)]\|_{HS(\ell_2, \ell_2)}|\mathcal{X}^n] < \infty$. For (i), first note that $A \mapsto \text{Tr}[A]$ is bounded on the space $\mathcal{B}_1(\ell_2)$ of trace class operators $\ell_2(\mathbb{N}) \rightarrow \ell_2(\mathbb{N})$. Moreover, from the structure of B it is obvious that $\text{Tr}[BA] \leq k(w, w)\text{Tr}[A] \leq c\text{Tr}[A]$ for any trace class A , where $c < \infty$ by Assumption 2. Combining these two facts, it suffices to show that $L[\tilde{\phi}(z)] \otimes L[\tilde{\phi}(z)] \in \mathcal{B}_1(\ell_2)$ almost surely for (i) to hold. This is true because

$$\text{Tr}[L[\tilde{\phi}(z)] \otimes L[\tilde{\phi}(z)]] = \sum_{i \in \mathbb{N}} \langle e_i, (L[\tilde{\phi}(z)] \otimes L[\tilde{\phi}(z)]) e_i \rangle_{\ell_2(\mathbb{N})} \quad (162)$$

$$= \sum_{i \in \mathbb{N}} \langle e_i, L[\tilde{\phi}(z)] \rangle_{\ell_2(\mathbb{N})}^2 \quad (163)$$

$$= \sum_{i \in \mathbb{N}} L_i[\tilde{\phi}(z)]^2 < \infty \quad (164)$$

with posterior probability 1, since we already showed earlier that $\sum_{i \in \mathbb{N}} \mathbb{E}[L_i[\tilde{\phi}(z)]^2|\mathcal{X}^n] < \infty$. We also already showed that (ii) holds earlier in the proof. Therefore, we can exchange the expectation with $\text{Tr} \circ B$, which gives us

$$\mathbb{E}[\text{Var}[\gamma(w, z)|\mathcal{X}^n, L]|\mathcal{X}^n] = \text{Tr}[B\mathbb{E}[L[\tilde{\phi}(z)] \otimes L[\tilde{\phi}(z)]^*]|\mathcal{X}^n] \quad (165)$$

$$= \text{Tr}[B(\mathbb{E}[L[\tilde{\phi}(z)]|\mathcal{X}^n] \otimes \mathbb{E}[L[\tilde{\phi}(z)]|\mathcal{X}^n]^* + \text{Cov}[L[\tilde{\phi}(z)]|\mathcal{X}^n])] \quad (166)$$

$$= \text{Tr}[B(\tilde{\Phi}_V^* \beta(z) \beta(z)^T \tilde{\Phi}_V + \Lambda \hat{k}(z, z))] \quad (167)$$

$$= \beta(z)^T \tilde{\Phi}_V B \tilde{\Phi}_V^* \beta(z) + \text{Tr}[B \Lambda \hat{k}(z, z)] \quad (168)$$

$$(169)$$

Substituting in the definition of B gives

$$\beta(z)^T \tilde{\Phi}_V B \tilde{\Phi}_V^* \beta(z) = \beta(z)^T (K_{VV} k(w, w) - K_{VV} A(w) K_{VV}) \beta(z) \quad (170)$$

$$\text{Tr}[B \Lambda \hat{k}(z, z)] = k(w, w) \sum_i \lambda_i \hat{k}(z, z) - \text{Tr}[A(w) \tilde{K}_{VV}] \hat{k}(z, z) \quad (171)$$

Re-arranging the terms we finally get $\text{Var}[\gamma(w, z)|\mathcal{X}^n] = S_1 + S_2 + S_3$ where

$$S_1 = \beta(z)^T K_{VV} (Ik(w, w) - A(w) K_{VV}) \beta(z) \quad (172)$$

$$S_2 = \hat{k}(z, z) (\text{Tr}[\tilde{K}_{VV} (\alpha(w) \alpha(w)^T - A(w))] \quad (173)$$

$$S_3 = \left(\sum_{i \in \mathbb{N}} \lambda_i \right) k(w, w) \hat{k}(z, z) \quad (174)$$

□

Corollary 3 (Theorem 3 for causal data fusion). *For the causal data fusion scenario in Corollary 1 we have the following modification of Theorem 3*

$$\mathbb{E}[\gamma(z)|\mathcal{X}^n] = \boldsymbol{\beta}^{(2)}(z)^T K_{V^{(2)}V^{(1)}} \boldsymbol{\alpha}^{(1)}(w) \quad (175)$$

$$\text{Var}[\gamma(z)|\mathcal{X}^n] = S_1 + S_2 + S_3 \quad (176)$$

where

$$S_1 = \boldsymbol{\beta}^{(2)}(z)^T K_{V^{(2)}V^{(2)}} \boldsymbol{\beta}^{(2)}(z) k(w, w) - \boldsymbol{\beta}^{(2)}(z)^T K_{V^{(2)}V^{(1)}} A^{(1)}(w) K_{V^{(1)}V^{(2)}} \boldsymbol{\beta}^{(2)}(z) \quad (177)$$

$$S_2 = \hat{\mathbf{k}}^{(2)}(z, z) (\text{Tr}[\tilde{K}_{V^{(1)}V^{(1)}}(\boldsymbol{\alpha}^{(1)}(w)\boldsymbol{\alpha}^{(1)}(w)^T - A^{(1)}(w)]) \quad (178)$$

$$S_3 = \left(\sum_{i \in \mathbb{N}} \lambda_i \right) k(w, w) \hat{\mathbf{k}}^{(2)}(z, z) \quad (179)$$

and $\boldsymbol{\alpha}^{(1)}(w) = D^{(1)}(w)(K_{W^{(1)}W^{(1)}} \odot K_{V^{(1)}V^{(1)}} + \sigma^2 I)^{-1} \mathbf{Y}^{(1)}$, $A^{(1)}(w) = D^{(1)}(w)(K_{W^{(1)}W^{(1)}} \odot K_{V^{(1)}V^{(1)}} + \sigma^2 I)^{-1} D^{(1)}(w)$, $D^{(1)}(w) = \text{diag}(\mathbf{k}^{(1)}(w))$, $\boldsymbol{\beta}^{(2)}(z) = (K_{Z^{(2)}Z^{(2)}} + \eta^2 I)^{-1} \mathbf{k}^{(2)}(z)$, $\hat{\mathbf{k}}^{(2)}(z, z) = k(z, z) - \mathbf{k}^{(2)}(z)^T \boldsymbol{\beta}^{(2)}(z)$, $\tilde{K}_{V^{(1)}V^{(1)}} = \int \mathbf{k}^{(1)}(v) \mathbf{k}^{(1)}(v)^T d\mu(v)$, $\mathbf{k}^{(1)}(w) = [k(w, W_1^{(1)}), \dots, k(w, W_{m_1}^{(1)})]^T$, $\mathbf{k}^{(2)}(z) = [k(z, Z_1^{(1)}), \dots, k(z, Z_{m_2}^{(2)})]^T$ and the equivalent definitions apply to $K_{W^{(1)}W^{(1)}}$ and $K_{V^{(i)}V^{(j)}}$ for $i, j \in \{1, 2\}$.

Proof. Follows immediately from the proof of Theorem 3 with the posteriors in Theorem 2 now modified according to Corollary 1. \square

Corollary 4 (Theorem 3 and Corollary 3 for $W = \emptyset$). *For the case $W = \emptyset$, the posteriors in Theorem 3 and Corollary 3 are identical except where now $K_{WW} = I$, $k(w, w) = 1$ and $\mathbf{k}(w) = \mathbf{1}$.*

Proof. Follows immediately from the proofs of Theorem 3 and Corollary 3 using the posteriors in Theorem 2 and Corollary 1 respectively, now modified according to Corollary 2. \square

C.4 Proof of Theorem 4

Theorem 4. *Under the conditions of Theorem 3, let $\{\mathcal{X}^n, \mathcal{X}^m\}$ be a partition of the dataset for $n, m > 0$. Let $\mu_{w,z} = \mathbb{E}[\gamma(w, z)|\mathcal{X}^n]$, $\sigma_{w,z} = \text{Var}[\gamma(w, z)|\mathcal{X}^n]$, $F_\alpha(t) = \mathbb{P}_{\mathcal{X}^n}(\mu_{w,z} + t_\alpha \sigma_{w,z} \leq t)$ and t_α be the $(1 - \alpha)$ quantile of $\mathcal{N}(0, 1)$. Let $\hat{\gamma}_m$ be the estimator for γ in Singh et al. (2024) using \mathcal{X}^m . Then, under the assumptions of Theorem 6.1 in Singh et al. (2024) and L -Lipschitzness of F_α*

$$\begin{aligned} & \|\mathbb{P}_{\mathcal{X}^n}(\gamma(w, z) \leq \mu_{w,z} + t_\alpha \sigma_{w,z}) \\ & - \hat{\mathbb{P}}_{\mathcal{Z}^n|\mathcal{X}^n}(\hat{\gamma}_m(w, z) \leq \mu_{w,z} + t_\alpha \sigma_{w,z})\|_{L_1(\mathbb{P}_{\mathcal{X}^m})} \\ & \leq \|\mathcal{D}(\mathbb{P}_{\mathcal{X}^n}, \mathbb{P}_{\mathcal{Z}^n|\mathcal{X}^n})\|_{L_1(\mathbb{P}_{\mathcal{X}^n})} + \mathcal{O}\left(m^{-\frac{1}{2} \frac{c-1}{c+\frac{1}{b}}}\right) \end{aligned} \quad (35)$$

\mathcal{D} is the Kolmogorov metric, $c \in (1, 2]$, $b \in [1, \infty)$.

Proof. To start note that by the triangle inequality we can split the deviation into $\mathcal{D}(\mathbb{P}_{\mathcal{X}^n}, \hat{\mathbb{P}}_{\mathcal{Z}^n|\mathcal{X}^n})$ and $|F_\alpha(\gamma(w, z)) - F_\alpha(\hat{\gamma}_m(w, z))|$.

$$|\mathbb{P}_{\mathcal{X}^n}(\gamma(w, z) \leq \mu_{w,z} + t_\alpha \sigma_{w,z}) - \hat{\mathbb{P}}_{\mathcal{Z}^n|\mathcal{X}^n}(\hat{\gamma}_m(w, z) \leq \mu_{w,z} + t_\alpha \sigma_{w,z})| \quad (180)$$

$$\begin{aligned} & \leq |\mathbb{P}_{\mathcal{X}^n}(\hat{\gamma}_m(w, z) \leq \mu_{w,z} + t_\alpha \sigma_{w,z}) - \hat{\mathbb{P}}_{\mathcal{Z}^n|\mathcal{X}^n}(\hat{\gamma}_m(w, z) \leq \mu_{w,z} + t_\alpha \sigma_{w,z})| \\ & + |\mathbb{P}_{\mathcal{X}^n}(\gamma(w, z) \leq \mu_{w,z} + t_\alpha \sigma_{w,z}) - \mathbb{P}_{\mathcal{X}^n}(\hat{\gamma}_m(w, z) \leq \mu_{w,z} + t_\alpha \sigma_{w,z})| \end{aligned} \quad (181)$$

$$\begin{aligned} & \leq \sup_{t \in \mathbb{R}} |\mathbb{P}_{\mathcal{X}^n}(t \leq \mu_{w,z} + t_\alpha \sigma_{w,z}) - \hat{\mathbb{P}}_{\mathcal{Z}^n|\mathcal{X}^n}(t \leq \mu_{w,z} + t_\alpha \sigma_{w,z})| \\ & + |\mathbb{P}_{\mathcal{X}^n}(\gamma(w, z) \leq \mu_{w,z} + t_\alpha \sigma_{w,z}) - \mathbb{P}_{\mathcal{X}^n}(\hat{\gamma}_m(w, z) \leq \mu_{w,z} + t_\alpha \sigma_{w,z})| \end{aligned} \quad (182)$$

$$= \mathcal{D}(\mathbb{P}_{\mathcal{X}^n}, \hat{\mathbb{P}}_{\mathcal{Z}^n|\mathcal{X}^n}) + |\mathbb{P}_{\mathcal{X}^n}(\gamma(w, z) \leq \mu_{w,z} + t_\alpha \sigma_{w,z}) - \mathbb{P}_{\mathcal{X}^n}(\hat{\gamma}_m(w, z) \leq \mu_{w,z} + t_\alpha \sigma_{w,z})| \quad (183)$$

$$= \mathcal{D}(\mathbb{P}_{\mathcal{X}^n}, \hat{\mathbb{P}}_{\mathcal{Z}^n|\mathcal{X}^n}) + |F_\alpha(\gamma(w, z)) - F_\alpha(\hat{\gamma}_m(w, z))| \quad (184)$$

Using the Lipschitz continuity of F_α , we get

$$\begin{aligned} & |\mathbb{P}_{\mathcal{X}^n}(\gamma(w, z) \leq \mu_{w,z} + t_\alpha \sigma_{w,z}) - \hat{\mathbb{P}}_{\mathcal{Z}^n | \mathcal{X}^n}(\hat{\gamma}_m(w, z) \leq \mu_{w,z} + t_\alpha \sigma_{w,z})| \\ & \leq \mathcal{D}(\mathbb{P}_{\mathcal{X}^n}, \hat{\mathbb{P}}_{\mathcal{Z}^n | \mathcal{X}^n}) + L \hat{\xi}_m(w, z) \end{aligned} \quad (185)$$

Where $\hat{\xi}_m(w, z) = |\gamma(w, z) - \hat{\gamma}_m(w, z)|$. Under the conditions of Theorem 6.1 in Singh et al. (2024), we have

$$\mathbb{P}\left(\hat{\xi}_m(w, z) \geq C \ln(4/\delta) m^{-\frac{1}{2} \frac{c-1}{c+1/b}}\right) \leq 2\delta \quad (186)$$

where $(c, b) = \operatorname{argmin}_{(\tilde{c}, \tilde{b}) \in \{(b_1, c_1), (b_2, c_2)\}} \left(\frac{\tilde{c}-1}{\tilde{c}+1/\tilde{b}}\right)$ and c_1, b_1, c_2, b_2 are defined as in Singh et al. (2024). After-re-arranging, this gives:

$$\mathbb{P}(\hat{\xi}(w, z) \geq t) \leq 8 \exp\left(-\frac{t}{C} m^{\frac{1}{2} \frac{c-1}{c+1/b}}\right) \leq A \exp(-Btm^{\frac{1}{2} \frac{c-1}{c+1/b}}) \quad (187)$$

for $A, B > 0$ appropriately chosen. Now, taking expectations of Eq. (185) we get

$$\|\mathbb{P}_{\mathcal{X}^n}(\gamma(w, z) \leq \mu_{w,z} + t_\alpha \sigma_{w,z}) - \hat{\mathbb{P}}_{\mathcal{Z}^n | \mathcal{X}^n}(\hat{\gamma}_m(w, z) \leq \mu_{w,z} + t_\alpha \sigma_{w,z})\|_{L_1(\mathbb{P}_{\mathcal{X}^m})} \quad (188)$$

$$\leq \|\mathcal{D}(\mathbb{P}_{\mathcal{X}^n}, \hat{\mathbb{P}}_{\mathcal{Z}^n | \mathcal{X}^n})\|_{L_1(\mathbb{P}_{\mathcal{X}^n})} + L \mathbb{E} \hat{\xi}_m(w, z) \quad (189)$$

Since $\mathbb{E} \hat{\xi}_m(w, z) = \int_0^\infty \mathbb{P}(\hat{\xi}_m(w, z) \geq t) dt$ we can write

$$\mathbb{E} \hat{\xi}_m(w, z) \leq A \int_0^\infty \exp(-Btm^{\frac{1}{2} \frac{c-1}{c+1/b}}) dt \quad (190)$$

$$= \frac{A}{B} m^{-\frac{1}{2} \frac{c-1}{c+1/b}} \quad (191)$$

Which implies the result. \square

C.5 Theorem 3 for Incremental Effects

Theorem 5 (Posterior moments of incremental effects). *Under the conditions of Theorem 3, we have that*

$$\mathbb{E}[\gamma(w, z) - \gamma(w', z') | \mathcal{X}^n] = \mathbb{E}[\gamma(w, z) | \mathcal{X}^n] - \mathbb{E}[\gamma(w', z') | \mathcal{X}^n] \quad (192)$$

$$\operatorname{Var}[\gamma(w, z) - \gamma(w', z') | \mathcal{X}^n] = \operatorname{Var}[\gamma(w, z) | \mathcal{X}^n] + \operatorname{Var}[\gamma(w', z') | \mathcal{X}^n] - 2\operatorname{Cov}[\gamma(w, z), \gamma(w', z') | \mathcal{X}^n] \quad (193)$$

$\mathbb{E}[\gamma(w, z) | \mathcal{X}^n]$, $\operatorname{Var}[\gamma(w, z) | \mathcal{X}^n]$ are defined as in Theorem 3 and

$$\operatorname{Cov}[\gamma(w, z), \gamma(w', z') | \mathcal{X}^n] = C_1 + C_2 + C_3 \quad (194)$$

where

$$C_1 = \boldsymbol{\beta}(z)^T K_{VV} (Ik(w, w') - A(w, w') K_{VV}) \boldsymbol{\beta}(z') \quad (195)$$

$$C_2 = \hat{k}(z, z') (\operatorname{Tr}[\tilde{K}_{VV}(\boldsymbol{\alpha}(w)\boldsymbol{\alpha}(w')^T - A(w, w'))]) \quad (196)$$

$$C_3 = \left(\sum_{i \in \mathbb{N}} \lambda_i\right) k(w, w') \hat{k}(z, z') \quad (197)$$

and all quantities except $A(w, w') := D(w)(K_{VV} \odot K_{WW} + \sigma^2 I)^{-1} D(w')$ are defined as in Theorem 3.

Proof. It suffices to derive the form of the covariance, which we do using the law of total covariance,

$$\operatorname{Cov}[\gamma(w, z), \gamma(w', z') | \mathcal{X}^n] = \operatorname{Cov}[\mathbb{E}[\gamma(w, z) | \mathcal{X}^n, L], \mathbb{E}[\gamma(w', z') | \mathcal{X}^n, L] | \mathcal{X}^n] + \mathbb{E}[\operatorname{Cov}[\gamma(w, z), \gamma(w', z') | \mathcal{X}^n, L] | \mathcal{X}^n] \quad (198)$$

All that remains is to take the required moments of these expressions. For the first term, we have

$$\begin{aligned} \operatorname{Cov}[\mathbb{E}[\gamma(w, z) | \mathcal{X}^n, L], \mathbb{E}[\gamma(w', z') | \mathcal{X}^n, L] | \mathcal{X}^n] &= \operatorname{Cov}[\mathbb{E}[\hat{m}(w, V) | \mathcal{X}^n, Z = z, L], \mathbb{E}[\hat{m}(w', V) | \mathcal{X}^n, Z = z', L] | \mathcal{X}^n] \\ & \quad (199) \end{aligned}$$

$$= \underbrace{\mathbb{E}[\mathbb{E}[\hat{m}(w, V) | \mathcal{X}^n, Z = z, L] \mathbb{E}[\hat{m}(w', V) | \mathcal{X}^n, Z = z', L] | \mathcal{X}^n]}_{I_1} - \underbrace{\mathbb{E}[\hat{m}(w, V) | Z = z, \mathcal{X}^n] \mathbb{E}[\hat{m}(w', V) | Z = z', \mathcal{X}^n]}_{I_2} \quad (200)$$

As before, we can expand I_1 as

$$\begin{aligned} I_1 &= \mathbb{E}[L[\tilde{\phi}(z)]^* \tilde{\Phi}_V^* \boldsymbol{\alpha}(w) \boldsymbol{\alpha}(w')^T \tilde{\Phi}_V L[\tilde{\phi}(z') | \mathcal{X}^n, Z]] \quad (201) \\ &= \underbrace{\mathbb{E}[(L[\tilde{\phi}(z)] | \mathcal{X}^n)^* \tilde{\Phi}_V^* \boldsymbol{\alpha}(w) \boldsymbol{\alpha}(w')^T \tilde{\Phi}_V \mathbb{E}[L[\tilde{\phi}(z') | \mathcal{X}^n, Z]]]}_{I_{11}} + \underbrace{\text{Tr}[\tilde{\Phi}_V^* \boldsymbol{\alpha}(w) \boldsymbol{\alpha}(w')^T \tilde{\Phi}_V \text{Cov}[L[\tilde{\phi}(z')], L[\tilde{\phi}(z)] | \mathcal{X}^n]}]_{I_{12}} \end{aligned} \quad (202)$$

Since $I_{11} = I_2$, we have $\text{Cov}[\mathbb{E}[\gamma(w, z) | \mathcal{X}^n, L], \mathbb{E}[\gamma(w', z') | \mathcal{X}^n, L] | \mathcal{X}^n] = I_{12}$. Since $\text{Cov}[L[\tilde{\phi}(z)], L[\tilde{\phi}(z')]] = \Lambda \hat{k}(z, z') = \Lambda \hat{k}(z', z)$, this simplifies to

$$\text{Cov}[\mathbb{E}[\gamma(w, z) | \mathcal{X}^n, L], \mathbb{E}[\gamma(w', z') | \mathcal{X}^n, L] | \mathcal{X}^n] = \text{Tr}[\tilde{\Phi}_V^* \boldsymbol{\alpha}(w) \boldsymbol{\alpha}(w')^T \tilde{\Phi}_V \Lambda] \hat{k}(z, z') \quad (203)$$

$$= \text{Tr}[\boldsymbol{\alpha}(w) \boldsymbol{\alpha}(w')^T \tilde{K}_{VV}] \hat{k}(z, z') \quad (204)$$

Where $[\tilde{K}_{VV}]_{i,j} = \sum_{l \in \mathbb{N}} \lambda_l^2 \phi_l(V_i) \phi_l(V_j) = \int_{\mathcal{Y}} k(V_i, t) k(t, V_j) d\mu(t)$. This is the first part of S_2 . Now for the second term, we have

$$\mathbb{E}[\text{Cov}[\gamma(w, z), \gamma(w', z') | \mathcal{X}^n, L] | \mathcal{X}^n] = \text{Tr}[B \mathbb{E}[L[\tilde{\phi}(z')] \otimes L[\tilde{\phi}(z)]^* | \mathcal{X}^n]] \quad (205)$$

$$= \text{Tr}[B(\mathbb{E}[L[\tilde{\phi}(z')] | \mathcal{X}^n] \otimes \mathbb{E}[L[\tilde{\phi}(z)] | \mathcal{X}^n]^* + \text{Cov}[L[\tilde{\phi}(z')], L[\tilde{\phi}(z)] | \mathcal{X}^n])] \quad (206)$$

$$= \text{Tr}[B(\tilde{\Phi}_V^* \boldsymbol{\beta}(z') \boldsymbol{\beta}(z)^T \tilde{\Phi}_V + \Lambda \hat{k}(z, z'))] \quad (207)$$

$$= \boldsymbol{\beta}(z)^T \tilde{\Phi}_V B \tilde{\Phi}_V^* \boldsymbol{\beta}(z') + \text{Tr}[B \Lambda \hat{k}(z, z')] \quad (208)$$

where now $B = Ik(w, w') - \tilde{\Phi}_V^* A(w, w') \tilde{\Phi}_V$ and $A(w, w') = D(w) (K_{WW} \odot K_{VV} + I\sigma^2)^{-1} D(w')$. Note we can exchange the expectation with $\text{Tr} \circ B$ using the same reasoning as Theorem 3. Substituting in the definition of B gives

$$\boldsymbol{\beta}(z)^T \tilde{\Phi}_V B \tilde{\Phi}_V^* \boldsymbol{\beta}(z') = \boldsymbol{\beta}(z)^T (K_{VV} k(w, w') - K_{VV} A(w, w') K_{VV}) \boldsymbol{\beta}(z') \quad (209)$$

$$\text{Tr}[B \Lambda \hat{k}(z, z')] = k(w, w') \sum_i \lambda_i \hat{k}(z, z') - \text{Tr}[A(w, w') \tilde{K}_{VV}] \hat{k}(z, z') \quad (210)$$

Re-arranging the terms we finally get $\text{Cov}[\gamma(w, z), \gamma(w', z') | \mathcal{X}^n] = C_1 + C_2 + C_3$ where

$$C_1 = \boldsymbol{\beta}(z)^T K_{VV} (Ik(w, w') - A(w, w') K_{VV}) \boldsymbol{\beta}(z') \quad (211)$$

$$C_2 = \hat{k}(z, z') (\text{Tr}[\tilde{K}_{VV} (\boldsymbol{\alpha}(w) \boldsymbol{\alpha}(w')^T - A(w, w'))]) \quad (212)$$

$$C_3 = \left(\sum_{i \in \mathbb{N}} \lambda_i \right) k(w, w') \hat{k}(z, z') \quad (213)$$

□

C.6 Theorem 3 for Average Causal Effects

The following corollary shows how to use our derived posteriors for γ to construct the posterior distribution on average causal effects, which correspond to marginal expectations of γ . Note, the following assumes we extend our Gaussian approximation of the posterior on $\gamma(w, z)$ to a GP approximation of the posterior on the causal function γ . In either case, the moments are parameterised by the true posterior moments, as derived in Theorem 3 and Theorem 5.

Corollary 5 (Posteriors on average causal effects). *Let the approximated posterior distribution for the causal function γ be $\hat{\mathbb{P}}_{\gamma | \mathcal{X}^n} = \mathcal{GP}(\mathbb{E}[\gamma(\bullet) | \mathcal{X}^n], \text{Cov}[\gamma(\bullet), \gamma(\bullet) | \mathcal{X}^n])$. Then the posterior distribution of $\mathbb{E}[\gamma(w, Z)]$ is $\mathcal{N}(\mathbb{E}[\mathbb{E}[\gamma(w, Z) | \mathcal{X}^n, Z] | \mathcal{X}^n], \mathbb{E}[\text{Cov}[\gamma(w, Z), \gamma(w, Z') | \mathcal{X}^n, Z, Z'] | \mathcal{X}^n])$ where $Z, Z' \stackrel{iid}{\sim} \mathbb{P}_Z$, as long as the absolute moments $\mathbb{E}[|\mathbb{E}[\gamma(w, Z) | \mathcal{X}^n, Z]| | \mathcal{X}^n]$ and $\mathbb{E}[|\text{Cov}[\gamma(w, Z), \gamma(w, Z') | \mathcal{X}^n, Z, Z']| | \mathcal{X}^n]$ are finite.*

Proof. Follows immediately from Proposition 3.2 in Chau et al. (2021a). □

Remark 4. *The result holds analogously for $\mathbb{E}[\gamma(W, Z)]$ and $\mathbb{E}[\gamma(W, z)]$.*

Remark 5. *In practice, one can compute the moments in Corollary 5 by using the derived moments in Theorem 3 and Theorem 5 and averaging them with respect to the empirical distribution $\hat{\mathbb{P}}_Z$.*

D Experiments

D.1 Ablation Study

In this experiment we aim to estimate the ATE $\mathbb{E}[Y|do(Z = z)]$ for the LHS causal graph in Fig. 1 in the main text.

D.1.1 Simulation Details

The data generating process for the LHS causal graph in Fig. 1 in the main text is given by

$$Z \sim \mathcal{U}(0, 1) \quad (214)$$

$$X_d|Z \sim \mathcal{N}(\sin(\alpha_d Z), \sigma_d^2), \quad d \in \{1, \dots, 5\} \quad (215)$$

$$Y|\mathbf{X} \sim \mathcal{N}(\boldsymbol{\beta}^T \sin(\mathbf{X}), \sigma_y^2) \quad (216)$$

Where $\boldsymbol{\alpha} = 10 \times [1, 1.75, 2.5, 3, 25, 4]$, $\boldsymbol{\beta} = 1/[1, 2, 3, 4, 5]$ and $(\sigma_d^2)_{d=1}^5, \sigma_y$ are set so that the signal to noise ratios are 2:1.

For each simulation we draw two i.i.d. datasets $(Y_i^{(1)}, \mathbf{X}_i^{(1)}, Z_i^{(1)})_{i=1}^n, (Y_j^{(2)}, \mathbf{X}_j^{(2)}, Z_j^{(2)})_{j=1}^n$ of size $n = 100$, and assume we only have access to the observations $\mathcal{D}_1 = (Y_i^{(1)}, \mathbf{X}_i^{(1)})_{i=1}^n$ and $\mathcal{D}_2 = (\mathbf{X}_j^{(2)}, Z_j^{(2)})_{j=1}^n$.

D.1.2 Causal Effect Identification

Using the rules of do-calculus, we have

$$\mathbb{E}[Y|do(Z = z)] = \int_{\mathcal{X}} \mathbb{E}[Y|do(Z = z), X = x] \mathbb{P}_{X|do(Z)}(dx|z) \quad (217)$$

$$= \int_{\mathcal{X}} \mathbb{E}[Y|do(Z = z), X = x] \mathbb{P}_{X|Z}(dx|z) \quad (Y \perp\!\!\!\perp Z \in \mathcal{G}_Z) \quad (218)$$

$$= \int_{\mathcal{X}} \mathbb{E}[Y|X = x] \mathbb{P}_{X|Z}(dx|z) \quad (Y \perp\!\!\!\perp Z|X \in \mathcal{G}_Z) \quad (219)$$

D.1.3 Implementation Details

True causal function: The true causal function is estimated by drawing 10^5 Monte Carlo samples from $\mathbb{P}_{Y|Z}(\cdot|Z = z)$ and averaging. We do this for $z \in \hat{\mathcal{Z}}$, where $\hat{\mathcal{Z}}$ is a uniformly spaced grid on $[0, 1]$ of size 100.

IMPspec: Our estimation target is $\gamma(w, z)$ as defined in Eq. (4) in the main text, where $V = \mathbf{X}$ and $W = \emptyset$ (i.e. $\gamma(w, z) = \gamma(z)$). Since we are in the causal data fusion setting and $W = \emptyset$, we estimate the posterior mean and variance of $\gamma(z)$ using the modification of Theorem 3 for this case (i.e. see Corollary 4 in Appendix C). All kernels are set as Gaussian kernels with per-dimension lengthscales. The kernel parameters and noise variances are optimised using the marginal likelihoods in Section 5.4. We use 1000 iterations of ADAM with a base learning rate of 0.1. The posterior confidence intervals are constructed using the procedure outlined in Section 5.3. We implement our method both with and without our spectral learning procedure for calibration optimisation, to do an ablation of this effect on calibration performance. When not using this procedure, we fix $\mu = \mathcal{N}(\bar{\mathbf{X}}, \hat{S})$, where $\hat{S} = \text{diag}(\hat{\text{Var}}(X_1)^{\frac{1}{2}}, \dots, \hat{\text{Var}}(X_5)^{\frac{1}{2}})$ and $\bar{\mathbf{X}} \approx \mathbf{0}$ is the empirical mean. When using this procedure, we set $\mu = \mathcal{N}(\bar{\mathbf{X}}, \omega \hat{S})$ and choose the optimal $\omega \in 2^{\{-4, -2, 0, 2, 4\}}$ that minimises the calibration error Eq. (34) for $\alpha \in \Gamma$, and $z \in \hat{\mathcal{Z}}$, where Γ is a uniformly spaced grid on $[0, 1]$ of size 101. We estimate Eq. (34) using a 50:50 sample split (i.e. $n = 50$ observations from each dataset are used to estimate $\mathbb{P}_{\mathcal{X}^{n/2}}$ via $\mathbb{P}_{\mathcal{Z}^{n/2}|\mathcal{X}^{n/2}}$ and the remaining $n = 50$ observations from each dataset are used to estimate $\hat{\gamma}(z)$ via our posterior mean (recall IMPspec’s posterior mean is equivalent to the original estimator in Singh et al. (2024) up to hyperparameter equivalence. We use 20 bootstrap replications to estimate $\mathbb{P}_{\mathcal{Z}^{n/2}|\mathcal{X}^{n/2}}$.

BayesIMP: We implement BayesIMP using the implementation in Proposition 5 in Chau et al. (2021b)⁸. The kernels k_Z, k_X are set as Gaussian kernels with per-dimension lengthscales, and the nuclear dominant kernel is set using their implementation $r_X = \int k_X(\cdot, x) k_X(\cdot, x) \mathcal{N}(0, \hat{S})[dt]$. We estimate the base kernel

⁸We found two typos in Proposition 5, which when removed significantly improved the performance of their method. All presented results for BayesIMP are for the case where these typos are fixed.

parameters and noise hyperparameters using (i) the marginal likelihood $p(\mathbf{y}|\mathbf{x}_1, \dots, \mathbf{x}_d) = \mathcal{N}(\mathbf{0}, R_{XX} + \sigma^2 I)$ and (ii) the marginal likelihood for $\langle \mathbb{E}[\psi(\mathbf{X})|Z], \psi(\mathbf{x}) \rangle_{\mathcal{H}_X}$ specified in their Proposition 3. We use 1000 iterations of ADAM with a base learning rate of 0.1. Since they do not provide details on how to set \hat{S} , we set \hat{S} identically to IMPspec.

Sampling GP: The baseline sampling GP we implement is essentially the method in Witty et al. (2020) in the case where there is no unobserved confounding. In particular, in this case their approach specifies $Y = f(X) + U$, $X_d = g_d(X) + V_d$ where $U \sim \mathcal{N}(0, \sigma^2)$, $V_d \sim \mathcal{N}(0, \eta_d^2)$, $f \sim \mathcal{GP}(0, k_X)$ and $g_d \sim \mathcal{GP}(0, k_{Z,d})$. The kernel parameters and noise variances are trained by maximising the usual marginal likelihoods for each respective dataset: $p(\mathbf{y}|\mathbf{x}_1, \dots, \mathbf{x}_d) = \mathcal{N}(\mathbf{y}|\mathbf{0}, K_{XX} + \sigma^2 I)$ and $\prod_{j=1}^d p(\mathbf{x}_j|z) = \prod_j \mathcal{N}(\mathbf{x}_j|\mathbf{0}, K_{ZZ,d} + \eta_d^2 I)$. We use 1000 iterations of ADAM with a base learning rate of 0.1. The causal effect is then estimated by sampling from the posterior predictive distributions $\prod_{j=1}^d p(\mathbf{x}_j|z, \mathcal{D}_2), p(\mathbf{y}|\mathbf{x}_1, \dots, \mathbf{x}_d, \mathcal{D}_1)$, which are again given by the usual formulae (Williams and Rasmussen, 2006). We use Gaussian kernels for k_X and each $k_{Z,d}$, with per-dimension lengthscales.

Calibration computation: To measure the calibration of posterior coverage probabilities, we specify a grid of 100 values of $\alpha \in [0, 1]$ and estimate Eq. (34) in the main text for each fixed confidence level α (rather than averaging over them). We estimate $\mathbb{P}_{\mathcal{X}^n}$ using the empirical distribution $\hat{\mathbb{P}}_{\mathcal{X}^n} = \frac{1}{T} \sum_{t=1}^T \delta_{\mathcal{X}_t^n}$ over the $T = 50$ trials (where \mathcal{X}_t^n is the dataset used for the t^{th} trial) and using the true causal function γ . Doing this recovers the calibration error profiles reported in the main text. We construct marginal calibration curves by estimating $\mathbb{P}_{\mathcal{X}^n}(\gamma(z) \in C_{z,\alpha}(\mathcal{X}^n))^9$ in the same way for each α and z , and averaging over the different values of z . As discussed in the main text, we report these profiles since it is standard in the calibration literature. However, we note these profiles can (unlike the error profiles) show near perfect calibration profiles even if a method is not well calibrated at every z .

We only get a single estimate of the calibration profile and error profile for each method from all the trials ran. To construct an approximate confidence interval around these results, we therefore use the empirical bootstrap, which samples with replacement from the empirical distribution $\hat{\mathbb{P}}_{\mathcal{X}^n} = \frac{1}{T} \sum_{t=1}^T \delta_{\mathcal{X}_t^n}$. We use 100 bootstrap replications of 50 sampled datasets each.

D.2 Synthetic Benchmark

In this experiment we aim to estimate the CATE $\mathbb{E}[Y|do(D = d), B = b]$ for the middle causal graph in Fig. 1 in the main text.

D.2.1 Simulation Details

We use the same data generating process as in Aglietti et al. (2020), which is:

$$U_1 = \epsilon_1 \tag{220}$$

$$U_2 = \epsilon_2 \tag{221}$$

$$F = \epsilon_3 \tag{222}$$

$$A = F^2 + U_1 + \epsilon_A \tag{223}$$

$$B = U_2 + \epsilon_B \tag{224}$$

$$C = \exp(-B) + \epsilon_C \tag{225}$$

$$D = \exp(-C)/10 + \epsilon_D \tag{226}$$

$$E = \cos(A) + C/10\epsilon_E \tag{227}$$

$$Y = \cos(D) + \sin(E) + U_1 + U_2\epsilon_Y \tag{228}$$

where all noise variables $\epsilon_\bullet \sim \mathcal{N}(0, 1)$.

For each simulation we draw a single dataset $(A_i, B_i, C_i, D_i, E_i, Y_i)_{i=1}^n$ of size $n = 100$.

⁹Note here $\mathcal{X}^n = \mathcal{D}_1 \cup \mathcal{D}_2$ as we are in the causal data fusion setting.

D.2.2 Causal Effect Identification

Using the rule of do-calculus, we have

$$\mathbb{E}[Y|do(D = d), B = b] = \int_{\mathcal{C}} \mathbb{E}[Y|do(D = d), B = b, C = c] \mathbb{P}_{C|do(D), B}(dc|d, b) \quad (229)$$

$$= \int_{\mathcal{C}} \mathbb{E}[Y|do(D = d), B = b, C = c] \mathbb{P}_{C|B}(dc|b) \quad (C \perp\!\!\!\perp D|B \in \mathcal{G}_{\overline{D}}) \quad (230)$$

$$= \int_{\mathcal{C}} \mathbb{E}[Y|D = d, B = b, C = c] \mathbb{P}_{C|B}(dc|b) \quad (Y \perp\!\!\!\perp D|B, C \in \mathcal{G}_{\overline{D}}) \quad (231)$$

D.2.3 Implementation Details

True causal function: Since $\mathbb{E}[Y|D = d, B = b, C = c] = \cos(d) + \mathbb{E}[\sin(E)|C = c] = \mathbb{E}[Y|D = d, C = c]$, we can estimate $\mathbb{E}[Y|do(D = d), B = b]$ for each pair (d, b) as follows. We first sample 10^5 Monte carlo samples from $\mathbb{P}_{C|B}(\cdot|b)$ and $P(A)$. This gives samples $(A_i, C_i)_{i=1}^{10^5}$ from $\mathbb{P}_{A, C|do(D=d), B=b}$. We then use each sample to sample from $\mathbb{P}_{E|C, A}$. This gives samples $(E_i)_{i=1}^{10^5}$ from $\mathbb{P}_{E|do(D=d), B=b}$. Averaging $\cos(d) + \sin(E)$ wrt these samples therefore estimates $\hat{\mathbb{E}}[Y|do(D = d), B = b]$.

IMPspec: Our estimation target is $\gamma(w, z)$ as defined in Eq. (4) in the main text, where now $W = (D, B)$ and $V = C$. We therefore estimate the posterior moments of γ using Theorem 3 in the main text. The kernels used, training, and calibration procedures are all identical to the Ablation study and we implement our full method which optimises the spectral representation.

BayesIMP: We implement BayesIMP using their equations in Proposition 5 extended for the case where $W \neq \emptyset$ in Eq. (4) in the main text. This extension is derived in Appendix A. Note that their derivations are for the causal data fusion setting. However, their method can be used in the single dataset setting $\mathcal{D}_1 = \mathcal{D}_2$ (in this case the concatenation is $\mathcal{D}_1 \cup \mathcal{D}_2 = \mathcal{D}_1 = \mathcal{D}_2$). The choice of kernels as well as the training and inference details are the same as in the Ablation study.

Sampling GP: The sampling GP specifies $Y = f(B, C, D) + U$ and $C = g(B) + V$, with f, g, U, V specified as in the Ablation study. The choice of kernels as well as the training and inference details are the same as in the Ablation study.

Calibration computation: See Ablation study.

D.3 CBO on Synthetic Benchmark and Healthcare Example

Causal Bayesian optimisation: In this experiment we use our method to construct a GP prior for Bayesian optimisation (BO) of several causal effects of interest. In general, in causal BO (CBO) (Aglietti et al., 2020), one aims to find $\operatorname{argmin}_{x \in \mathbb{X}} \mathbb{E}[Y|do(x)]$ or $\operatorname{argmax}_{x \in \mathbb{X}} \mathbb{E}[Y|do(x)]$ by querying as few values of the treatment as possible. At the start, one typically has no interventional data, and so has to construct a GP prior for $\mathbb{E}[Y|do(X = \cdot)] \sim \mathcal{GP}(m, k)$ (either naively or by using observational data). Each iteration recovers an observation $(\hat{x}, \mathbb{E}[Y|do(X = \hat{x})])$, which is then used to condition the GP prior on. Note that in practice to recover this observation one would have to run a large scale experiment under the intervention $do(X = \hat{x})$, and return an estimated $\mathbb{E}[Y|do(X = \hat{x})]$ using a very large empirical average. At each iteration the GP is used to construct an acquisition function. This function determines the next optimal search location for x by using the posterior uncertainty estimates to optimally trade off exploration and exploitation. GPs are popular surrogates for BO tasks as they are flexible, non-parametric models with good generalisation and uncertainty quantification properties (Williams and Rasmussen, 2006); enable acquisition functions to be computed in closed form; and are efficient with their use of the data (Shahriari et al., 2015).

In our case, we aim to find the optimal intervention that (i) minimises the CATE $\mathbb{E}[Y|do(D = d), B = b]$ in the synthetic benchmark (middle causal graph in Fig. 1 in the main text), (ii) maximises the ATT $\mathbb{E}[Y|do(B = b), B = b']$ in the synthetic benchmark (middle causal graph in Fig. 1 in the main text), and (iii) minimises the ATE $\mathbb{E}[\text{VOL}|do(\text{Statin})]$ in a real Healthcare example under causal data fusion (RHS causal graph in 1 in the main text). We search for the optimal intervention level, whilst fixing $B = 0$ for the CATE and ATT in the synthetic benchmark. We note that despite the ATT being considered a counterfactual quantity, it is a ‘single-world’ counterfactual quantity, and can be estimated experimentally (Richardson and Robins, 2013).

D.3.1 Simulation Details

Synthetic benchmark: The data generating process for the synthetic benchmark is already described above. For the task of minimising the CATE $\mathbb{E}[Y|do(D = d), B = b]$ wrt D we draw datasets of size $n = 100$, and for the task of maximising the ATT $\mathbb{E}[Y|do(B = b), B = b']$ we draw dataset sizes of $n = 500$.

Healthcare example: For the first dataset \mathcal{D}_1 (see Fig. 1 in the main text), we use the same data generating process as in [Chau et al. \(2021b\)](#):

$$\text{age} = \mathcal{U}[15, 75] \quad (232)$$

$$\text{bmi} = \mathcal{N}(27 - 0.01 \cdot \text{age}, 0.7) \quad (233)$$

$$\text{aspirin} = \sigma(-8.0 + 0.1 \cdot \text{age} + 0.03 \cdot \text{bmi}) \quad (234)$$

$$\text{statin} = \sigma(-13 + 0.1 \cdot \text{age} + 0.2 \cdot \text{bmi}) \quad (235)$$

$$\text{cancer} = \sigma(2.2 - 0.05 \cdot \text{age} + 0.01 \cdot \text{bmi} - 0.04\text{statin} + 0.02 \cdot \text{aspirin}) \quad (236)$$

$$\text{PSA} = \mathcal{N}(6.8 + 0.04 \cdot \text{age} - 0.15 \cdot \text{bmi} - 0.6 \cdot \text{statin} + 0.55 \cdot \text{aspirin} + \text{cancer}, 0.4) \quad (237)$$

and for each simulation we draw $n = 100$ observations. For the second dataset \mathcal{D}_2 (see Fig. 1 in the main text), we did not have access to the original data used in ([Chau et al., 2021b](#)), but we still were able to construct a simulator based on real data. In particular, we use the estimated linear model ($\text{VOL} = \hat{\beta}\text{PSA}$) of the effect of prostate specific antigen (PSA) on cancer volume (VOL) in [Carvalho et al. \(2010\)](#) as a simulator, by setting $\text{VOL} = \hat{\beta}\text{PSA} + U$, where $U \sim \mathcal{N}(0, \sigma^2)$ with σ^2 set to match the estimated $R^2 = 0.13$ in their study. For each simulation we draw $n = 100$ observations for \mathcal{D}_2 using this model (note we use the data generating process above to first draw observations for PSA).

D.3.2 Causal Effect Identification

We have already derived the identification formulae for the CATE $\mathbb{E}[Y|do(D = d), B = b]$ in the synthetic benchmark using the back-door criterion. The ATT $\mathbb{E}[Y|do(B = b), B = b']$ in the synthetic benchmark can be identified using the do calculus on a counterfactual graph which has an added node B' with the same parents as B but all outgoing edges removed (see Theorem 1 in ([Shpitser and Pearl, 2012](#))). We call this graph \mathcal{G}' .

$$\mathbb{E}[Y|do(B = b), B = b'] = \int_{\mathcal{C}} \mathbb{E}[Y|do(B = b), B' = b', C = c] \mathbb{P}_{C|do(B), B'}(dc|b, b') \quad (238)$$

$$= \int_{\mathcal{C}} \mathbb{E}[Y|do(B = b), B' = b', C = c] \mathbb{P}_{C|do(B)}(dc|b) \quad (C \perp\!\!\!\perp B' | B \in \mathcal{G}'_B) \quad (239)$$

$$= \int_{\mathcal{C}} \mathbb{E}[Y|do(B = b), B' = b', C = c] \mathbb{P}_{C|B}(dc|b) \quad (C \perp\!\!\!\perp B \in \mathcal{G}'_B) \quad (240)$$

$$= \int_{\mathcal{C}} \mathbb{E}[Y|B' = b', C = c] \mathbb{P}_{C|B'}(dc|b) \quad (Y \perp\!\!\!\perp B | B', C \in \mathcal{G}'_B) \quad (241)$$

$$= \int_{\mathcal{C}} \mathbb{E}[Y|B = b', C = c] \mathbb{P}_{C|B}(dc|b) \quad (242)$$

Lastly, the ATE $\mathbb{E}[\text{Vol}|do(\text{Statin})]$ for the healthcare example can be identified as follows

$$\mathbb{E}[\text{Vol}|do(\text{Statin})] = \int \mathbb{E}[\text{Vol}|do(\text{Statin}), \text{PSA}] \mathbb{P}(d\text{PSA}|do(\text{Statin})) \quad (243)$$

$$= \int \mathbb{E}[\text{Vol}|\text{PSA}] \mathbb{P}(d\text{PSA}|do(\text{Statin})) \quad (\text{Vol} \perp\!\!\!\perp \text{Statin} | \text{PSA} \in \mathcal{G}_{\overline{\text{Statin}}}) \quad (244)$$

$$= \int \int \mathbb{E}[\text{Vol}|\text{PSA}] \mathbb{P}(d\text{PSA}|\text{Statin}, \text{Age}, \text{BMI}) \mathbb{P}(d(\text{Age} \times \text{BMI})) \quad (245)$$

Where the last-line follows from the fact that (Age, BMI) satisfies the back-door criterion wrt $(\text{Statin}, \text{PSA})$.

D.3.3 Implementation Details

True causal function: (Synthetic benchmark) Since $\mathbb{E}[Y|B = b, C = c] = \mathbb{E}[\cos(D)|C = c] + \mathbb{E}[\sin(E)|C = c] = \mathbb{E}[Y|C = c]$, we can estimate $\mathbb{E}[Y|do(B = b), B = b']$ for each pair (b, b') as follows. We sample 10^5 Monte

carlo samples from $\mathbb{P}_{C|B}(\cdot|b)$ and $P(A)$ which gives samples $(A_i, C_i)_{i=1}^{10^5}$ from $\mathbb{P}_{A,C|do(B=b),B=b'}$. We then use each sample to sample once from $\mathbb{P}_{E|A,C}$ and $\mathbb{P}_{D|C}$. This gives samples $(D_i, E_i)_{i=1}^{10^5}$ from $\mathbb{P}_{D,E|do(B=b),B=b'}$. Averaging $\cos(D) + \sin(E)$ wrt these samples therefore estimates $\mathbb{E}[Y|do(B=b), B=b']$. See Section D.2 for estimation strategy for $\mathbb{E}[Y|do(D=d), B=b]$. (Healthcare example) Since $\mathbb{E}[\text{Vol}|do(\text{Statin})]$ is a marginal interventional quantity, one can estimate it by simply modifying the data generating process so that $\text{Statin} = s$ in the case $do(\text{Statin} = s)$.

The following settings are constant across all BO experiments, and so from now on we will assume we are optimising an abstract causal function $f : \mathcal{X} \rightarrow \mathbb{R}$, and x is the intervention value. Note that we target the CATE and ATT above while fixing the conditioning variable B to zero, so this also covers those cases.

General BO settings: For all methods and causal effects we use the expected improvement (EI) acquisition function, and run 10 BO iterations. The kernel hyperparameters of each method are updated every $K = 3$ iterations. We assess the performance of each method by the cumulative regret scores $\sum_{i=1}^{10} |f(x^*) - f(x_i^{best})|$ and also through analysing the convergence profiles of $f(x_i^{best})_{i=1}^{10}$ (here $x_i^{best} = \text{argmin}_{x \in \{x_1, \dots, x_i\}} |f(x^*) - f(x)|$ is the current best intervention). Cumulative regret rankings of methods can be sensitive to the number of iterations run. We focus on performance after 10 iterations (rather than a larger number) because in most real-life situations it is challenging to run more than 10 full scale experimental studies sequentially. Moreover, in healthcare situations this can be unethical: an exploratory intervention for a cancer drug dosage could cost livelihoods. We emphasise that finding the optimum (or achieving the same performance) in just two or three fewer iterations can have substantial practical impact.

IMPspec: The implementation used for the ATT in the synthetic example $\mathbb{E}[Y|do(B=b), B=b']$ is the same as for the CATE $\mathbb{E}[Y|do(D=d), B=d]$ (see Section D.2). The ATE in the healthcare example is of the form $\gamma(s) = \mathbb{E}_{\text{Age, BMI}}[\gamma(\text{Statin} = s, \text{Age}, \text{BMI})]$, where $\gamma(\text{Statin}, \text{Age}, \text{BMI})$ is derived from the two-stage model $(\text{Statin}, \text{Age}, \text{BMI}) \rightarrow \text{PSA}, \text{PSA} \rightarrow \text{Vol}$. The posterior on $\gamma(\text{Statin}, \text{Age}, \text{BMI})$ can therefore be estimated using the modification of Theorem 3 for the causal data fusion setting and where $W = \emptyset$, which is Corollary 4. The posterior on $\gamma(s)$ then follows from an application of Corollary 5 and Remark 5 in Appendix C. For all CBO tasks, we use IMPspec to construct GP prior for the causal effects using the posterior mean and covariance derived for each causal function: $f \sim \mathcal{GP}(\mathbb{E}[\gamma(\cdot)|\mathcal{X}^n], \text{Cov}[\gamma(\cdot), \gamma(\cdot)|\mathcal{X}^n]) + k_{RBF}$. Here k_{RBF} is a Gaussian kernel. The choice of IMPspec’s kernels as well as the training and inference details are the same as in the Ablation study.

BayesIMP: The implementation used for the ATT in the synthetic example $\mathbb{E}[Y|do(B=b), B=b']$ is the same as for the CATE $\mathbb{E}[Y|do(D=d), B=d]$ (see Section D.2). For the ATE in the Healthcare example we use the exact implementation in Proposition 5 in Chau et al. (2021b). The choice of BayesIMP’s kernels as well as the training and inference details are the same as in the Ablation study. For the CBO tasks the implementation is the same as IMPspec.

CBO: Aglietti et al. (2020) construct the CBO prior $f \sim \mathcal{GP}(\hat{\mathbb{E}}[Y|do(\cdot)], \sqrt{\hat{\text{Var}}(Y|do(\cdot)) + k_{RBF}}$, where k_{RBF} is a Gaussian (radial basis function) kernel and $\hat{\mathbb{E}}[Y|do(X)], \hat{\text{Var}}(Y|do(X))$ are estimated from observational data. We estimate these functions using the approach in Singh et al. (2024), using the same kernels and hyperparameters as our method. Note, to use this approach for to estimate the variance, we estimate $\hat{\mathbb{E}}[Y^2|do(X)]$ and then compute $\hat{\text{Var}}(Y|do(X)) = \hat{\mathbb{E}}[Y^2|do(X)] - \hat{\mathbb{E}}[Y|do(X)]^2$.

BO: The standard BO approach does not make use of observational data, and so simply uses $f \sim \mathcal{GP}(0, k_{RBF})$ as the prior (see Aglietti et al. (2020) for further details).

D.4 Additional Results

D.4.1 Ablation Study

Here we include results for additional ablations of IMPspec and Bayesimp using simulations from the LHS causal graph in Fig. 2 (see simulation details in Appendix D.1). The first ablation we run is the effect of sample splitting in IMPspec’s spectral learning procedure to optimise calibration, versus using the full dataset to estimate both $\mathbb{P}_{\mathcal{X}^n}$ and $\hat{\gamma}$. We also run two ablations for BayesIMP. The first ablation aims to quantify the effect of using the marginal likelihood $\log p(\mathbf{y}|\mathbf{x}_1, \dots, \mathbf{x}_d)$ to optimise the parameter ς of the variance of the measure $\mathcal{N}(0, \varsigma \hat{S})$ used to construct the nuclear dominant kernel for r_V . This is important since, as we discuss in Appendix A, it is plausible that the nonstationarity of the nuclear dominant kernel leads to systematic

underfitting, and this nonstationarity is controlled by ζ . The second ablation aims to quantify the effect of Monte carlo approximating the nuclear dominant kernel during training and inference time. This is relevant because except in special cases nuclear dominant kernels are not available in closed form, and so Monte Carlo approximation will in general be required. Note that we require $m = \alpha n$ samples with $\alpha \geq 1$ during training to ensure invertibility of the gram matrix R_{VV} . However if $\alpha > 1$ then the time complexity of computing R_{VV} exceeds $\mathcal{O}(n^3)$. We therefore set $\alpha = 1$ during training. At inference time we set $n = 10^5$ since these matrices are only computed once.

The results of these ablations from 50 trials are displayed in Table 4. We see that optimising the measure variance of the nuclear dominant kernel does improve performance, however does not fully resolve the underfitting problem compared to our method. We also see a notable reduction in performance when Monte carlo approximating the kernel. As mentioned, Monte carlo approximation is necessary for nuclear dominant kernels constructed with various base kernels (e.g. Matérn, Gamma exponential, Rational quadratic) - even when using the Gaussian measure. This therefore demonstrates another limitation of using nuclear dominant kernels.

Turning to IMPspec, we see that calibration performance is reduced when not sample splitting. One possible reason for this is that, by not sample splitting, there is a correlation induced between the estimator for $\hat{\gamma}$ and the estimator for $\hat{\mathbb{P}}_{\mathcal{X}^n}$ in Eq. (34). Since we found all methods were slightly overconfident in their uncertainty estimates, this could result in the calibration procedure choosing a spectral representation that induces a smaller posterior variance than is optimal, hence leading to more overconfidence than otherwise.

Method	RMSE	Calibration Error
BayesIMP-approx	0.366 ± 0.156	0.136 ± 0.015
BayesIMP	0.314 ± 0.082	0.143 ± 0.009
BayesIMP-opt	0.269 ± 0.086	0.094 ± 0.010
IMPspec-nosplit (ours)	0.223 ± 0.046	0.087 ± 0.009
IMPspec (ours)	0.223 ± 0.046	0.065 ± 0.008

Table 4: Ablation study mean \pm standard deviation of RMSE and calibration error from 50 trials. Monte carlo approximating the nuclear dominant kernel during training (BayesIMP-approx) degrades performance. Optimising the integrating measure variance of the nuclear dominant kernel (BayesIMP-opt) partially reduces the underfitting problem. Not using sample splitting with our posterior calibration procedure (IMPspec-nosplit) worsens IMPspec’s performance.

Ablation for IMPspec posterior approximation

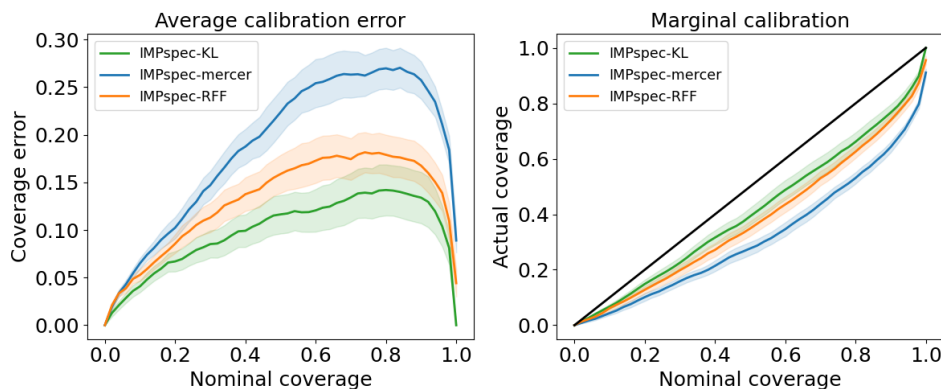


Figure 8: Calibration profiles from 50 trials of the ablation study (i.e. LHS causal graph of Fig. 1) for different posterior approximation methods using IMPspec (with fixed spectral representation). KL = $KL(P, Q)$ projection of the posterior P onto the space of Gaussians (i.e. our proposed approach in the paper - see Section 5.3). Merc = Truncated posterior approximation using 10^4 Mercer features, RFF = Truncated posterior approximation using 10^4 Random Fourier features (see Appendix A for details on Mercer and RFF). Our proposed approach gives the most accurate uncertainty quantification.